Public Interest Energy Research (PIER) Program

FINAL PROJECT REPORT

HYDRODYNAMIC SEPARATION OF NEUTRALLY BUOYANT PARTICLES FROM WASTEWATER

Reducing Energy Demands and Increasing Energy Yields

Prepared for: California Energy Commission
Prepared by: Palo Alto Research Center (PARC), Inc

MARCH 2015
CEC-500-2016-025

Prepared by:

Primary Author(s):
Cory Lancaster
Norine Chang
Mark Stephenson
Armin R. Völkel

PARC, Inc.
3333 Coyote Hill Road
Palo Alto, CA 94304

Contract Number: PIR-11-006

Prepared for:

California Energy Commission

Anish Gautam
Contract Manager

Anish Gautam
Project Manager

Virginia Lew
Office Manager
Energy Efficiency Research Office

Laurie ten Hope
Deputy Director
Energy Research and Development

Robert Oglesby
Executive Director

DISCLAIMER

This report was prepared as the result of work sponsored by the California Energy Commission. It does not necessarily represent the views of the Energy Commission, its employees or the State of California. The Energy Commission, the State of California, its employees, contractors and subcontractors make no warrant, express or implied, and assume no legal liability for the information in this report; nor does any party represent that the uses of this information will not infringe upon privately owned rights. This report has not been approved or disapproved by the California Energy Commission nor has the California Energy Commission passed upon the accuracy or adequacy of the information in this report.

ACKNOWLEDGEMENTS

The authors would like to acknowledge the support of the Sunnyvale Water Pollution Control Facility, namely Operations Manager Bryan Berdeen and staff, for providing the site for this pilot study.

PREFACE

The California Energy Commission Public Interest Energy Research (PIER) Program supports public interest energy research and development that will help improve the quality of life in California by bringing environmentally safe, affordable, and reliable energy services and products to the marketplace.

The PIER Program conducts public interest research, development, and demonstration (RD&D) projects to benefit California.

The PIER Program strives to conduct the most promising public interest energy research by partnering with RD&D entities, including individuals, businesses, utilities, and public or private research institutions.

PIER funding efforts are focused on the following RD&D program areas:

- Buildings End-Use Energy Efficiency
- Energy Innovations Small Grants
- Energy-Related Environmental Research
- Energy Systems Integration
- Environmentally Preferred Advanced Generation
- Industrial/Agricultural/Water End-Use Energy Efficiency
- Renewable Energy Technologies
- Transportation

Hydrodynamic Separation of Neutrally Buoyant Particles from Wastewater – Reducing Energy Demands and Increasing Energy Yields is the final report for the novel hydrodynamic separation technology for wastewater treatment project PIR-11-006, conducted by PARC, Inc. The information from this project contributes to PIER's Industrial/Agricultural/Water End-Use Energy Efficiency Program.

For more information about the PIER Program, please visit the Energy Commission's website at www.energy.ca.gov/research/ or contact the Energy Commission at 916-654-4878.

ABSTRACT

This report describes the Palo Alto Research Center's efforts in bringing their Hydrodynamic Separation technology out of the laboratory and into a pilot-scale demonstration at a wastewater treatment plant. The Palo Alto Research Center successfully fabricated and tested two generations of semi-automatically assembled stacks of mass produced, injection-molded parts using an ultraviolet gluing and curing process. The researchers manufactured working hydrodynamic seperation channels that separated and concentrated neutrally buoyant organic solids from primary effluent from a wastewater treatment plant. By reducing the organic loading from the primary effluent (using the hydrodynamic separation technology), there will also be direct reducdtion in the energy demand for secondary treatment at wastewater treatment plants.Due to unforeseen limitations in the pilot system, only two stages of second-generation stacks could be tested at the Sunnyvale wastewater treatment plant. The researchers found that the best performance of harvest efficiency (the mass capture rate in the concentrate stream) for the first and second stage occured at the beginning of testing. Harvest efficiency performance deteriorated during testing due to fouling of the separation channels. To return the harvest efficiency to pre-pilot performance level, it was necessary to clean the first stage channels using backflow and high pressure. The researchers determined that design and manufacturing flaws detected during this study could easily be corrected to reduce fouling, improve flow split to the intended ratios, and facilitate assembly. Theoretical best-case performance suggests that energy savings for typical wastewater treatment plants could be approximately $1,650 per year per million gallons per day of wastewater treatment plant capacity.

Keywords: Hydrodynamic separation, wastewater treatment, organics harvesting from primary effluent, energy recovery

Please use the following citation for this report:

Lancaster, Cory, Norine Chang, Mark Stephenson, Armin R. Völkel. (PARC, Inc.). 2015. ***Hydrodynamic Separation of Neutrally Buoyant Particles From Wastewater – Reducing Energy Demands and Increasing Energy Yields.*** California Energy Commission. Publication number: CEC-500-2016-025.

TABLE OF CONTENTS

Acknowledgements i

PREFACE ii

ABSTRACT iii

TABLE OF CONTENTS iv

LIST OF FIGURES vi

LIST OF TABLES ix

Executive Summary 1

Introduction 1

Project Goals and Objectives 2

Project Results 2

Project Benefits 4

CHAPTER 1: Background and Problem Statement 1

1.1 Energy and Wastewater Treatment 1

1.2 Hydrodynamic Separation 2

1.3 Goals and Objectives 3

Chapter 2: Potential Benefits from Harvesting Organics from Primary Effluent 5

2.1 Conceptual HDS System Design 6

2.2 Process Modeling Exercise 7

CHAPTER 3: Feasibility of Separating Solids From Primary Effluent 11

3.1 Survey of Different Sources 11

3.2 San Francisco Public Utility Commission (SFPUC) Southeast Plant Results 12

3.3 East Bay Municipal Utility District (EBMUD) Plant Results 14

3.4 Sunnyvale Water Pollution Control Plant Results 16

CHAPTER 4: HDS Manufacturing 23

4.1 Pre-fabrication Considerations 23

4.1.1 HDS Channel Design 23

4.1.2 HDS Channel Fabrication Criteria 24

4.1.3 HDS system Fabrication Criteria 26
4.1.4 CFD modeling of Stacked Channels 27
4.2 Channel Fabrication Options 28
4.2.1 Extruded Plastic Channels 28
4.2.2 Injection Molded Channels 29
4.3 Stack Assembly Options 30
4.3.1 Hot Plate Welding 30
4.3.2 Electromagnetic Welding 31
4.3.3 Compression Gasketing 32
4.3.4 Ultrasonic Welding 32
4.3.5 Ultra-Violet Gluing and Curing 33
4.4 Final HDS Part Fabrication, Assembly Solution for PIER Project 34
CHAPTER 5: Pilot Unit Design, Testing and Operation, and Installation 37
5.1 Pilot Unit Design 37
5.2 Pilot Unit Testing and Operation 39
5.2.1 Pilot Unit Testing 43
5.2.2 Pilot Installation 46
CHAPTER 6: Pilot Demonstration in a Wastewater Plant 49
6.1 First-Generation HDS Stacks – Summary 49
6.2 Differences – First- and Second-Generation HDS Stacks 54
6.3 Second-generation Stacks - Performance 56
6.3.1 Baseline Testing 56
6.3.2 Pilot Testing 58
CHAPTER 7: Energy Benefits of HDS 68
CHAPTER 8: Technology Transfer Activities 72
CHAPTER 9: Conclusions and Recommendations 74
9.1 General Conclusions 74
9.2 Recommendations for Future Work 76

GLOSSARY **77**

REFERENCES **79**

LIST OF FIGURES

Figure 1: Energy use at a conventional activated sludge facility. 1

Figure 2: HDS Channels are rectangular in cross section and separation relies on internal forces induced by channel geometry and flow rate to concentrate particles in a force minimum near the outside wall. 2

Figure 3: Relationships between TSS, COD, and BOD for raw influent (left) and primary effluent (right). 6

Figure 4: The Anticipated Performance of Four HDS Stacks in Series (units of mg/L TSS) 7

Figure 5: Typical Domestic Wastewater Treatment Facility Designed for TSS, BOD Removal, and Nitrification. 9

Figure 6: Domestic Wastewater Treatment Facility Designed to Include HDS 9

Figure 7: Primary Effluent (left), HDS Effluent (middle), and HDS Concentrate (right) for HDS Separation Test Using SFPUC Southeast Plant Primary Effluent Collected on 11-8-13 13

Figure 8: Mass Rate PSD for HDS Separation Test Using SFPUC Southeast Plant Primary Effluent Collected on 11-8-13 13

Figure 9: Cumulative Mass Rate PSD for HDS Separation Test Using SFPUC Southeast Plant Primary Effluent Collected on 11-8-13 14

Figure 10: Micrograph of Primary Effluent Collected from EBMUD, 11-13-13 15

Figure 11: Mass Rate PSD for HDS Separation Test Using EBMUD Primary Effluent Collected on 11-13-13 15

Figure 12: Cumulative Mass Rate PSD for HDS Separation Test Using EBMUD Primary Effluent Collected on 11-13-13 16

Figure 13: Primary Effluent (left), HDS Effluent (middle), and HDS Concentrate (right) for HDS Separation Test Using Sunnyvale Primary Effluent Collected on 11-21-13 17

Figure 14: Mass Rate PSD for HDS Separation Test Using Sunnyvale Primary Effluent Collected on 11-21-13 18

Figure 15: Cumulative Mass Rate PSD for HDS Separation Test Using Sunnyvale Primary Effluent Collected on 11-21-13 18

Figure 16: Micrograph of Primary Effluent Collected from Sunnyvale on 11-26-13 19

Figure 17: Mass Rate PSD for HDS Separation Test Using Sunnyvale Primary Effluent Collected on 11-26-13 20

Figure 18: Cumulative Mass Rate PSD for HDS Separation Test Using Sunnyvale Primary Effluent Collected on 11-26-13 20

Figure 19: Mass Rate PSD for HDS Separation Test Using Sunnyvale Primary Effluent Collected on 11-26-13 22

Figure 20: Cumulative Mass Rate PSD for HDS Separation Test Using Sunnyvale Primary Effluent Collected on 11-26-13 22

Figure 21: Example of CFD Model Results for a Cross Section of an HDS Channel- Flow Fields (top); Pressure Fields (bottom) 24

Figure 22: Laser Printer (left); Printing Acrylic Top Layer (middle); Gluing Middle and Top Layer of HDS Channel (right) 25

Figure 23: Two Different Exit Channel Designs 26

Figure 24: Circuit Approximations (left), CFD Modeling (right) of Channel Stacks 28

Figure 25: Extruded plastic channel components, left to right, top to bottom: channel cross section; full turn channel; 3D printed manifold fittings; glued manifold; gasketed, compression manifold; extruded manifold concept; integrated extruded channels and extruded manifold concept. 29

Figure 26: Molded part design first-generation part (left); molded part design, second-generation part (middle); actual molded parts – first generation (right, bottom); second-generation (right, top). 30

Figure 27: Hot Plate Tooling Method (top), Different Joint Types (bottom) 31

Figure 28: Emmabond Process (left); Electromagnetically Welded HDS Part Sample (right) 31

Figure 29: Single HDS Part with Gasket (left); 1 mgd Assembled Unit (right) 32

Figure 30: Recommended Injection Molding Detail for Ultrasonic Welding Assembly 33

Figure 31: Robotically Gluing (left), and Curing (right) a First-Generation, 72-Channel HDS Stack 34

Figure 32: Improved HDS Assembly Table with Clamps Instead of Weights for Second-Generation Stack Assembly 34

Figure 33: Second-Generation HDS Part, Molding Modeling Results - Warp in Z, New Design, Run 3, 0.088″ Thick, Four Gates, Warp in Z, 235 °C Melt Temperature, 60 °C Mold Temperature, 3X Deformation Scale 36

Figure 34: Early (November 2012) P&ID Schematic of Proposed HDS Pilot System 37

Figure 35: Four Stages of HDS Channels in Series for PIER Pilot 38

Figure 36: Isographs of Final PIER Pilot System, from Design Drawings by Intuitech, Inc. 39

Figure 37: Pilot Unit Upon Delivery Without HDS Stacks and with Stage 1 Components..... 40

Figure 38: Weir boxes and weir configuration (left); with TSS meters and weir box lid (right)... 41

Figure 39: Bag filters and TSS Instrument Controllers (left); Surrogate Nodes for HDS (right) .. 42

Figure 40: Main Control Panel with HMI (left); Overview Display (middle); Process Control Display (right)..... 42

Figure 41: Process-Operating Set Points for 144:27:5:1 Channel Configuration at 80:20 Flow 43

Figure 42: Clean Water Through Nodes - Influent Flow, Effluent Flow, and Inlet Pressure for Stage1 44

Figure 43: Clean Water Through Nodes - Influent Flow, Effluent Flow, and Inlet Pressure for Stage 4 45

Figure 44: Pressure Versus Flow, Stage 4 46

Figure 45: Aerial View of the Sunnyvale WPCP Plan with the Pilot Testing Site Circled in Red (left); Pad Location at End of Primary Clarifiers for Pilot Installation 46

Figure 46: Pilot system after arrival at Sunnyvale with shipping box in front (left); pilot system inside the canvas tent (right). 47

Figure 47: Schematic Diagram of the Fluidic Setup 47

Figure 48: Components of the Fluidic Setup: Influent Grinder Pump in the Primary Effluent Launder (left); Effluent Storage Tank (a modified refuse container) (middle); Effluent Sump Pump (right) 48

Figure 49: First-Generation Stacks Installed in Pilot 49

Figure 50: Split Ratio Deterioration with Stack Height 50

Figure 51: Pressure Anomaly Correlates with Deteriorating Split Ratio 51

Figure 52: 10x Concentration Increase with Forced 80:20 Split 52

Figure 53: Influent, 4th Stage Concentrates with Forced Split 53

Figure 54: Setup for Testing First-Generation 27-Channel Stacks (left); Performance (right) with ¼" Tubing on Effluent and Concentrate Exits (which can be seen in the photo, leading from the exits to the raised tank) 54

Figure 55: 1st (top of each photo) and 2nd (bottom of each photo) Generation Stacks (bottom of each photo)..... 55

Figure 56: Flaws of Second-Generation Parts - Ejector Pin Mark in Middle of Effluent Channel (left); 73:27 Geometric Flow Split Design Error (right) 56

Figure 57: Lab Setup for Testing Second-Generation 5-Channel (left) and 144-Channel Stack (right), with a Free-Surface Discharge at the Exits 57

Figure 58: Lab Results of the Second-Generation 5-Channel (left) and 144-Channel Stack (right), with a Free-Surface Discharge at the Exits 57

Figure 59: Pilot Testing of the First Stage (left) and Third Stage (right) Stacks, with a Free-Surface Discharge at the Exits 59

Figure 60: TSS Results for 4 Days of Pilot Testing 60

Figure 61: Particulate COD Results for 4 Days of Pilot Testing 60

Figure 62: 1st Stage Influent (left of each photo) and 3rd Stage Concentrate (right of each photo) for Beginning (left) and End (right) of 4-Hour Run of Pilot Operation (October 28rd) 62

Figure 63: 1st Stage Inlet Pressure 63

Figure 64: Stage 3 Inlet Pressure. 63

Figure 65: 200um bag filter holds water after 4 hours of operation (left); Inlet manifold debris accumulation (middle); after cleaning with a brush (right). 64

Figure 66: Solids accumulating on the splitter and ejector pin marks for the 1st Stage (left); 3rd Stage (right). 64

Figure 67: Algae pieces lodged in channel near inlet channel (left); lodged in effluent channel (right). 65

Figure 68: Stage 1 Inlet Manifold Debris Accumulation after 4 Hours without the Bag Filter 66

Figure 69: Confirmation test of the 1st stage second-generation stack, flow rate of 36 lpm, showing 85 percent mass capture of neutrally buoyant 45-53um standard spheres. 67

Figure 70: Mass rate particle size distribution of primary effluent input, single channel HDS effluent, and single channel HDS concentrate. From lab separation of primary effluent from Sunnyvale Wastewater plant performed November 21, 2013. 76

LIST OF TABLES

Table 1: Fabricated and Tested HDS Designs (from Hsieh et al., 2013) 3

Table 2: Performance Assumptions for Four Stages in Series 7

Table 3: Implications for 1 mgd HDS system of four stages in series starting with 100 mg/L TSS with the ideal performance presented in Table 2. 7

Table 4: Influent Characteristics, Primary Treatment Parameters 8

Table 5: Size and Performance of a 25 mgd Wastewater Treatment Plant with & without HDS. 10

Table 6: Primary Effluent Survey Summary 12

Table 7: Single Channel Harvest Efficiency Results – Using Primary Effluent Collected from the SFPUC Southeast Plant, 11-8-13 12

Table 8: Single Channel HE Results – Using Primary Effluent Collected from EBMUD, 11-13-13 14

Table 9: Single Channel HE Results – Using Primary Effluent Collected from Sunnyvale, 11-21-13 17

Table 10: Single Channel HE Results – Using Primary Effluent Collected from Sunnyvale, 11-26-13 19

Table 11: Single Channel HE Results – Using Primary Effluent Collected from Sunnyvale, 11-27-13 21

Table 12: Results and Statistics of Flow Stability Test 44

Table 13: Results of the Stage 4 Pressure Versus Flow Test 45

Table 14: Performance of "New", Second-Generation Stacks with Neutrally Buoyant, 45-53um Spheres 58

Table 15: Performance Between 1st and 2nd Generation 27 Channel Stacks with Neutrally Buoyant 45-53um Spheres 58

Table 16: Harvest Efficiencies with Primary Effluent During Four-Days of 4-Hour Pilot Operation 61

Table 17: Split Ratios During Four-Days of 4-Hour Pilot Operation 61

Table 18: Performance of "Dirty", Second-Generation Stacks with Neutrally Buoyant Spheres Between 45-53um 66

Table 19: Performance of the 144 channel second-generation stack with neutrally buoyant spheres between 45-53um – the impact of fouling and cleaning. 67

Table 20: Table of performance assumptions for an ideal HDS system of 4 stages in series. 68

Table 21: Implications for 1 mgd HDS system of 4 stages in series starting with 100 mg/L TSS with the ideal performance presented in Table 20. 68

Table 22: Table of performance based on average, actual results measured during pilot testing. 69

Table 23: Implications for 1 mgd HDS system of four stages in series starting with 100 mg/L TSS with the actual performance presented in Table 22. 69

Table 24: Assumptions Used for the Three Components Used to Calculate Energy Benefits of HDS 70

Table 25: Energy comparison of a theoretical plant without HDS (baseline), with an ideal HDS system, and an HDS system based on average performance documented during the pilot study. 71

EXECUTIVE SUMMARY

Introduction

Over the span of 33 months, the Palo Alto Research Center (PARC) investigated the feasability of using a novel hydrodynamic separation (HDS) technology to harvest neutrally buoyant organics from wastewater that has undergone primary treatment.

Most of California's wastewater treatment facilities are largely dependent upon energy intensive processes due for innovation. Considering that an average energy consumption of 2,300 kilowatt-hour per million gallons per day (kWh/mgd) are required for wastewater treatment, about 2 terawatt hours (TWh) are needed to power the 608 wastewater treatment plants in California; in total, these plants process over 1.3 trillion gallons of wastewater every year. This is a significant burden on California investor owned utilities (IOUs), which own 70 percent of transmission and distribution infrastructure, and 25 percent of the power generation facilities in California.

To run pumps, blowers, solids handling equipment, mixers, and other miscellaneous operations, a considerable amount of energy is necessary. For example, the largest and most common power demand used for treating activated sludge treatment requires the support of activated sludge blowers. These blowers supply oxygen, which sustains biological carbon oxidation and nitrification produced by a diverse and robust microbial population called *activated sludge*. Air delivery mechanisms for carbon oxidation and nitrification account for up to 60 percent (1,400 kWh/mgd) of electrical energy demands for modern activated sludge treatment facilities.

Easily concentrated particulate organics (settled in primary clarifiers and concentrated as primary solids) and biomass grown on soluble organics (excess biological growth in bioreactors and removed as secondary solids) can be sent to anaerobic digesters to be converted into biogas made up of 65 percent methane. The biogas can be used in primary movers, turbines, and converted into electricity and heat in a process known as cogeneration. The produced energy can decrease the requirement of a wastewater treatment facility, ultimately reducing overall cost. Typical anaerobic digestion processes, for every one million gallons per day (MGD) of wastewater treatment, produces about 10,000 cubic feet of biogas, with typical cogeneration process from biogas producing about 500 kWh/mgd of energy.

Technologies that either reduce energy consumption or increase energy production are highly desirable. PARC's novel HDS technology has the potential of accomplishing both: by removing solids that otherwise could not be captured in conventional primary treatment processes and concentrating the removed solids and sending them to anaerobic digesters, the load on aeration systems is reduced. This process lowers energy requirements for aeration and the energy yield increases through biogas production and cogeneration. Ultimately, this project sought to investigate HDS technology in light of its potential application.

Project Goals and Objectives

This project sought to acheive two specific goals. The first goal was to demonstrate the scalability of PARC's HDS technology: the researchers wanted to prove that stacks of channels, capable of processing tens of thousands to millions of gallons per day, can be produced commercially. PARC's experience thus far has been with very small stacks (less than 10 channels) of hand-assembled channels; however, hand-assembly does not lend itself well to commercialization. Identifying a practical manufacturing process that results in functional channels was a critical and logical next step.

The second goal was to demonstrate that PARC's HDS technology can provide energy savings by harvesting neutrally buoyant organic solids to reduce loads to aeration systems. In addition, the system can provide increased energy generation by sending the harvested organics directly to anaerobic digesters for biogas production and cogeneration of electricity and heat. While other HDS channel designs have supplementary applications in wastewater treatment, mixed-liquor suspended solids thickening for example, the goal of this project was to evaluate one particular HDS channel design for organics harvesting to address energy needs as targeted by the California Energy Commission's (Energy Commission) Public Interest Energy Research (PIER) program.

To meet these goals, the researchers considered three main objectives. Two of the objectives involved exploration in manufacturing, bench testing, and pilot testing at a wastewater treatment plant. The first objective was to find a scalable means of reliably manufacturing and assembling multiple layers of HDS channels, and to establish a production process that fabricates parts assembled in an automated manner. The second objective was to evaluate the applicability of HDS for organics harvesting from primary effluent in wastewater treatment at different wastewater facilities. The third objective involved pilot testing, which addressed both scalability and wastewater applicability goal; it demonstrated that a manufactured and scaled HDS unit can be field-deployed, perform under adverse conditions, and harvest organics, which all indicate potential energy savings and gains.

Project Results

For the first stage of the project, primary effluent was collected from three local wastewater treatment plants: the San Francisco Public Utility Commission's Southeast wastewater treatment plant (SFPUC Southeast), the East Bay Municipal Utility District wastewater treatment plant (EBMUD), and the Sunnyvale Water Pollution Control Facility (Sunnyvale). Samples were brought back to the water laboratory at PARC and evaluated for solids separability with HDS using a single half-turn channel with a 73 to 27 flow split. The flow split was made from clear Acrylonitrile Butadiene Styrene (ABS) and glued with an ultraviolet (UV) -curable glue by Cascade Designs, Inc. (CDI) in Seattle, Washington. The researchers evaluated HDS performance by measuring three characteristics of the influent, effluent, and concentrate streams; these are the volumetric flow split, the total suspended solids concentration, and the particle size distribution. With the incorporation of flow rates and total suspended solids (TSS) measurements, the researchers defined a performance metric for mass removal in the concentrate stream, otherwise known as *harvest efficiency*.

The second stage of the project involved determining a workable manufacturing and assembly approach for fabricating stacks of HDS channels. The authors evaluated extruded and injection molding processes for making plastic HDS parts, ultimately deciding injection molding was more feasible and practical. They then explored five methods for assembling multiple injection-molded layers to create stacks of HDS channels. These methods included hot plate welding, electromagnetic welding, compression gasketing, ultrasonic welding, and UV gluing and curing. The selected assembly method dictated the design of the injection molded part. Manufacturing and assembly were by far the most challenging part of the project, and the researchers arrived at a semi-automated method of UV gluing and curing injection molded layers after two part designs and countless gluing trials by our manufacturing partners, CDI. A full set of stacks needed for the pilot were tested with a standard, a neutrally buoyant sphere between 45 and 53 micrometers (um), and performed well. While this approach did succeed in producing functional stacks of channels, hot plate welding seems a more appropriate method for commercialization. More research and development is needed to investigate hot plate welding of injectionmolded parts to create stacks of HDS channels.**c**

The third stage of the project involved designing, fabricating, installing, and testing an HDS pilot system at a wastewater treatment plant. Intuitech, Inc. built a pilot unit, consisting of four stages of HDS stacks in series, collaboratively conceived by the team). The cascading design allowed for sequential solids separation and concentration. The 36 liters per minute (lpm) pilot unit was installed at the Sunnyvale Water Pollution Control Plant where it could pump primary effluent through the channels and then discharge both concentrate and effluent streams back to the main plant.

Due to unforeseen flaws in the pilot design related to system hydraulics that could not be fixed without expensive and time-consuming modifications, pilot testing was limited to two stages. The testing was conducted in a series with free-surface discharges, and comprised four-hours of testing for four days, for a total of 16 hours of operation. During that period, the total suspended solids, chemical oxygen demand, flow rate, and pressure of both stages were measured for influent, effluent, and concentrate streams.

Harvest efficiency generally deteriorated from the beginning to the end of a four-hour period of operation as well as the first to the fourth day of operation. Deterioration was attributed to debris build-up at certain points in the channel. The clear plastic parts allowed visualization and documentation of where this buildup occurred. The best harvest efficiency was 70 percent, while the worst harvest efficiency was 32 percent. Also, the third stage generally performed worse than the first stage, for unknown reasons. The impact of debris buildup on flow split was inconsistent—in some cases, buildup improved flow split.

After the four days of pilot testing, the first and third stage stacks of HDS channels were brought back to PARC's lab to be re-tested with standards. For the first test, the inlet manifolds were brushed clean as before, but no efforts were made to clean the insides of the channels. The channels were tested again with neutrally buoyant spheres between 45 and 53 um, using starting concentrations between 200 and 400 milligrams per liter (mg/L). The 144 channel stack was then cleaned using a combination of hot tap water, back flushing, soapy water, and high-

pressure (20 pounds per square inch [psi]) both forward and backwards through the inlet, concentrate, and effluent channels in combination and individually. Approximately 40 liters (L) of clean water was pumped through the stack for about five minutes for each rinse, with the rinse water replaced with clean water approximately 15 times. The researchers repeated a separation experiment with a solution of neutrally buoyant spheres between 45 and 53 um, as before, to determine if the initial "new" performance could be recovered with cleaning. The difference between "new" and "cleaned" performance was negligible, indicating that the stacks could indeed be cleaned.

Project Benefits

Using the findings presented in this report, The researchers calculated the energy impact for a wastewater treatment facility without HDS, with an ideal HDS system, and with an actual system. Anaerobic digestion, aeration, and pumping were the only impacts considered for energy generation, as all other plant energy demands will be equal. The full analysis is presented in Chapter 7.

To summarize, an ideal HDS system saves about 40 kWh/mgd, or about $1,650 every year per million gallons per day per year (mgd/year), in energy costs when compared to a conventional activated sludge plant. If an HDS system with a similar performance outcome to the pilot study were installed, it would cost about 220 kWh/mgd, or about $9,335/mgd/year more in energy costs compared to a conventional activated sludge plant. Despite the fact that this iteration does not provide a benefit over conventional treatment, muchcan still be improved. The best-case savings of $1,650/mgd/year is an unlikely incentive for commercialization of HDS for harvesting of organics from primary effluent. While these conclusions are disappointing, this project has allowed the researchers to prove that stacks of HDS channels can be assembled in a commercial fashion, which is advantageous when investigating other promising HDS applications such as algae dewatering and activated sludge recycling.

CHAPTER 1:
Background and Problem Statement

1.1 Energy and Wastewater Treatment

California's portfolio of wastewater treatment facilities is largely dependent upon energy intensive processes that are ripe for innovation. Considering an average energy consumption of 2,300 kWh/mgd for wastewater treatment, about 2 TWh is needed to power the 608 wastewater treatment plants in California that treat 1.3 trillion gallons of wastewater every year. This is a significant burden on California investor owned utilities (IOUs), which own 70% of transmission and distribution infrastructure, and 25% of the power generation facilities in California.

Electricity is needed at wastewater treatment facilities to run pumps, blowers, solids handling equipment, mixers and miscellaneous other operations (Figure 1). The largest power demand for activated sludge treatment processes (the most common process-type in California) is to power blowers that supply oxygen to support biological carbon oxidation and nitrification by a diverse and robust microbial population called "activated sludge". Air delivery mechanisms for carbon oxidation and nitrification account for up to 60% of the electrical energy demands for a modern activated sludge treatment facility (1,400 kWh/mgd).

Figure 1: Energy use at a conventional activated sludge facility.

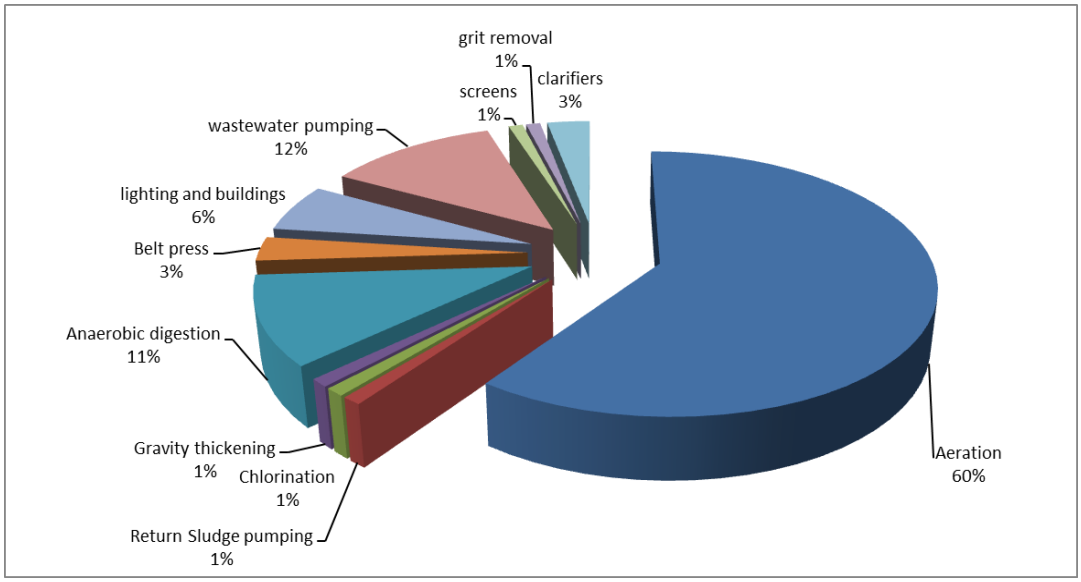

Particulate organics that can be easily concentrated (i.e., settled in primary clarifiers and concentrated as primary solids) and biomass grown on soluble organics (i.e., excess biological growth in bioreactors and removed as secondary solids) can be sent to anaerobic digesters and be converted to biogas (65% methane), which is then burned in primary movers (turbines) and

converted to electricity and heat in a process known as cogeneration. This energy can reduce the requirement of a wastewater treatment facility, reducing cost. Typical anaerobic digestion processes, for every one million gallon per day (MGD) of wastewater treatment, produce about 10,000 cubic feet of biogas, and typical cogeneration process from this biogas produces about 500 kWh/mgd of energy.

Technologies that either reduce energy consumption or increase energy production are highly desirable. Palo Alto Research Center's (PARC) novel hydrodynamic solids separation (HDS) technology has the potential of accomplishing both: by removing solids that otherwise couldn't be captured in conventional primary treatment processes and concentrating these removed solids and sending them to anaerobic digesters, the load on aeration systems is reduced, lowering energy requirements for aeration, and the energy yield is increased through biogas production and cogeneration. This demonstration project investigated the HDS technology in light of this potential application.

1.2 Hydrodynamic Separation

Since 2008, PARC has been developing its hydrodynamic separation (HDS) technology as an innovative solid-liquid separation alternative. Relying on no physical barriers, HDS carefully balances a combination of fluidic forces to separate particles (solids, flocs, and emulsions) from the entraining fluid. Centrifugal force creates transverse flow patterns in a curved channel, which under certain circumstances manifest themselves as a pair of Dean Vortices, as shown in Figure 2.

Figure 2: HDS Channels are rectangular in cross section and separation relies on internal forces induced by channel geometry and flow rate to concentrate particles in a force minimum near the outside wall.

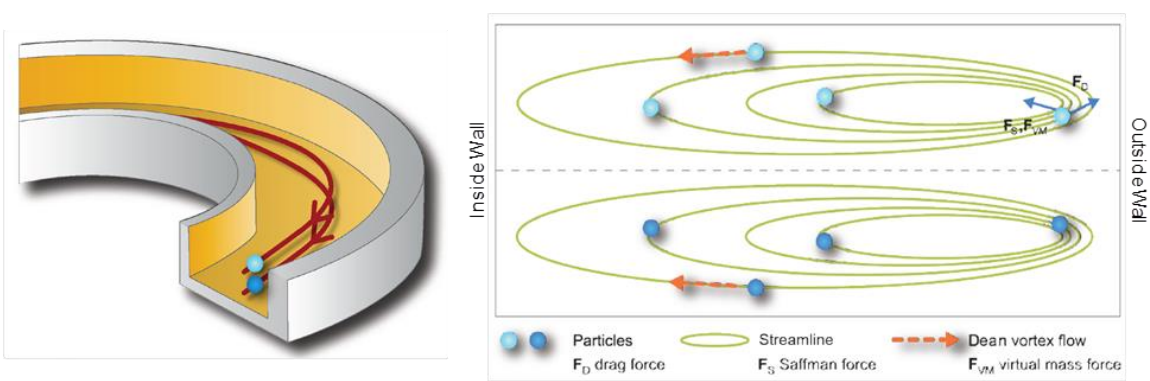

Starting with proof of concept experiments obtained with micro-channels in the laboratory (Seo, Lean, & Kole, 2007), the team at PARC has shown the efficacy of this novel separation technology with numerous sample types including: particles and flocs in produced water, wastewater, agriculture water, and algae dewatering. As well as suspended solid harvesting from various industrial processes, including harvesting organic solids from primary clarifier effluents and recycling activated sludge post-biological treatment. The most distinctive

advantage of the HDS technology, the fact that it effectively separates neutrally buoyant particles, was illustrated by achieving 96% recovery of 45um polystyrene beads rendered neutrally buoyant by density-matching to a mixture of 50:50 H_2O and D_2O (Hsieh et al., 2013).

The design (radius of curvature and channel height and width), operating conditions (pressure and flow rate), and water properties (viscosity and temperature) ultimately affect which particles of a certain size and shape concentrate along the outside wall at the end of the curved channel. Table 1 (Hsieh et al., 2013) shows three design permutations. This study uses the "particle separator" design, capable of capturing particles between 20 and 100 um. Strategically splitting the flow after separation occurs, results in a "concentrate" stream with more solids and an "effluent" stream with fewer solids. Stacking many curved channels in parallel increases throughput. Running several HDS modules in series can further thickening, using the concentrate output of one stage as the input for the next stage.

Table 1: Fabricated and Tested HDS Designs (from Hsieh et al., 2013)

Channel dimensions for current prototypes	R_C [mm]	Height [mm]	Width [mm]	*Q* [ml/min]	*V* [m/s]	d*P* [psi]	d*P* [kPas]	Pr (5k gpm) [kw]	d_c [micron]
Floc separator	198	1.1	5	200	0.61	1.3	9.9	2.8	70
3 × floc separator	198	1.1	15	600	0.61	1.2	9.1	2.6	70
Particle separator	198	0.4	6	250	1.73	10/20*	75.8/151.6	21.7/43.5	20

R_C radius of curvature.
Q flow rate at room temperature and water viscosity.
V linear velocity of liquid at room temperature and water viscosity.
d*P* pressure drop (single channel) at room temperature and water viscosity.
* half turn / full turn.
Pr (5k gpm) HDS fluidic-only power requirement for 5,000 gallon per min.
d_c estimated cut-off size (>90%).

1.3 Goals and Objectives

There were two specific goals of this project. The first goal was to demonstrate scalability of PARC's HDS technology: that is, to show that stacks of channels capable of processing tens of thousands of gallons per day or more can be produced commercially. PARC's experience thus far has been with very small stacks (<10 channels) of hand-assembled channels. Hand-assembly does not lend itself well to commercialization. Identifying a practical manufacturing process that results in functional channels was therefore the critical and logical next step, and outlined as the first goal of this project.

The second goal was to specifically demonstrate that PARC's HDS technology has applications in the field of wastewater treatment to provide energy savings by harvesting neutrally buoyant organic solids to reduce loads to aeration systems and to provide increased energy generation by sending those harvested organics directly to anaerobic digesters for biogas production and ultimately cogeneration of electricity and heat. While other HDS channel designs have other potential applications in wastewater treatment (mixed-liquor suspended solids thickening, for example), the goal of this project was to evaluate one particular HDS channel design for organics harvesting to address energy needs as targeted by the PIER program.

The three objectives required to meet these two goals involve explorations in manufacturing, bench testing, and pilot testing at a wastewater treatment plant. The first objective is to find a scalable means of reliably manufacturing and assembling multiple layers of HDS channels, and to establish a production process that fabricates parts that can be assembled in an automated manner. The second objective is to evaluate the applicability of HDS for organics harvesting from primary effluent in wastewater treatment at different wastewater treatment facilities. The third objective is pilot testing which will address both scalability and wastewater applicability goals, as it will demonstrate that a manufactured and scaled HDS unit (in our case, 36 lpm) can be field-deployed and perform under adverse conditions and harvest organics that can indicate potential energy savings and potential energy gains.

CHAPTER 2:
Potential Benefits from Harvesting Organics from Primary Effluent

To understand what exactly can be captured or harvested by HDS, it is first helpful to understand what the constituents are in both a raw influent wastewater and the effluent from a primary clarifier, broken down into meaningful components. Using a commercially available process simulator, BioWin (EnviroSim, Ltd.), first the authors evaluated the impact of solids removal on organic constituents, and then they performed a process modeling exercise that compared the impact of a 25 mgd facility, with and without an HDS system, on size and performance.

The constituents typically measured in wastewater are actually "lumped" parameters – each is comprised of many other components. Total suspended solids (TSS), biochemical oxygen demand (BOD), and chemical oxygen demand (COD) are three such lumped parameters. Complicating matters, the constituents that make up each of these parameters register as portions or fractions of the other parameters. Fortunately, process engineers and plant operators, over decades, have established correlations between these different lumped parameters, and the typical relationships have been quantified for use in the industry. The simulator software gives users the ability to adjust these relationships based on a standard COD "currency", which can be measured for a given wastewater source and then correlated to TSS and BOD (part of rigorous calibration exercises). These relate particulate and soluble, biodegradable and non-biodegradable components of wastewater.

Typical values of TSS, COD, and BOD relationships for a raw influent and a primary effluent (assuming 60% removal of solids) are shown in Figure 3. These parameters can be changed within a model to closely track in actual wastewater. These values presented as an example were also used in the modeling exercise.

Figure 3: Relationships between TSS, COD, and BOD for raw influent (left) and primary effluent (right).

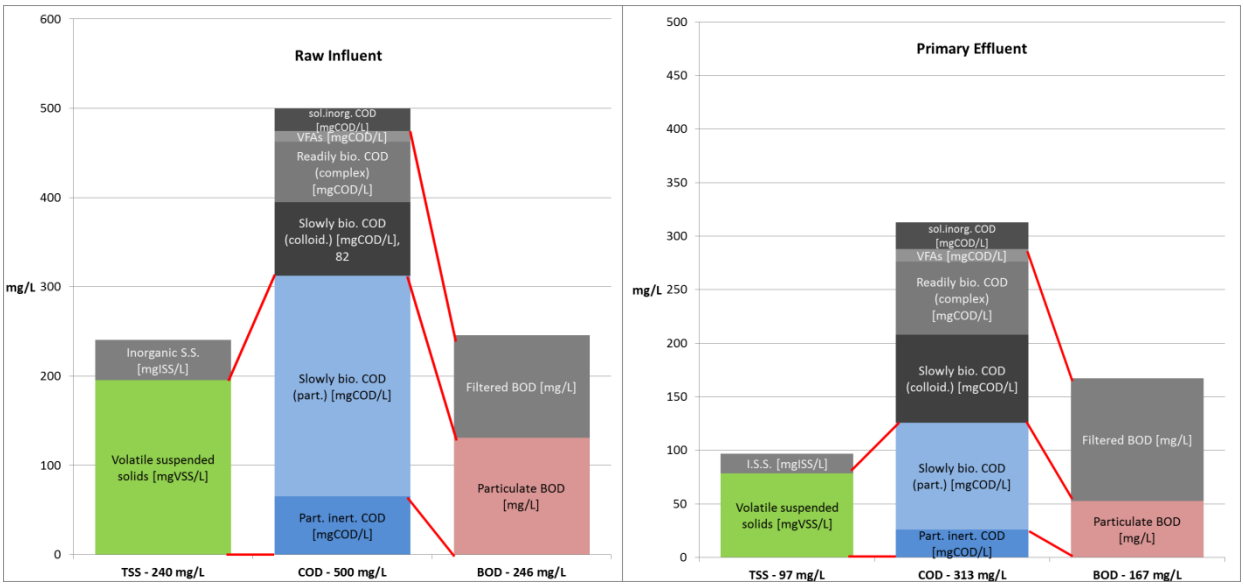

Figure 3 shows that approximately 100 mg/L of TSS, which contains about 50 mg/L of particulate BOD, typically remains in the effluent of primary clarifiers. It is these neutrally buoyant small particles that are being targeted for capture, as they are capable of being harvested by HDS. Removing inorganic solids reduces the solids inventory in bioreactors; removing organic solids both reduces the solids inventory as well as the oxygen demand. The biodegradable organics can then subsequently benefit biogas production in digesters.

2.1 Conceptual HDS System Design

Four stages of 80:20 split particle separators are required to thicken solids to greater than 3% (30,000 mg/L), a typical minimum needed to feed to a digester, assuming a 70%/90%/90%/90% capture rate (harvest efficiency, see below) for stages 1-4, respectively (Figure 4). The concentrate flow rate will be less than 0.2% of the influent flow, with 99.8% of the flow passing through. Preliminary lab investigations using primary effluent collected from local treatment plants demonstrated that a single, ½-turn particle separator with an 80:20 flow split could achieve a 70% percent harvest efficiency of solids. It was assumed that increases in harvest efficiency to 90% could be achievable due to pre-conditioning of solids and process optimization. The overall result would be a mass capture of 51% after four stages. Table 2 presents the flow split and harvest efficiency assumptions, while Table 3 presents the impact of these assumptions on a 1 million gallon per day (mgd) HDS system starting with an influent concentration of 100 mg/L TSS and assuming ideal performance. This system would have 13,104 HDS channels per mgd, each with a flow rate of 0.25 lpm, have an output of 3.2% solids with a flow rate of 1 gallon per minute (gpm), and the combined effluent would have a TSS concentration of 49 mg/L.

Table 2: Performance Assumptions for Four Stages in Series

	Flow split		Harvest Efficiency	
Stage	**Effluent**	**Concentrate**	**Effluent**	**Concentrate**
Stage 1	80%	20%	30%	70%
Stage 2	80%	20%	10%	90%
Stage 3	80%	20%	10%	90%
Stage 4	80%	20%	10%	90%

Table 3: Implications for 1 mgd HDS system of four stages in series starting with 100 mg/L TSS with the ideal performance presented in Table 2.

		flow rates [gpm]			mass flow rates [%]			solids concentration [mg/L]		
stage	# channels	Inf.	Eff.	Conc.	Inf.	Eff.	Conc.	Inf.	Eff.	Conc.
1	10500	694	556	139	100%	30%	70%	100	38	350
2	2100	139	111	28	70%	7%	63%	350	44	1575
3	420	28	22	6	63%	6%	57%	1575	197	7088
4	84	6	4	1	57%	6%	**51%**	7088	886	**31,894**

Figure 4: The Anticipated Performance of Four HDS Stacks in Series (units of mg/L TSS)

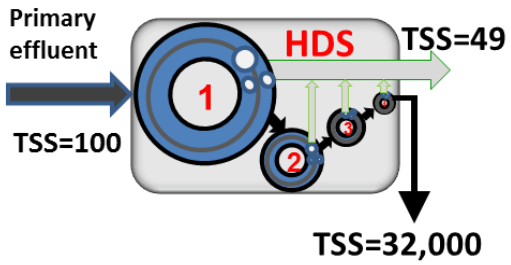

2.2 Process Modeling Exercise

The process modeling software, BioWin, was used to simulate the effect of HDS on overall performance of a hypothetical 25 mgd domestic wastewater treatment facility. Imbedded within the software is a complex set of partial differential equations that mathematically describe the physical, chemical, and biological reactions that occur during treatment. The software can be used to simulate steady-state as well as the dynamic behavior of different treatment processes based on the controlled environment that defines the plant – the volumes, flow rates, aeration rates, temperature, chemical dosing rates, and so forth are the "knobs" that allow operators to optimize performance.

The baseline process that was modeled for this exercise includes a primary clarifier, a plug-flow arrangement of five aerobic bioreactors sized for carbon oxidation and nitrification, secondary

clarification, gravity belt thickening of primary solids, and waste activated sludge to ~ 5% solids, mesophilic anaerobic digestion for 30 days, and a belt filter press for final thickening to 20% cake for landfill disposal. Sidestreams were returned to the head of the plant. Influent and primary treatment process characteristics are shown in Table 4.

The same process was sized and simulated assuming an HDS system was installed between the primary clarifiers and the bioreactors. HDS is not a process that can be simulated with BioWin, per se. However, the assumed percent mass removal and effective concentration of solids can be input using a generic solids separation device within the model to show what the effect is downstream of the HDS system to both the biological treatment process and the anaerobic digestion process. The comparison between the two simulations is presented in Table 5.

Table 4: Influent Characteristics, Primary Treatment Parameters

Raw influent	Value	Primary Treatment (clarifiers)	Value
Average daily flow (mgd)	25	VSS removal, % (mass)	55%
flow (mgd)	33	ISS removal, % (mass)	77%
COD, mg/L	500	TSS removal, % (mass)	59%
BOD, mg/L	246	Primary Effluent (PE) TSS, mg/L	99
TSS, mg/L	240	PE BOD, mg/L	174
VSS, mg/L	195	PE particulate BOD, mg/L	59
Phosphorus, mg/L	6	PE VSS, mg/L	89
Ammonia, mg/L	26	PE VSS:TSS ratio	0.90
Temperature, C	10	Primary solids, %solids	1.4%

Installing a full-scale HDS system with performance similar to what was described above could reduce the required footprint of the secondary treatment bioreactors by about 20, reduce the amount of oxygen needed in these bioreactors by about 10%, and increase the amount of biogas produced by 25% (Table 5). The digesters themselves may need to be slightly larger if the same concentration were to be maintained; however, most digesters can accommodate a 10% fluctuation in concentration. The total mass of cake to be disposed of is about the same.

A net-present worth analysis that incorporates both capital and operating costs will demonstrate if this technology provides a cost benefit over the baseline treatment configuration. Without an understanding of size and cost of an HDS system at this point, such an analysis is premature. However, it is clear that there are potential benefits of HDS for decreasing overall footprint and energy use while increasing energy yield. A detailed analysis of energy benefits is presented in Chapter 6.

Figure 5: Typical Domestic Wastewater Treatment Facility Designed for TSS, BOD Removal, and Nitrification.

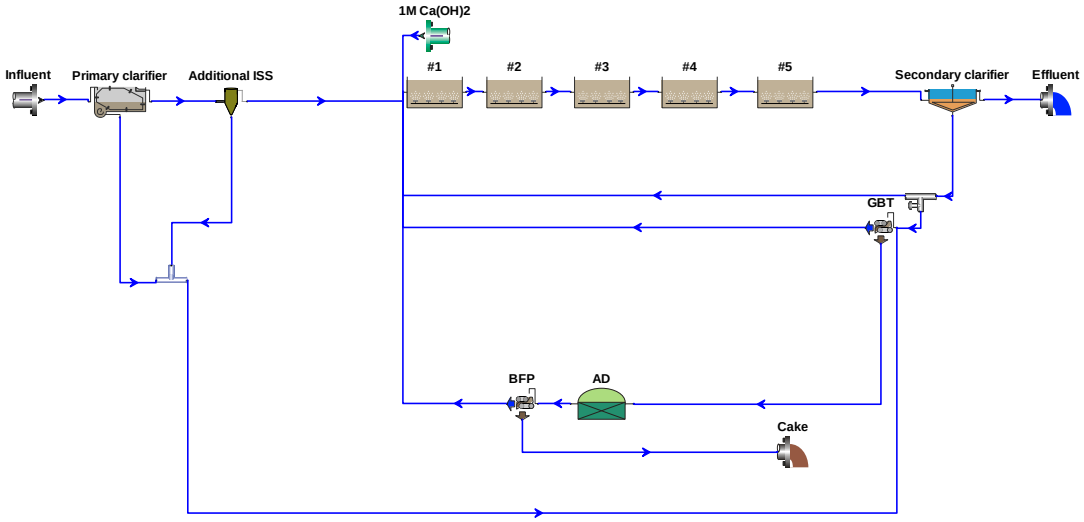

Figure 6: Domestic Wastewater Treatment Facility Designed to Include HDS

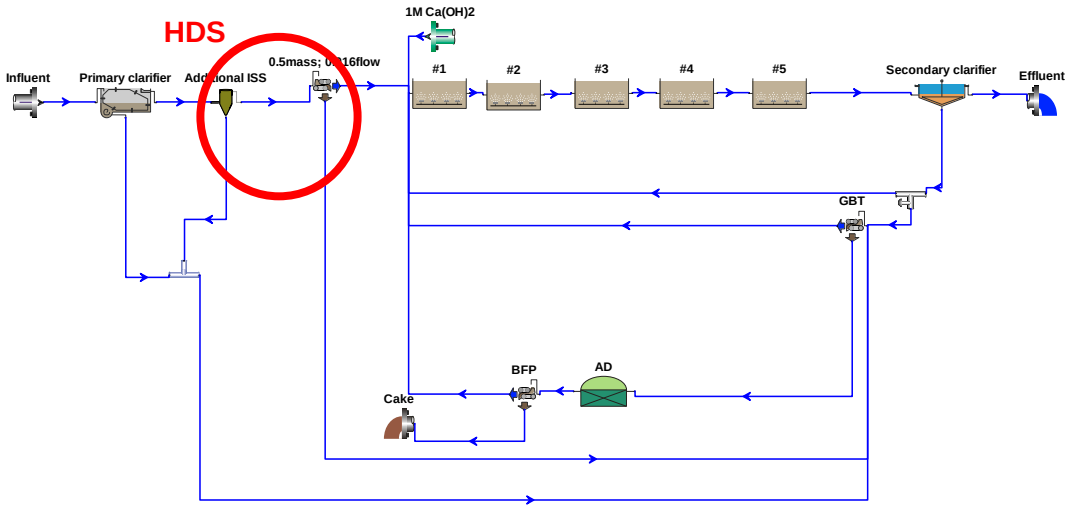

To summarize Table 5, implementing a well-performing HDS process could reduce the required footprint of the secondary treatment bioreactors by about 20%, reduce the amount of oxygen needed in these bioreactors by about 10%, and increase the amount of biogas produced by 25%. The digesters themselves may need to be slightly larger if the same concentration were to be maintained; however, most digesters can accommodate a 10% fluctuation in concentration. The total mass of cake to be disposed of is about the same.

Table 5: Size and Performance of a 25 mgd Wastewater Treatment Plant with & without HDS

	Parameter	Without HDS	With HDS	
HDS				
	concentrate:effluent flow	N/A	0.16%	Assuming 80:20 flow split for 4 stages in series
	Influent TSS, mg/L	N/A	99	
	Effluent TSS, mg/L	N/A	48	Assuming ~ 50% total mass capture (70%/90%/90%/90% for each stage in series)
	Effluent BOD, mg/L	N/A	143	
	Effluent particulate BOD	N/A	29	
	Effluent VSS	N/A	43	
	Concentrate TSS, mg/L	N/A	32199	
	Overall % removal (mass)	**N/A**	**52%**	
Secondary treatment				
	Design aerobic Solids Residence Time (SRT)	11	11	This is the residence time of the MLSS under aeration
	Aeration tank volume, m^3	**36,480**	**25,700**	aeration tanks are 30% smaller with HDS
	MLSS, mg/L	3,850	3,850	The modeling was adjusted so these values were the same, so the design of the secondary clarifiers would be the same
	MLSS VSS:TSS ratio	0.82	0.83	
	WAS VSS solids, kg/day	10,400	7,630	The quantity of secondary solids is 27% less
	SRT, days	13	13	This includes both the aerobic SRT and the SRT in the clarifiers (approximately 2 days)
	tOUR, kg/day	**39,170**	**34,670**	(OUR = oxygen uptake rate) Overall Oxygen needed is 12% less
	Nitrogenous OUR, kg/day	16,070	16,160	As most nitrogen is in a soluble form, HDS does little to reduce the nitrogen load to the secondary process and hence the amount of oxygen needed for nitrification does not change significantly
	Carbonaceous OUR, kg/day	**23,110**	**18,510**	Oxygen requirement for carbon oxidation is 20% less with HDS
Anaerobic Digester				
	VSS load to digesters, kg/day	**22,460**	**25,180**	VSS load to digesters is 12% more with HDS
	% solids to digesters	5.1%	5.0%	
	Digester SRT	30	30	
	Digester volume, m^3	17,010	18,710	Digesters need to be slightly larger (10%) with HDS if the same digester concentration is maintained
	VSS destruction, %	54%	59%	
	gas flow rate, m^3/min	7.9	9.9	Gas flow rate is 24% greater with HDS
	% methane	63%	63%	Methane content is the same
	Cake, kg/day	15,430	15,530	Essentially the same

CHAPTER 3:
Feasibility of Separating Solids From Primary Effluent

3.1 Survey of Different Sources

In proposing that neutrally buoyant organic solids could be captured with HDS from primary effluent, PARC performed nearly a dozen preliminary separation experiments to validate the concept in 2011 and 2012. Primary effluent was collected from three local wastewater treatment plants: the San Francisco Public Utility Commission's Southeast wastewater treatment plant (SFPUC Southeast), the East Bay Municipal Utility District wastewater treatment plant (EBMUD), and the Sunnyvale Water Pollution Control Facility (Sunnyvale). Samples were brought back to the water laboratory at PARC and evaluated for solids separability with HDS using hand fabricated, full-turn and half-turn channels with different channel dimensions, flow rates, and split ratios. That data is not included herein, as it was exploratory. As part of this study, PARC repeated these experiments separating primary effluent from the three local treatment plants using a single half-turn channel with a 73:27 flow split made specifically for this project using the first-generation part design that was largely based on what was learned during the preliminary separation experiments. The part was made from clear ABS and glued together with UV curable glue by Cascade Designs, Inc. (CDI). The results presented herein from separation testing and evaluations were standardized.

HDS performance is evaluated by measuring three characteristics of the influent, effluent, and concentrate streams. These are the volumetric flow split, the total suspended solids, and the particle size distribution. The volumetric flow split is measured simply with graduated cylinders and a stopwatch, and the total suspended solids test is measured by the procedure outlined in Standard Methods Method 2540. The particle size distribution (PSD) requires a PSD analyzer. PARC uses a Horiba LA-950 Mie scatter analyzer. By using properties of light and refraction, the instrument makes estimates on particle size based on refractive index and assuming spherical particles.

Incorporating volume and TSS measurements, the researchers have defined a performance metric for mass removal in the concentrate stream, which they are calling the "harvest efficiency". First, a mass balance can be calculated to help gauge the precision of the analyses. The harvest efficiency is then calculated as the concentrate mass divided by the influent mass. While primary effluent from a fourth wastewater treatment facility was evaluated, and hand-assembled channels were often tested alongside the injection molded channel, only the results that are from the injection molded channel and have mass-balances within +/- 10% are presented herein. A summary table is shown in Table 6.

Table 6: Primary Effluent Survey Summary

Plant, experiment date	HE
SFPUC Southeast, 11-08-11	70%
EBMUD, 11-13-13	56%
Sunnyvale, 11-21-13	53%
Sunnyvale, 11-26-13	62%
Sunnyvale, 11-27-13	60%

3.2 San Francisco Public Utility Commission (SFPUC) Southeast Plant Results

The SFPUC Southeast Plant is a 150 mgd pure-oxygen plant with circular primary clarifiers, and discharges to San Francisco Bay. The primary effluent sample collected from this plant on 11-8-13 from this plant separated the best of all the samples from the three plants tested at 70% harvest efficiency (Table 7). Note how the mode (the most abundant particle size) of the primary effluent (Figure 8) is slightly lower than the theoretical cutoff size of the channel designs employed (20um). Particles below the cutoff size are not differentially separated within the channel. The particle size distribution (PSD) data for the three streams of each separation experiment (primary effluent (HDS influent), HDS effluent, and HDS concentrate, Figure 7)) are presented as mass rates verses particle size (Figure 8, to show the magnitude of the particle size bins in relation to each other) and as cumulative mass rates verses particle size (Figure 9, to show the total mass rates as presented in Table 7).

Table 7: Single Channel Harvest Efficiency Results – Using Primary Effluent Collected from the SFPUC Southeast Plant, 11-8-13

SFPUC Southeast, 11-08-13	Flow rate (L/min)	Concentration (mg/L)	Mass rate(mg/min)
Primary Effluent (HDS Influent)	0.250	138	35
HDS Effluent	0.183	73	13
HDS Concentrate	0.068	358	24
(effluent mass+concentrate mass)/influent mass		Mass balance	109%
Concentrate mass/influent mass		Harvest Efficiency	70%

Figure 7: Primary Effluent (left), HDS Effluent (middle), and HDS Concentrate (right) for HDS Separation Test Using SFPUC Southeast Plant Primary Effluent Collected on 11-8-13

Figure 8: Mass Rate PSD for HDS Separation Test Using SFPUC Southeast Plant Primary Effluent Collected on 11-8-13

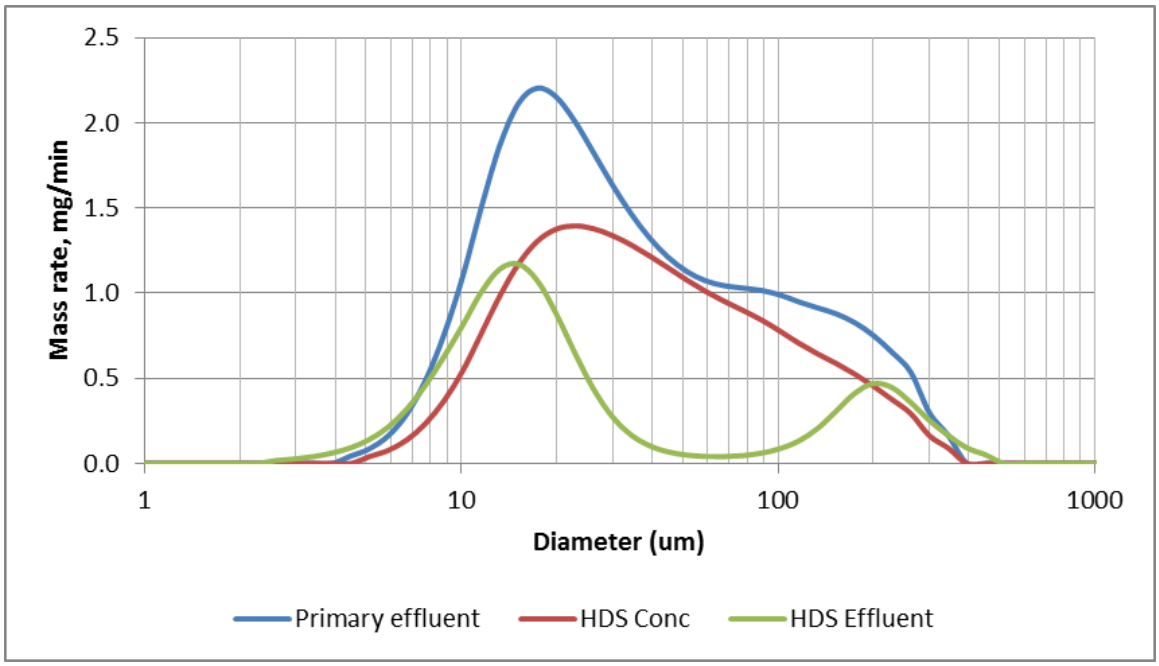

Figure 9: Cumulative Mass Rate PSD for HDS Separation Test Using SFPUC Southeast Plant Primary Effluent Collected on 11-8-13

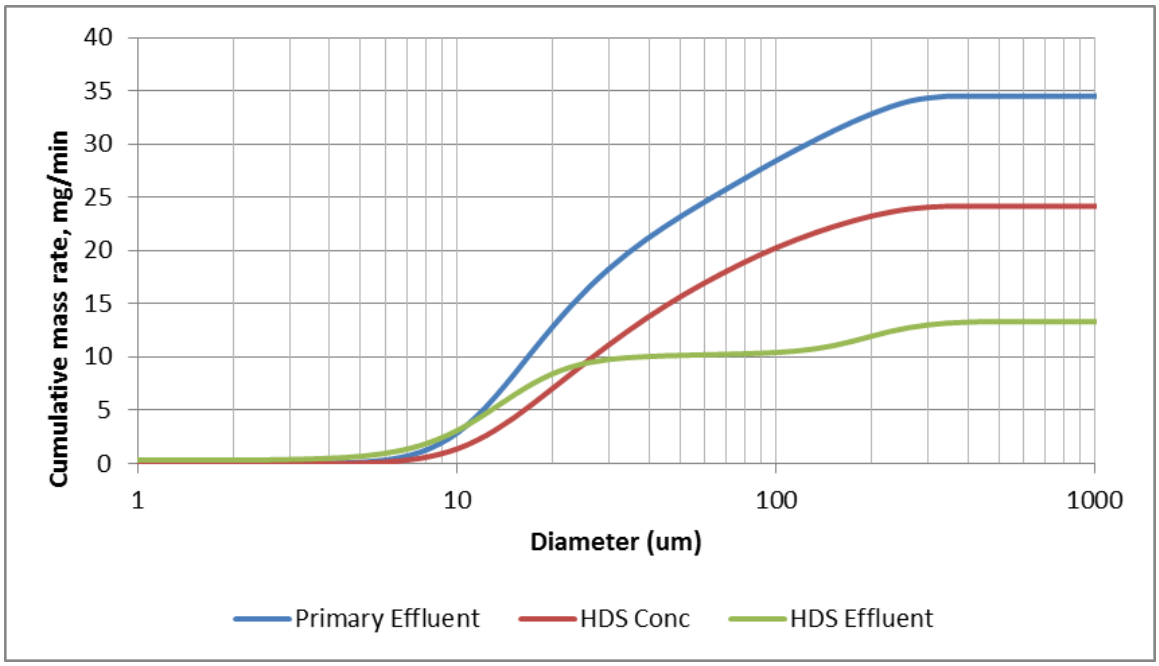

3.3 East Bay Municipal Utility District (EBMUD) Plant Results

The East Bay Municipal Utility District wastewater treatment plant is a 120 mgd pure oxygen plant with rectangular primary clarifiers. Like the SFPUC Southeast plant, it discharges to San Francisco Bay. The primary effluent sample collected on 11-13-13 for this experiment had a high concentration of solids, at 189 mg/L, and had moderate separability in a single HDS channel (56% - Table 8), despite the mode particle size (60 um) being significantly larger than the cutoff size (Figure 11). The PSD data for the three streams of each separation experiment (primary effluent (HDS influent), HDS effluent, and HDS concentrate) are presented as mass rates verses particle size (Figure 11, to show the magnitude of the particle size bins in relation to each other) and as cumulative mass rates verses particle size (Figure 12, to show the total mass rates as presented in Table 8). A micrograph of the primary effluent sample showing some solid particles is presented in Figure 10.

Table 8: Single Channel HE Results – Using Primary Effluent Collected from EBMUD, 11-13-13

EBMUD, 11-13-13	Flow rate (L/min)	Concentration (mg/L)	Mass rate(mg/min)
Primary Effluent (HDS Influent)	0.250	189	47
HDS Effluent	0.183	86	16
HDS Concentrate	0.068	390	26
(effluent mass+concentrate mass)/influent mass		Mass balance	90%
Concentrate mass/influent mass		Harvest Efficiency	56%

Figure 10: Micrograph of Primary Effluent Collected from EBMUD, 11-13-13

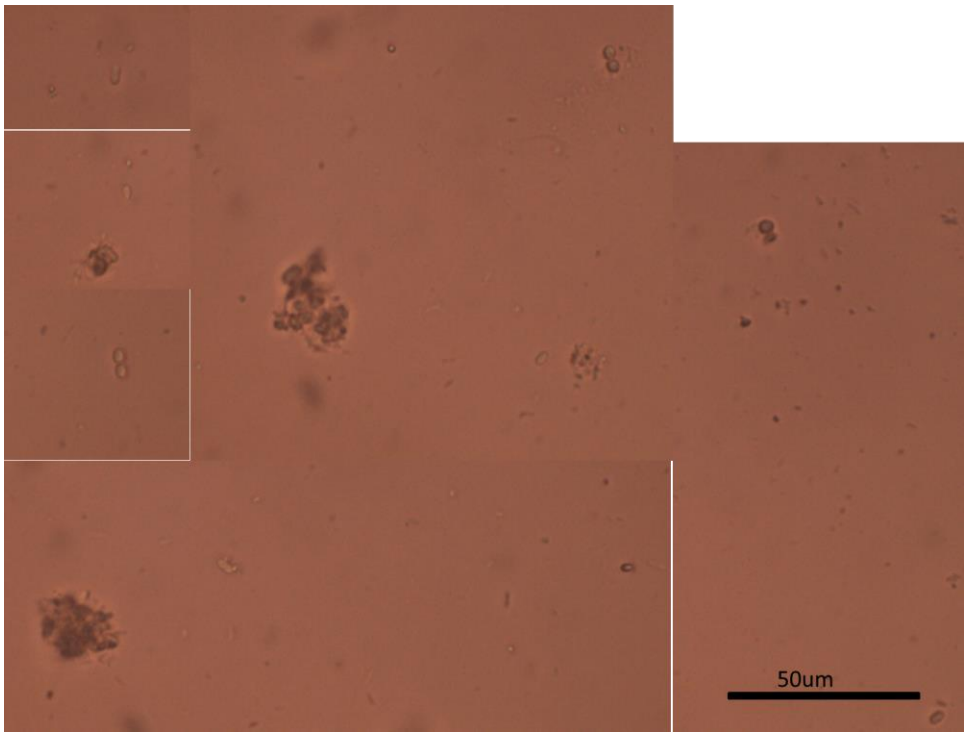

Figure 11: Mass Rate PSD for HDS Separation Test Using EBMUD Primary Effluent Collected on 11-13-13

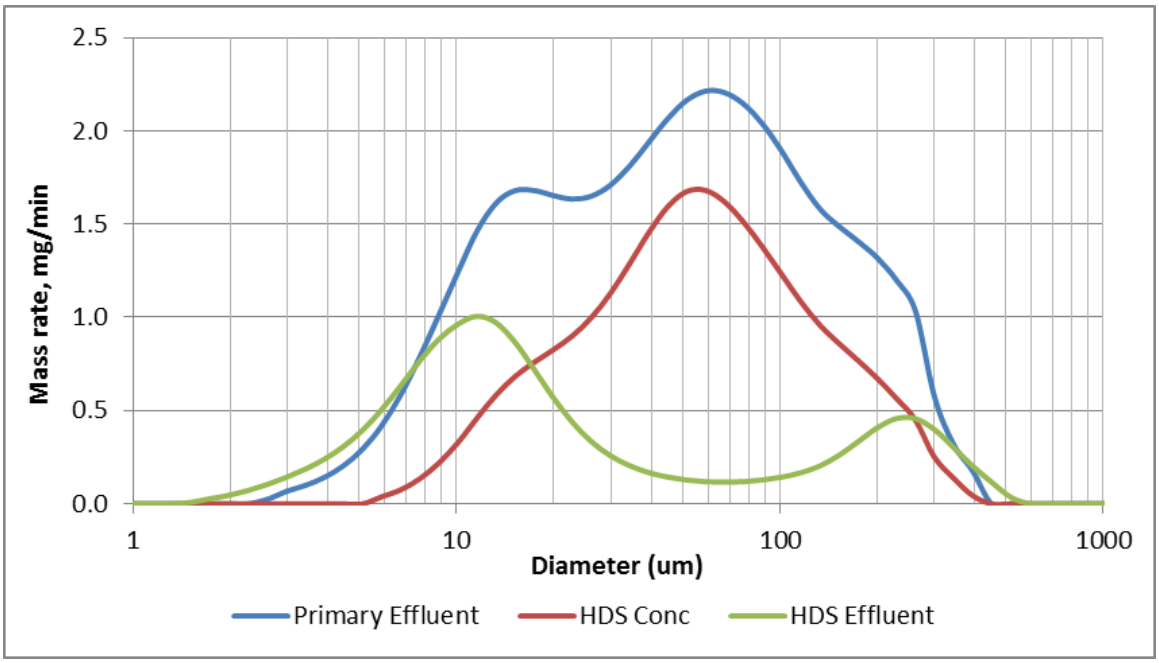

Figure 12: Cumulative Mass Rate PSD for HDS Separation Test Using EBMUD Primary Effluent Collected on 11-13-13

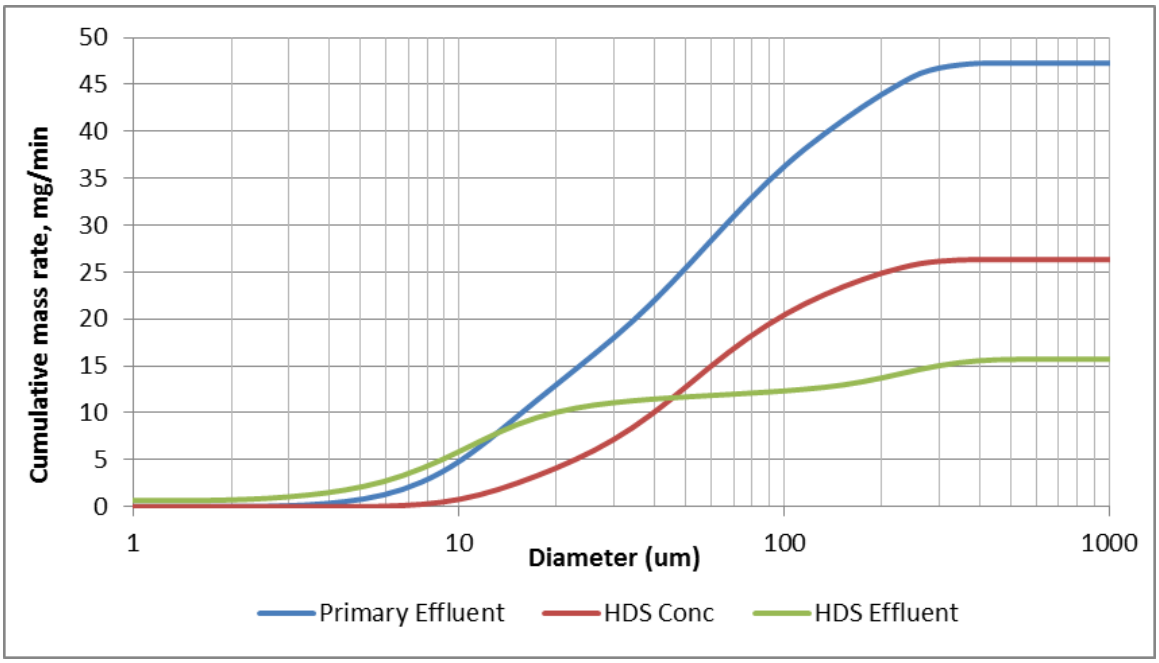

3.4 Sunnyvale Water Pollution Control Plant Results

The Sunnyvale plant is a 30 mgd plant that relies heavily on waste stabilization ponds, a rarity for both this location, the highly urban San Francisco bay area, and size, 440 acres. The primary clarifiers are rectangular, and perform exceptionally well, with the lowest concentrations of all three plants evaluated. Samples were collected for analysis from the primary effluent channel on 11-21, 11-26, and 11-27, and the results of the separation tests are presented herein. The primary effluent from Sunnyvale ranged from 45 to 93 mg/L. The mode of the primary effluent samples taken from Sunnyvale were all less than 20um, and therefore below the cutoff size of the channel design. The harvest efficiencies ranged from 53% to 62%. The PSD data for the three streams of each separation experiment (HDS influent, HDS effluent, and HDS concentrate) are presented as mass rates verses particle size (Figures 14, 17 and 19, to show the magnitude of the particle size bins in relation to each other) and as cumulative mass rates verses particle size (Figures 15, 18, and 20, to show the total mass rates as presented in Tables 9, 10, and 11, respectively).

Table 9: Single Channel HE Results – Using Primary Effluent Collected from Sunnyvale, 11-21-13

Sunnyvale, 11-21-13	**Flow rate (L/min)**	**Concentration (mg/L)**	**Mass rate(mg/min)**
Primary Effluent (HDS Influent)	0.250	77	19
HDS Effluent	0.183	44	8
HDS Concentrate	0.068	152	10
(effluent mass+concentrate mass)/influent mass		Mass balance	95%
Concentrate mass/influent mass		Harvest Efficiency	53%

Figure 13: Primary Effluent (left), HDS Effluent (middle), and HDS Concentrate (right) for HDS Separation Test Using Sunnyvale Primary Effluent Collected on 11-21-13

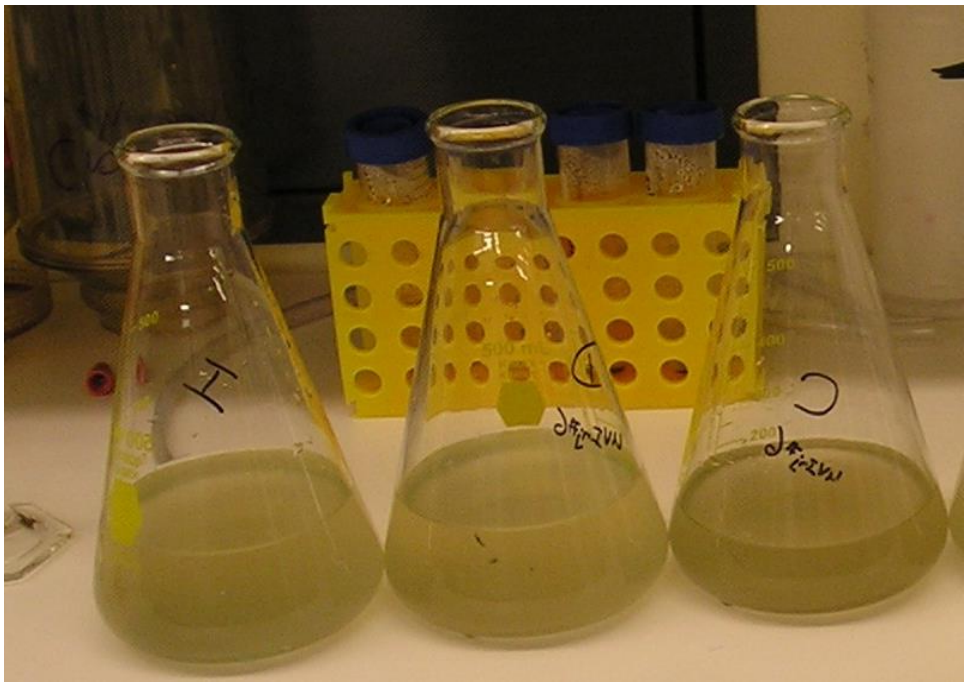

Figure 14: Mass Rate PSD for HDS Separation Test Using Sunnyvale Primary Effluent Collected on 11-21-13

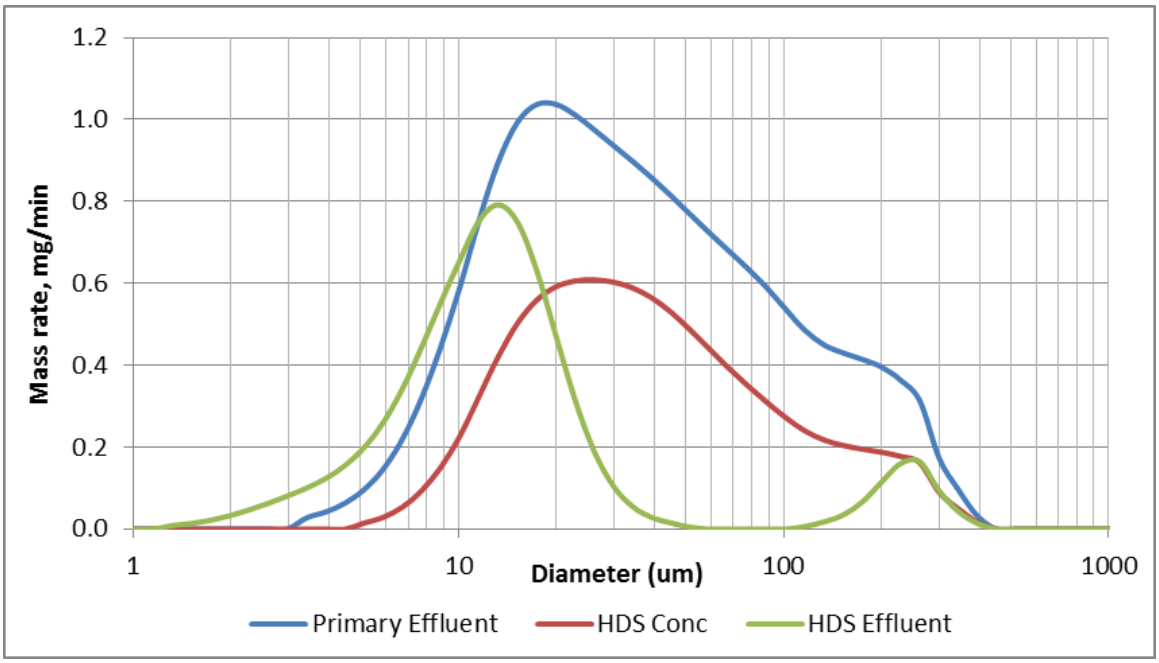

Figure 15: Cumulative Mass Rate PSD for HDS Separation Test Using Sunnyvale Primary Effluent Collected on 11-21-13

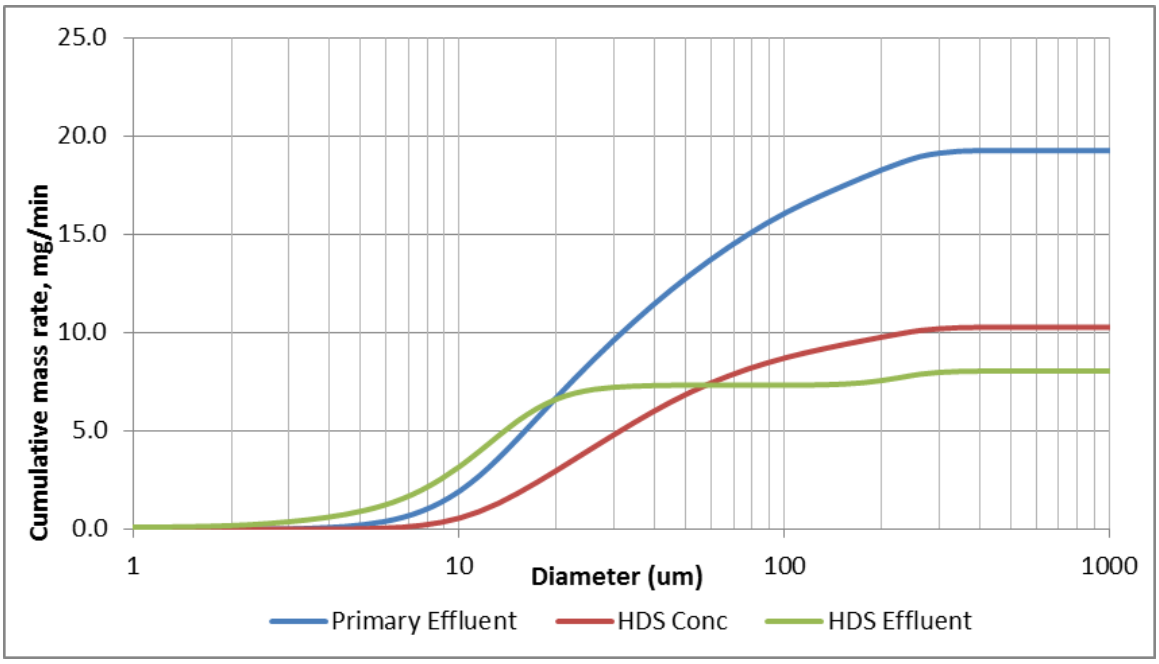

Table 10: Single Channel HE Results – Using Primary Effluent Collected from Sunnyvale, 11-26-13

Sunnyvale, 11-26-13	**Flow rate (L/min)**	**Concentration (mg/L)**	**Mass rate(mg/min)**
Primary Effluent (HDS Influent)	0.250	93	23
HDS Effluent	0.183	54	10
HDS Concentrate	0.068	212	14
(effluent mass+concentrate mass)/influent mass		Mass balance	104%
Concentrate mass/influent mass		Harvest Efficiency	62%

Figure 16: Micrograph of Primary Effluent Collected from Sunnyvale on 11-26-13

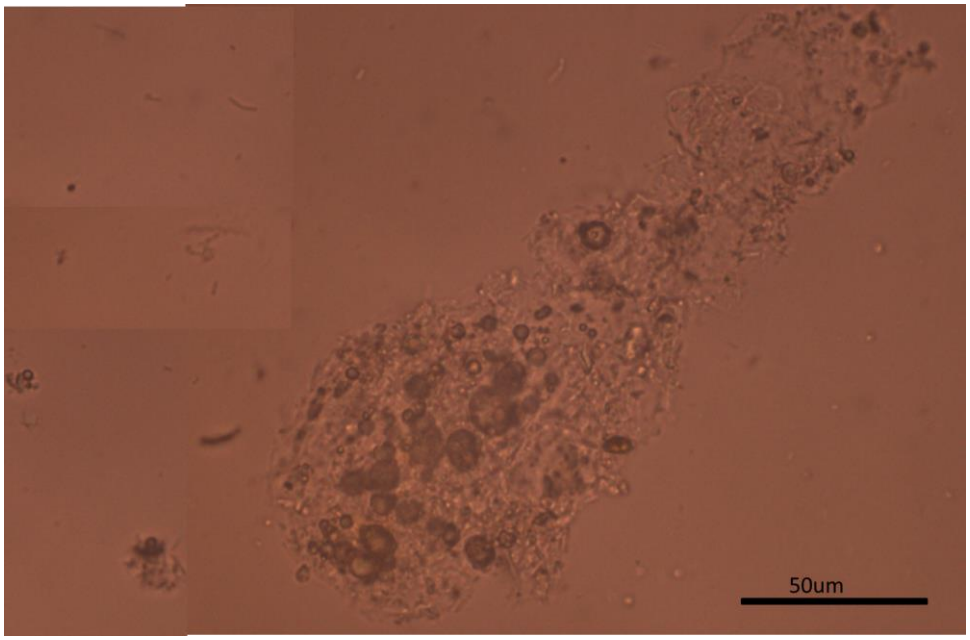

Figure 17: Mass Rate PSD for HDS Separation Test Using Sunnyvale Primary Effluent Collected on 11-26-13

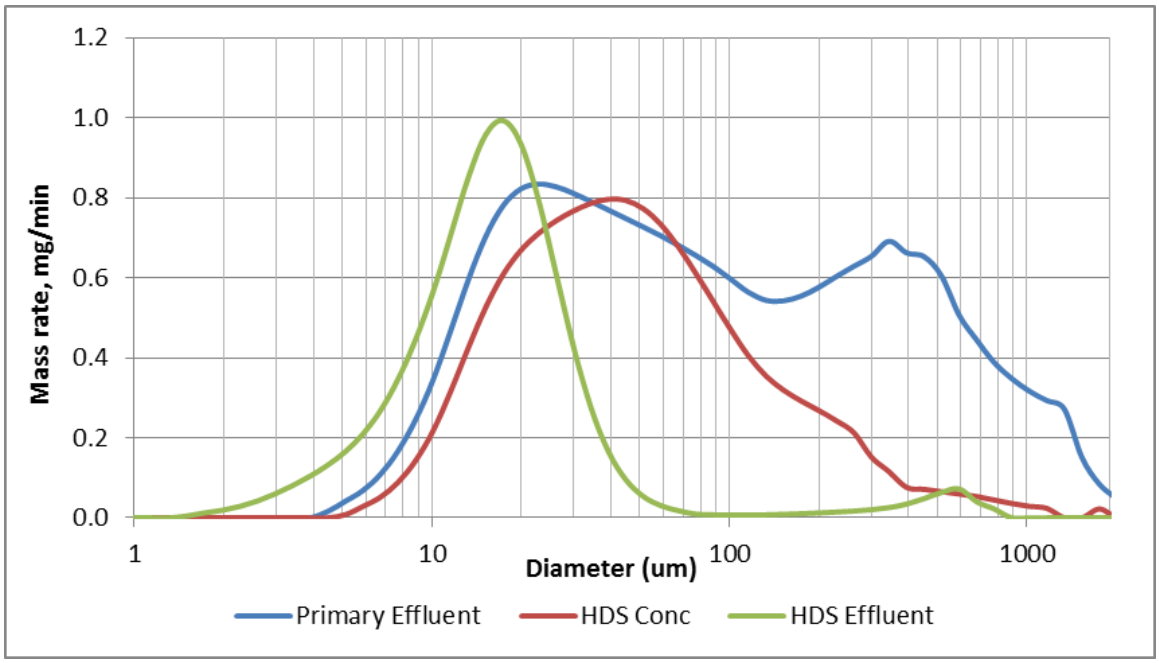

Figure 18: Cumulative Mass Rate PSD for HDS Separation Test Using Sunnyvale Primary Effluent Collected on 11-26-13

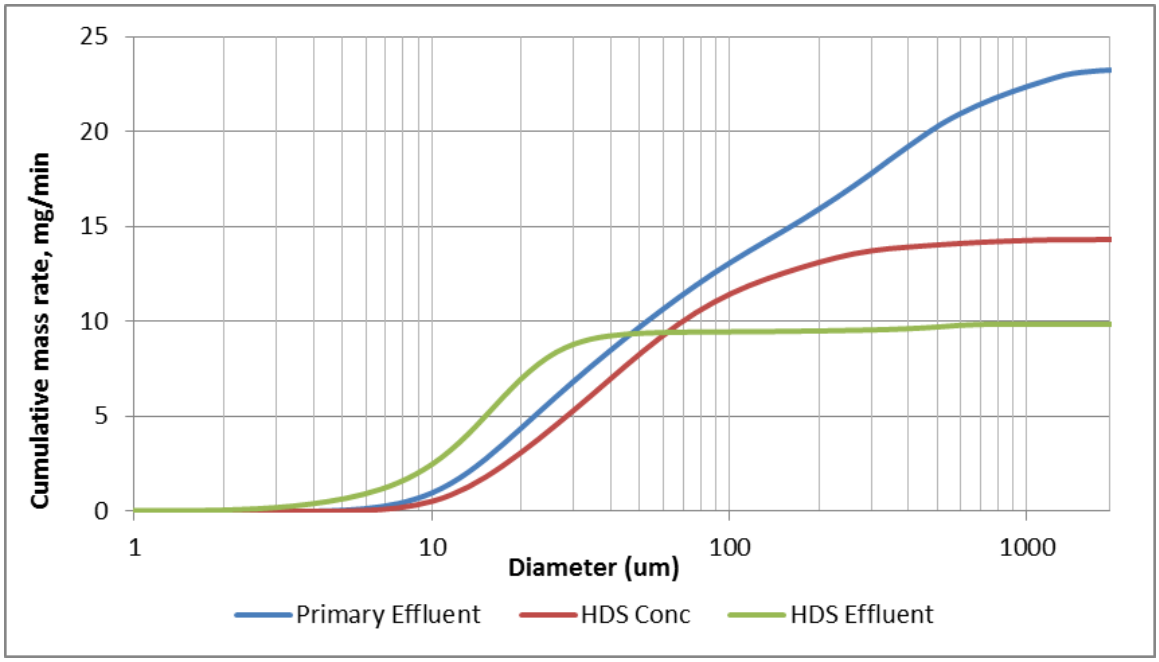

Table 11: Single Channel HE Results – Using Primary Effluent Collected from Sunnyvale, 11-27-13

Sunnyvale, 11-27-13	Flow rate (L/min)	Concentration (mg/L)	Mass rate(mg/min)
Primary Effluent (HDS Influent)	0.250	45	11
HDS Effluent	0.183	19	3
HDS Concentrate	0.068	100	7
(effluent mass+concentrate mass)/influent mass		Mass balance	91%
Concentrate mass/influent mass		Harvest Efficiency	60%

Figure 5: Primary Effluent (left), HDS Effluent (middle), and HDS Concentrate (right) for HDS Separation Test Using Sunnyvale Primary Effluent Collected on 11-27-13

Figure 19: Mass Rate PSD for HDS Separation Test Using Sunnyvale Primary Effluent Collected on 11-26-13

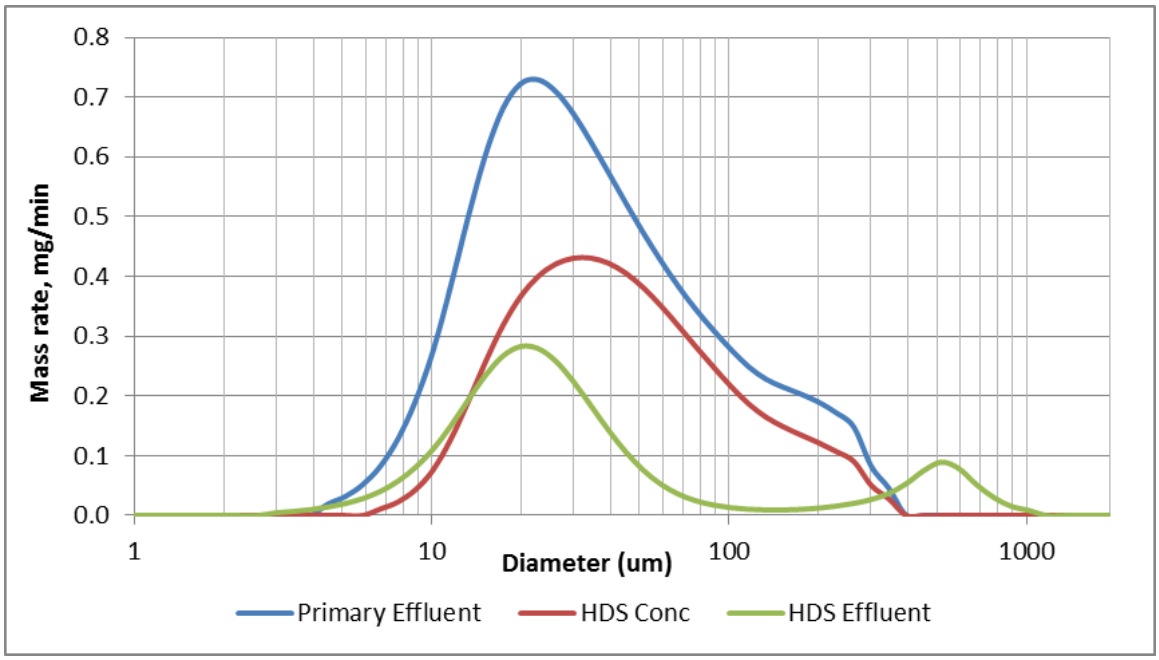

Figure 20: Cumulative Mass Rate PSD for HDS Separation Test Using Sunnyvale Primary Effluent Collected on 11-26-13

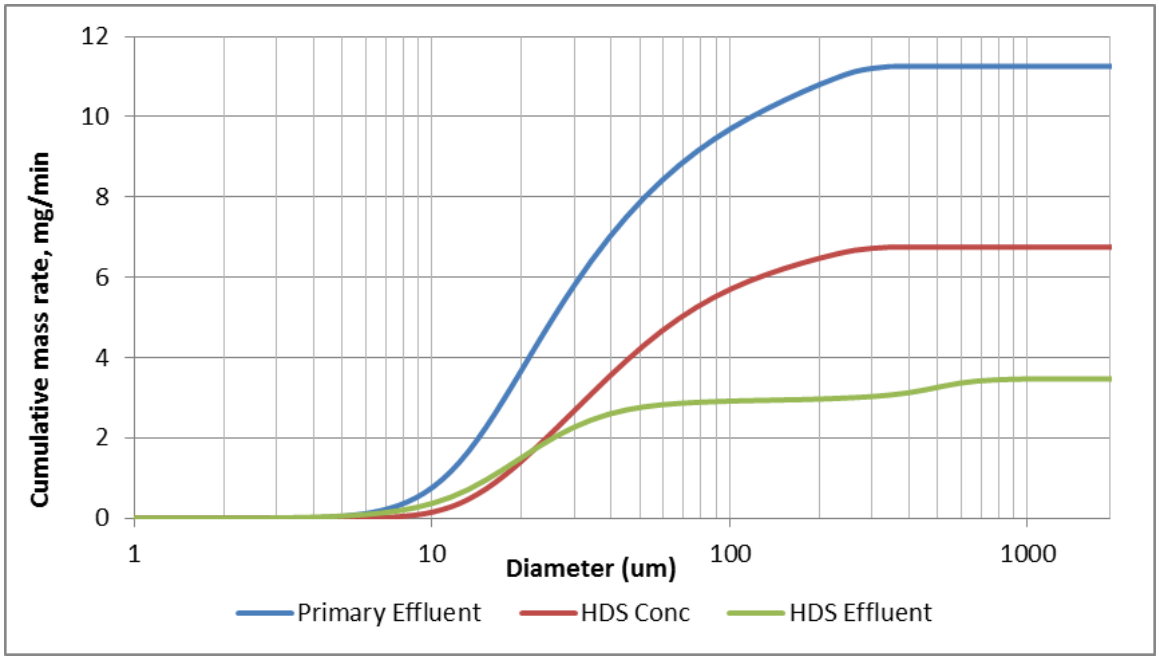

CHAPTER 4:
HDS Manufacturing

4.1 Pre-Fabrication Considerations

To scale the HDS technology to process tens of thousands to millions of gallons per day to create a functional product that can accomplish the project objectives, it is important to consider the channel design, the channel fabrication criteria, and the system fabrication criteria. These are presented below.

4.1.1 HDS Channel Design

PARC's hydrodynamic separation technology is based on the interaction of particles and hydrodynamic forces within a curved channel. The design of the channel geometry and the flow split will depend on the application and the quality and size of the particles to be separated. The fundamental physics and computational fluid dynamic (CFD) modeling procedures employed to fine-tune HDS channel designs for specific particle sizes and applications could easily comprise an entire report. Examples of CFD output include plots of the pressure and the flow field in a cross section of an HDS channel (Figure 21). What is important to understand is that there are many influencing variables that can be carefully adjusted to allow for the formation of vortices that separate solids of the intended size. Changes to one variable will change other variables, or change the size of the particle that can be separated. The intent of the PIER study is to capture particles from primary effluent in the range of 20-400 um. PARC's half-turn "particle separator" design (the specifics of which are presented in Table 1) was determined to be suitable for this application based on initial experiments done with primary effluent samples in PARC's lab.

Figure 21: Example of CFD Model Results for a Cross Section of an HDS Channel- Flow Fields (top); Pressure Fields (bottom)

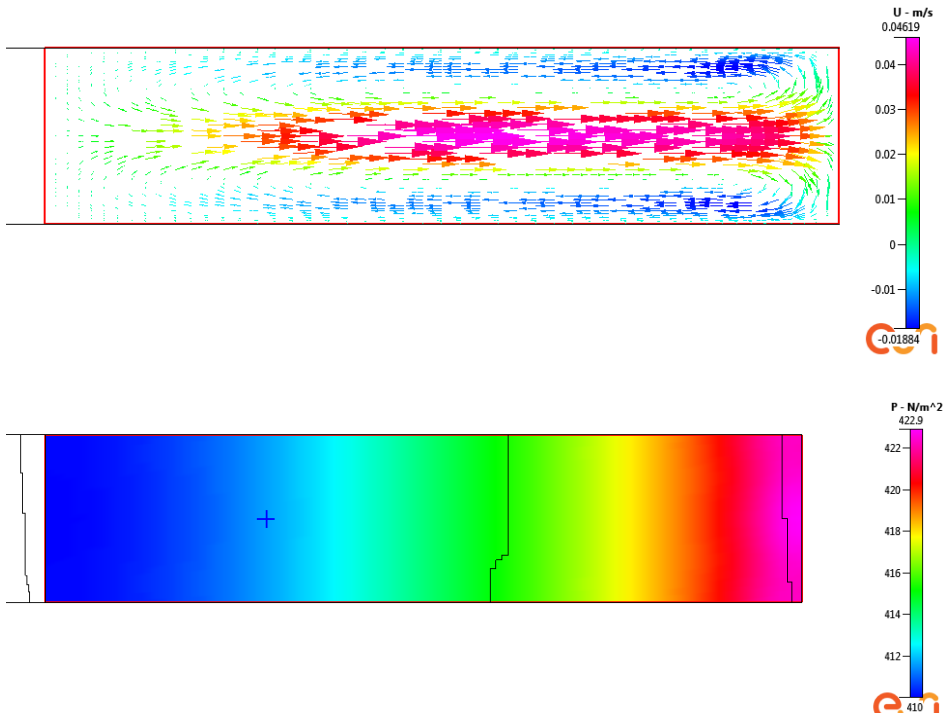

The channel through which fluid and particles flow and where separation can occur is simply a void in space – the materials and assembly methods only needs to be such that specific geometric and surface finish criteria are met. The application will determine how the channels will be best designed, fabricated, and assembled to accomplish the desired objective. This chapter presents HDS channel fabrication criteria and HDS system criteria used as the basis of design for the PIER project. This chapter also presents the options considered for fabrication and assembly, as well as the chosen fabrication method of stacking injection-molded layers that could be robotically glued and cured with UV sensitive adhesive.

4.1.2 HDS Channel Fabrication Criteria

PARC has spent the last 7 years custom fabricating and assembling HDS channels to test the various designs. Until now, mostly single channels for testing of designs and applications have been fabricated by hand in PARC's in-house shop. The authors have used layers of laser-printed acrylic and polycarbonate sheets, which are glued together with solvent glues (Weld-on #4, carbon tetra furan). Computer-Aided Design (CAD) files are edited based on design changes for different needs, and a laser printer reads the file and prints the desired shape on a sheet of appropriate thickness. Such articles typically last no more than a few weeks to a few months, and are extremely difficult to assemble in stacks. Threaded taps (1/4 - 20 NPT) are glued to the exits to accommodate nylon hose-barb fittings to connect to small diameter tubes for influent, effluent, and concentrate flows. Figure 22 shows some of the steps involved in making hand-assembled channels.

Figure 22: Laser Printer (left); Printing Acrylic Top Layer (middle); Gluing Middle and Top Layer of HDS Channel (right)

The intent of the PIER study is to demonstrate scalability, which is not possible with PARC's custom method of fabrication. Listed below are fabrication criteria for mass produced HDS channels.

4.1.2.1 Interior Channel Surfaces

The interior channel surfaces must be very smooth, and there can be no glue or material hanging into the channel. Laminar flow is needed for the establishment of vortices that set up inside the channel and cause the particle separation. Rough surfaces will cause turbulence, disrupt the vortices, and affect solids separation. This is particularly true for the top and bottom surfaces, less so for the side walls. In addition, the top and bottom channel walls have to be parallel to each other, as any wedge-shaped cross-section geometry changes the flow patterns and reduces separation efficiency.

4.1.2.2 Channel Height

More than any other dimension, maintaining a uniform and exact channel height is critical. The tolerance on the channel height can be no more than +/- 5 %. With the particle separator used for this project having a channel height of 400 um, that results in a tolerance of +/- 20um. When gluing or gasketing layers together, any resulting thickness must be accounted for such that the top of a particle separator channel is not more than 420 um (ideally 400 um for this channel design) from the bottom of the inside of the channel.

4.1.2.3 Channel Width

The channel width is less critical than the channel height, but should be within +/- 10 percent of the intended width. For this project, the channel width was 6 mm.

4.1.2.4 Pressure Requirement

A completed article must withstand at least 5 times the operating pressure at room temperature and not leak, either externally or internally. The research team designed the channels for 5 times the operating pressure, which was an arbitrary number and rigorous failure testing may be helpful in refining this value. For a 400 um high half-turn channel that has a design operating pressure of 12 psi, that equates to a maximum pressure of about 60 psi.

4.1.2.5 Exit Sealing

More than any other area, the sealing/water tightness between the exit channels is also critical. Flow migrating "across" a poorly sealed split will affect not only the flow split, but the particle separation as well.

4.1.2.6 Splitter Tip

Depending on the application, the tip of the flow splitter either can be a sharp tip or rounded. In both cases, the walls in the splitter region have to be vertically well defined and free of burrs or anything that might catch particles and facilitate a build-up of solids.

4.1.2.7 Flow Split Geometry

HDS channels are designed to have a specific flow split, for example, 80:20, 50:50, and so forth, depending on the objective of the application. The geometry of the exit channels, that is, channel width, length, and curvature, is optimized through CFD simulations to correspond to a selected flow split when connected to ambient pressure as part of the channel design. Examples of different exit channel designs are shown in Figure 23. The flow split intended for this project was 80:20, but, for reasons explained later, was ultimately 73:27.

Figure 23: Two Different Exit Channel Designs

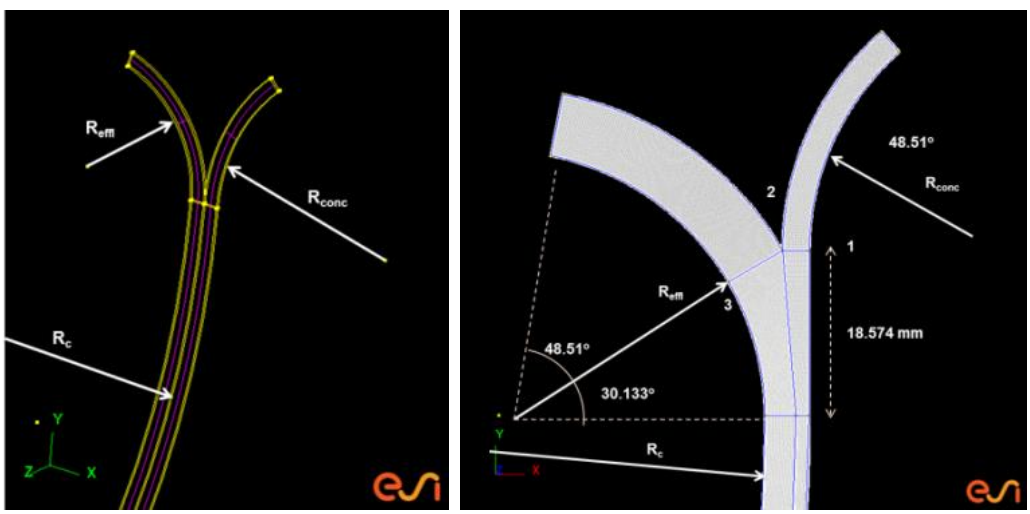

4.1.3 HDS system Fabrication Criteria

While establishing a specific particle size range to be removed is important when designing a single HDS channel, the specific application is just as important when considering how multiple channels will be integrated together to process higher flow rates. A *"stack"* is the term used herein to describe a module of multiple channels operated in parallel and connected to a common source.

4.1.3.1 Throughput

The quantity of flow to be processed per stack of HDS channels influences the design of the stack inlet and exits. For this project, the researchers had four stacks with throughput flow rates

of – 36 lpm, 6.75 lpm, 1.25 lpm, and 0.25 lpm (corresponding to 144, 27, 5, and 1 channel stacks). The capacity of each downstream stack is dependent on the flow split criteria defined above.

4.1.3.2 Means of Fluidic Connection Between Channels

The common inlet to and common exits from a stack of channels is called a manifold, and can be a pipe or a channel with a free surface. The size of the manifolds affects the velocity of the flow within them and ultimately the pressure, thus affecting the head losses of the system. All the channels in a stack share the same inlet and outlet manifolds, which have to be engineered to carry the necessary flow without adding substantial hydraulic losses that would impact separation.

4.1.3.3 Means of Fluidic Connections Between Stacks

The fluidic elements integrated into an HDS system downstream of a stack of HDS channels will introduce headlosses that can affect the backpressure on the exit manifolds and therefore affect the flow split. Pipes, elbows, flow meters, and so forth contribute to head loss. One way to make an HDS system function more independently of the system is to integrate active flow split controls with flow meters and flow control valves. A second way is to design these downstream fluidic elements such that the head losses downstream of the two exits are equal. As will be explained in later chapters, this was one criterion not adequately considered at the beginning of this project.

4.1.3.4 Particle Concentration

Hydrodynamic separation requires hydrodynamic forces to move the particles into a band and keep them there. Increasing the particle concentration will increase the resulting band width and, if high enough, will ultimately hinder the band formation altogether. For solid and weakly interacting particles, the researchers have successfully demonstrated separation of source waters with up to about 7000 parts per million (ppm) solids loading. They have not defined an upper limit. For fluffy and/or strongly interacting particles, the maximum concentration may be as small as a few 100 to 1000 ppm solids loading in the source water. Very high concentrations may require different splits – for example, 100 mg/L input may separate ideally with an 80:20 (effluent:concentrate) split, whereas a 10,000 mg/L input may require a 50:50 split, and a 20,000 mg/L input may require a 20:80 (effluent:concentrate) split.

4.1.4 CFD modeling of Stacked Channels

An important parameter when considering HDS scale up is the impact of manifold design on flow rate and flow distribution. For this, CFD simulations were performed in early 2013 comparing channel stacking to electric circuits to determine the effects of such resistance. Using analytical arguments and simple calculations, as well as the CFD results, the authors have concluded that the inlet and outlet manifolds will not have a noticeable effect on the flow distribution when stacking thousands of channels as long as the outlet ports are sized accordingly, because the manifold resistances are much lower than the channel resistance (Figure 24). Therefore, the first-generation stacks of channels had 25.4 millimeter (mm) exit outlets, which were enlarged to 38.1 mm exits for the second-generation stacks.

Figure 24: Circuit Approximations (left), CFD Modeling (right) of Channel Stacks

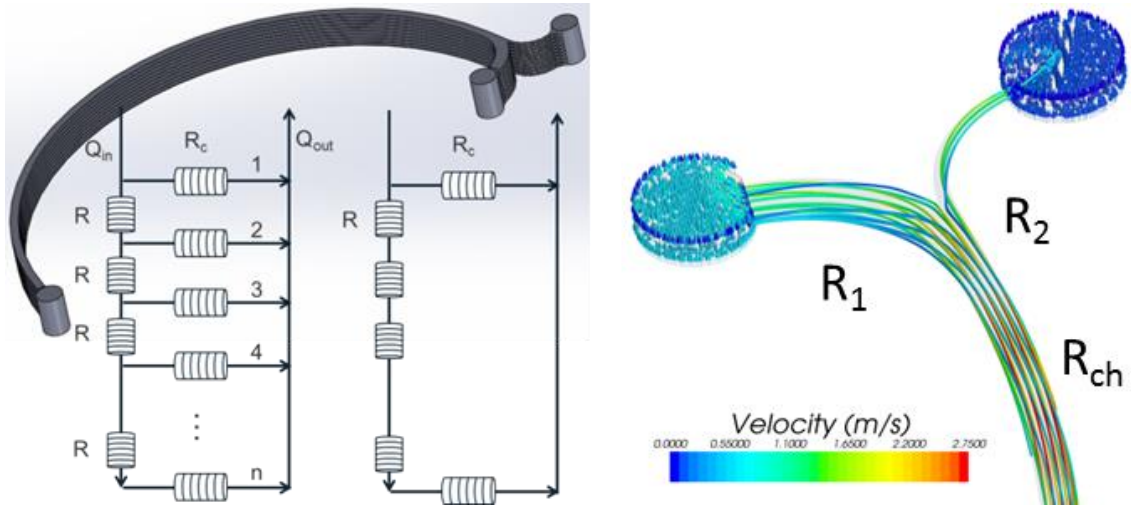

4.2 Channel Fabrication Options

There are many possible ways that channels can be made, as long as the specifications for both HDS channels and HDS systems, as described above, are met. The research team considered two of the more promising methods to make stacks of HDS channels, an extruded method and injection molded method, both using plastics (such as acrylonitrile butadiene styrene ABS, polymethyl methacrylate, and poly vinyl chloride), discussed in detail below.

4.2.1 Extruded Plastic Channels

This method of fabrication involves extruding plastic through a die to create a straight channel, and then bending the straight channel to a desired radius of curvature. The curved channel then needs to be attached to the inlet and exit manifolds to create a functional HDS channel. The researchers worked with GenPlex Custom Plastic Extrusions in September of 2012. They developed a tool and process to make custom curved extruded channels that met specifications for HDS applications. This fabrication method was not continued beyond the prototype single channels shown in Figure 25, primarily due to the challenges and difficulty in assembly of large stacks of channels.

Figure 25: Extruded plastic channel components, left to right, top to bottom: channel cross section; full turn channel; 3D printed manifold fittings; glued manifold; gasketed, compression manifold; extruded manifold concept; integrated extruded channels and extruded manifold concept

4.2.2 Injection Molded Channels

Injection molding is the process by which melted plastic is injected into a cavity that is a void that resembles the desired part. The process requires a custom milled "tool" that comprises of a two-part mold typically machined out of stainless steel, a means of delivering melted plastic to the mold through "gates", and ejector pins that push the part out of the mold. Injection molding typically requires a significant initial investment for the manufacturing of a tool that is specific to a single design. Gate placement, plastic material flow rates and injection pressures, heating and cooling cycle times and temperatures, and ejector pin placement are all dependent on the material properties of the plastics being used. These important parameters need to be considered for successful part production to meet design criteria. Our design consisted of a single part or layer that had a male and a female side, so that a single part could be stacked to create multiple HDS channels between each of these identical parts, facilitating scaling to many channels in parallel. Three sides of the channel itself are formed on one face of each layer, which are completed with stacking by the back face of the next layer. The inlet and outlets of the channel were designed in such a way that a tubular manifold formed as stacks of parts were assembled to create multiple parallel channels. The channels are thus integrally manifolded together at the ends with 25.4 mm first-generation/38.1 mm second-generation inlets and outlets. A stack of n channels would therefore consist of $n+1$ layers.

The research team worked with REVA of Carlsbad, California to manufacture appropriate tools and injected molded parts of ABS plastic, beginning in February 2013, with an assembly method that consisted of the gluing approach using a tongue-and-groove configuration, according to the specifications of their sister company, Forcast 3D. Forcast 3D specializes in assembly, and claimed to have a reliable gluing assembly process.

When their approach was unsuccessful, the researchers were forced to consider alternative assembly methods, of which there are many. Each assembly method, as they learned and will discuss in the following section, requires a specific joint detail to be incorporated into the part design. While the researchers were eventually able to glue the parts together thanks to the expertise of Cascade Designs, Inc. (CDI) of Seattle, Washington (as will be discussed in the following section summarizing assembly methods), there were still unavoidable problems with the final produced stacks that lead to the second-generation design specifically considered gluing for assembly. Other problems with the first-generation design warranted a second effort. Following the assembly methods, a discussion presents these issues and the efforts made to correct them. Figure 26 shows the two different part designs, as well as the final produced parts. It should be noted that the second-generation part is one half the first-generation layer height and one third the first-generation layer volume.

Figure 26: Molded part design first-generation part (left); molded part design, second-generation part (middle); actual molded parts – first generation (right, bottom); second-generation (right, top).

4.3 Stack Assembly Options

There are a number of different options for assembling injection-molded parts. Herein are descriptions of assembly options for injection-molded layers that have HDS channels integrated into them. Feasible assembly options include hot plate welding, compression gasketing, electromagnetic welding, ultrasonic welding, and UV gluing and curing.

4.3.1 Hot Plate Welding

Hot plate, as the name describes, is a process which uses a Teflon-coated heating platen that comes in contact with opposing plastic parts to be joined (Figure 27, top). Heat is applied to the platen which then softens the plastic. When the correct temperature is reached in the plastics, the platen is withdrawn and the two components are pressed together. They are held in position for a few seconds to let the polymer combine and then release, forming a hermetic seal joining two layers of injection molded HDS parts. Both Silvey Plastics Consulting and Branson Ultrasonics Corporation believed this was a feasible assembly solution. Branson recommended a cross section that included a butt joint and flash trap design (Figure 27, bottom) that would be the mating surface for hot plate welding. The flash trap would capture excess melted material so as not to impact the height of the HDS channel. Injection molded parts would need to be custom designed for this assembly approach. An indexing table or platform integrated with the hot plate tool would be required for production of stacks of multiple channels.

Figure 27: Hot Plate Tooling Method (top), Different Joint Types (bottom)

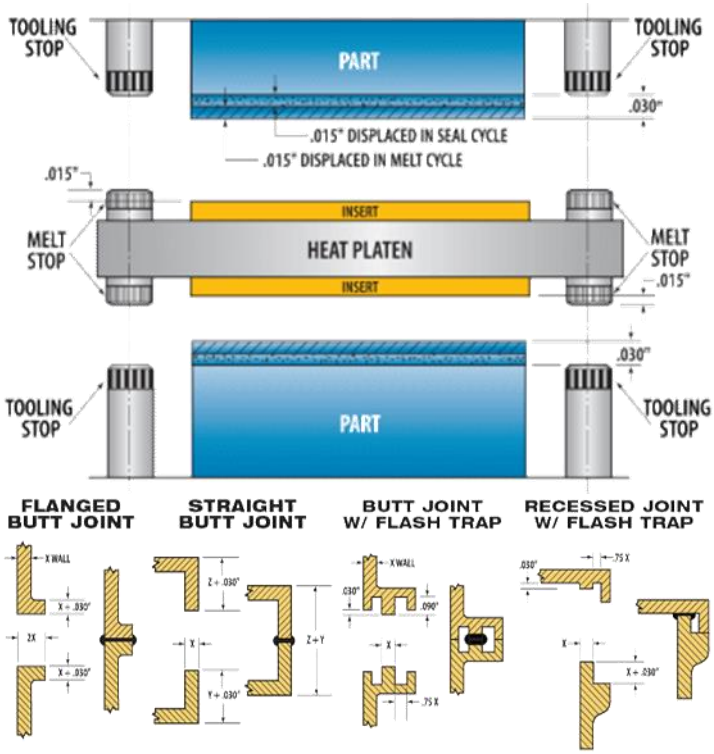

Source: forwardtech.com.

4.3.2 Electromagnetic Welding

A proprietary process by Emmabond (Norwood, New Jersey) uses strips of electromagnetic material placed along a bond line or joint that, upon application of high-frequency induction energy and heat, fuses the three components (two parts and the electromagnetic material) together. The process is shown in Figure 28 (left). The researchers had samples of first-generation injection molded HDS layers successfully bonded with this method, below, right, in August 2013. They suggest seven different joint-detail types that work well with the Emmabond process.

Figure 28: Emmabond Process (left); Electromagnetically Welded HDS Part Sample (right)

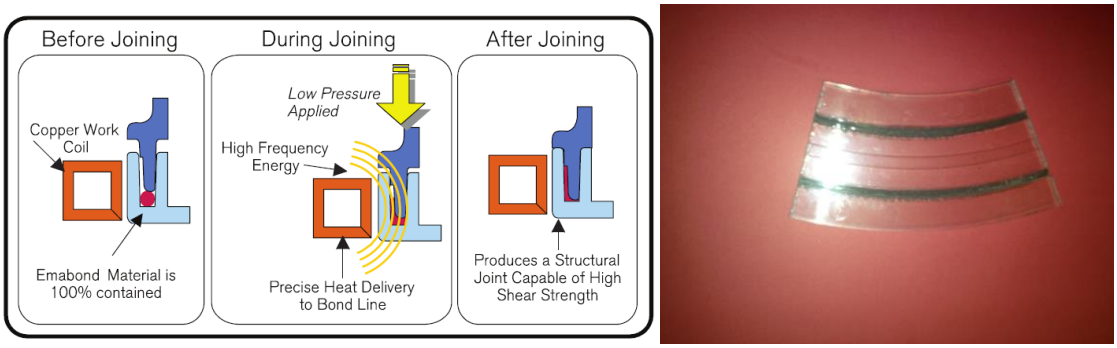

4.3.3 Compression Gasketing

This assembly method involves inserting a gasket within a groove of an injection molded part, and bolting the layers together sandwiched between two plates to create a seal. Our partners in China had success assembling large stacks of HDS layers to create channels that did not leak by February 2014; successful particle separation was not achieved for other reasons. Namely, the variation in part thickness and part warping of the first-generation parts caused the stacks to lean with increasing stack height, and a poor pairing of channel design with the intended application and particle size distribution. Their manual assembly method was labor intensive. Injection molded parts would best be custom designed for compression gasketing assembly.

Figure 29: Single HDS Part with Gasket (left); 1 mgd Assembled Unit (right)

4.3.4 Ultrasonic Welding

A manufacturing consultant (Silvey's Plastic Consulting) and an ultrasonic welding tool manufacturer (Branson Ultrasonics Corporation) evaluated this method. Silvey did not think ultrasonic welding was suitable, as he did not believe a single horn (the tool that applies the energy to the part) or the machine was big enough to accommodate our parts, and was concerned the joint between multiple horns would provide poor sealing that may result in leaks. Branson recommended that multiple actuators/heads, as many as four complete systems, would be needed to weld the entire part simultaneously. They also indicated multiple horns with flat-face details would be needed, using a tongue and groove joint with a textured bottom groove surface with an energy director on the tongue. They did not indicate the joints between the horns would be problematic. The figure below shows a detail of the recommended energy director on the tongue and textured bottom groove. Injection molded parts would need to be custom designed for ultrasonic welding.

Figure 30: Recommended Injection Molding Detail for Ultrasonic Welding Assembly

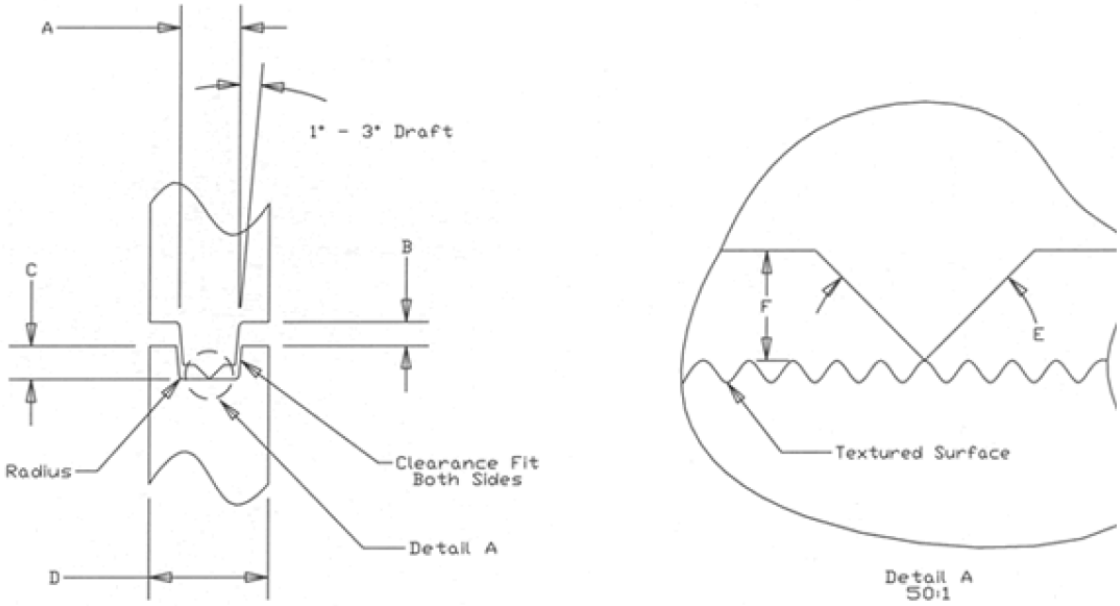

4.3.5 Ultra-Violet Gluing and Curing

Gluing is the process of applying a bead of adhesive between two mated surfaces and allowing the chemical process to join two parts together. For gluing injected molded HDS parts, ideally a specific joint detail is required that accommodates overflow of glue, called a "trap", so excess glue does not flow into the HDS channels of injection molded parts, and so the glue bond does not change the intended internal dimensions of the channel. As was mentioned in the section describing the injection molding process, the first-generation parts were not designed specifically for gluing. CDI, with their expertise in assembly and manufacturing, were able to devise a solution that allowed for the gluing of these non-ideal parts. They proposed using clear ABS plastic for the molded parts, and proposed using glue that was quickly cured in a matter of seconds when exposed to a high intensity UV light. While the additive manufacturing process required manually stacking parts one on top of the other, a programmable robot performed the gluing and curing process. By using a robotic gluing attachment (Figure 31, left) and a robotic UV light curing attachment (Figure 31, right) CDI was able to fabricate the stacks of HDS needed for the pilot. The process requires an indexing table that needed to be manually adjusted for each new part. The first-generation stack assembly method employed a weight to hold down the part being glued, seen in Figure 31 (right); the second-generation stack assembly method employed clamps integrated into the articulating table (Figure 32).

Figure 31: Robotically Gluing (left), and Curing (right) a First-Generation, 72-Channel HDS Stack

Figure 32: Improved HDS Assembly Table with Clamps Instead of Weights for Second-Generation Stack Assembly

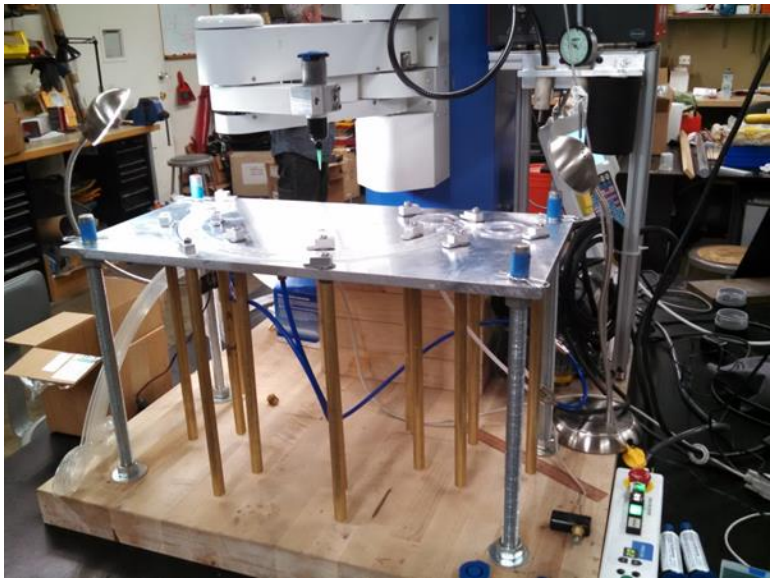

4.4 Final HDS Part Fabrication, Assembly Solution for PIER Project

As has been described above, our initial design and fabrication of injection molded ABS plastic layers resulted in flawed first-generation parts that did not lend themselves to easy assembly. Perseverance by CDI provided an assembly solution that resulted in channel stacks that had reasonable performance and did not leak. This first attempt at producing working stacks of HDS channels, despite its shortcomings, succeeded in offering insight into what could be done better.

Because of a combination of the first-generation part design the part thickness, resulting tool design, and the injection molding parameters (injection pressure, temperature, gate size and location, cooling time, and so forth) the parts would warp slightly as conic sections while curing. This warping resulted in deviations of the stack height along the channel that multiplied as more layers were added (for example, the 72 channel stack that was half of the 1st stage had a difference of 0.31" of stack height from the middle to the ends). The warping also made the gluing process increasingly difficult, as a planar surface was needed for the robotic application and curing steps. The warping is suspected to have affected the internal integrity of the channel height, although this was not quantitatively confirmed. The generic first-generation part design also necessitated a gluing solution resulting in a "glue gap" that increased the effective internal channel height. The channel height was measured by destructively cutting open glued channel stacks at one end and using feeler gauges along the channel length (23 measurements for each of the three single channel assemblies). This overall impact was an internal channel height that was, on average, nearly 20 percent greater than the intended channel height of 400 um.

After initial testing of the first-generation stacks in the lab and at the pilot (described in detail in Chapter 7) and a number of brainstorming and design sessions, CDI came up with a part design that addressed the warping issues and tailored the joint detail specifically for gluing. Given that they had already developed a familiarity with the gluing process, the researchers felt it was prudent to continue along this assembly path rather than to switch to a different assembly method such as hot plate welding.

The second-generation part design was begun in February 2014, and, notably, included input from all parties – the injection molding company (REVA), the company responsible for assembly (CDI), and PARC. This collaborative design effort built upon what was learned during the first-generation HDS manufacture, assembly, and testing process. Part of the re-design also included, critically and for the first time, rigorous numerical molding modeling to test and modify the second-generation part design as needed before a physical tool was fabricated, saving time, money, and reducing uncertainty. Molding modeling was subcontracted to Hawkridge Systems of Mountain View, California by CDI. They performed a baseline simulation of the existing first-generation part to test the validity of the model, and performed four simulation runs of the molding process, with each including some design and molding parameter modifications to improve the predicted warpage. These included changes to part thickness, injection pressure, and gate placement. The best run resulted in a part that had less than 10 percent of the warpage in the first generation-parts, while also providing a part half the height and one third the volume of the first generation-part. Figure 33 presents a screenshot of the molding modeling results showing the projected deformation of the second-generation part.

Figure 33: Second-Generation HDS Part, Molding Modeling Results - Warp in Z, New Design, Run 3, 0.088" Thick, Four Gates, Warp in Z, 235 °C Melt Temperature, 60 °C Mold Temperature, 3X Deformation Scale

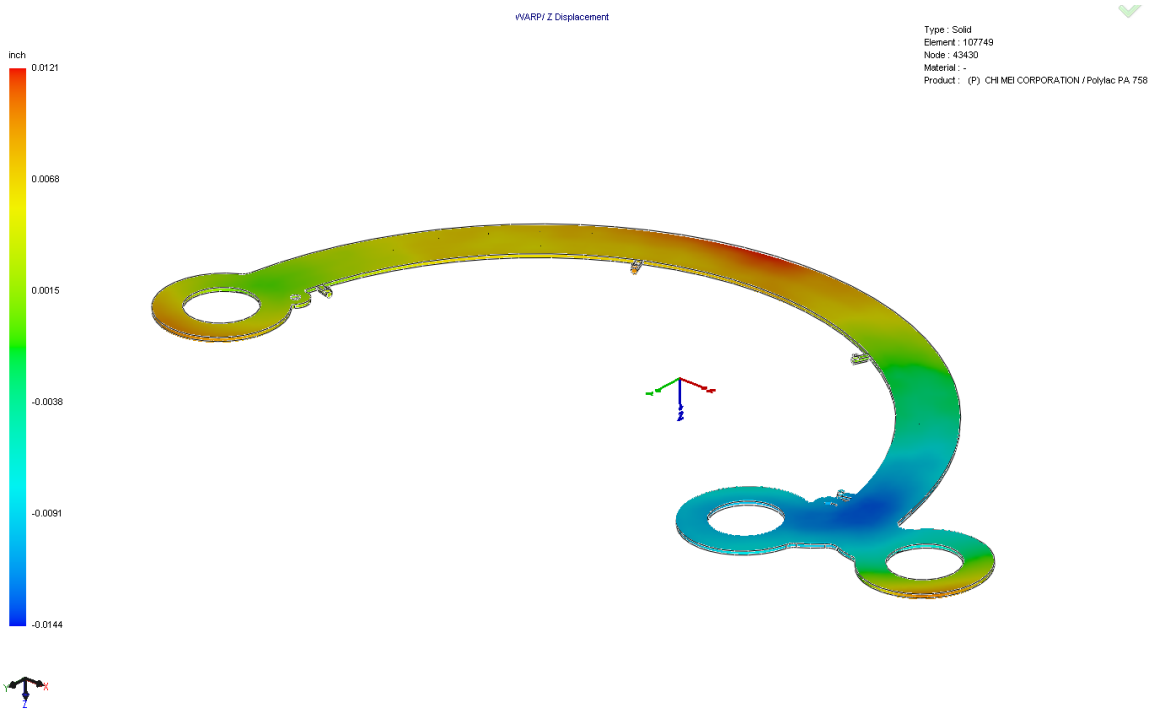

CHAPTER 5:
Pilot Unit Design, Testing and Operation, and Installation

This chapter consists of descriptions of the design process of the pilot unit fabricated by Intuitech, Inc., steps taken to evaluate its performance in preparation for operating the pilot unit, and installation of the pilot unit on site at the Water Pollution Control Plant (WPCP) in Sunnyvale, California. Given the schedule and lead-time requirements for both the fabrication of HDS stacks and a pilot unit, the research team pursued both efforts in parallel.

5.1 Pilot Unit Design

An initial design meeting between consulting engineering firm CDM Smith, a fabrication firm, Intuitech, Inc., that specializes in building pilot units for the water, wastewater, and chemical processing industries, and PARC staff at PARC"s facility in Palo Alto was held in September 2012. After discussing functional requirements for HDS, needs and objectives of the study, practical implications in the field, and limitations imposed by pilot system designs, the team began to develop concepts of what the pilot unit would eventually consist of. Figure 34 shows an early iteration of the pilot piping and instrumentation diagram (P&ID).

Figure 34: Early (November 2012) P&ID Schematic of Proposed HDS Pilot System

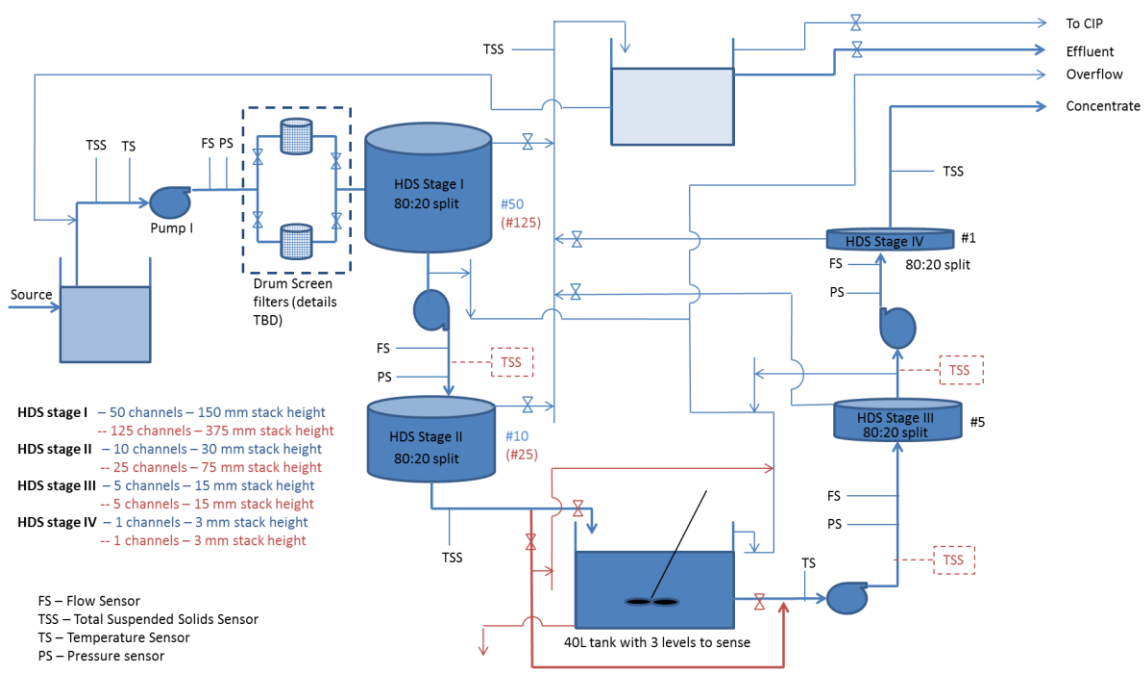

To achieve an adequate increase in the concentration of solids from the primary effluent, a 4-stage HDS channel arrangement is required. The pilot unit designed around these four stages needed to include all supporting components – pumps, meters, valves, piping, gauges, controls,

and so forth. To compensate for any variations in concentrate and effluent flow rate and to prevent starvation of downstream systems and pumps, each upstream stage has a slightly higher capacity than needed - about 3 % more concentrate flow than is needed for each subsequent stage. The final configuration consists of 144 channels in two stacks of 72 channels for Stage 1, 27 channels in a single stack for Stage 2, 5 channels in a single stack for Stage 3, and a 1 channel stack for Stage 4. Figure 35 shows conceptually how to configure the four stages in series to take in primary effluent, pass concentrate through each stage to be sent to a digester, and combine the effluents of each stage to be sent to secondary treatment.

Figure 35: Four Stages of HDS Channels in Series for PIER Pilot

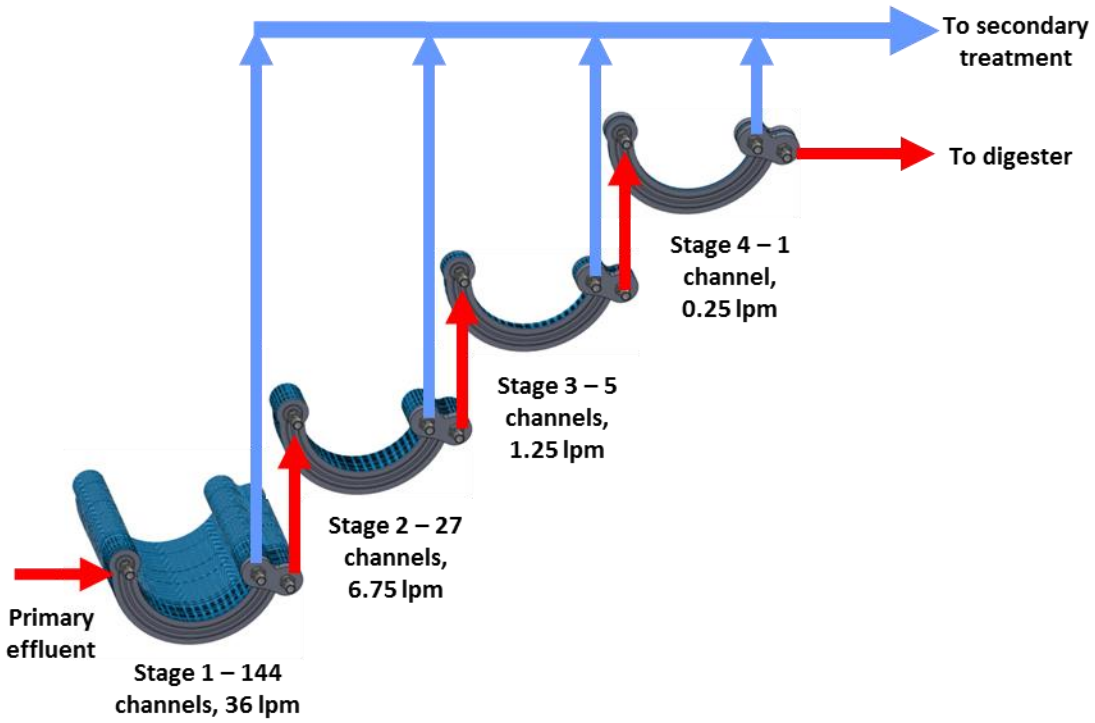

PARC approved a final design following multiple iterations between the various parties. Figure 3 shows isographs of the pilot unit featured on the cover of the final design drawings submitted in June 2013.

Figure 36: Isographs of Final PIER Pilot System, from Design Drawings by Intuitech, Inc.

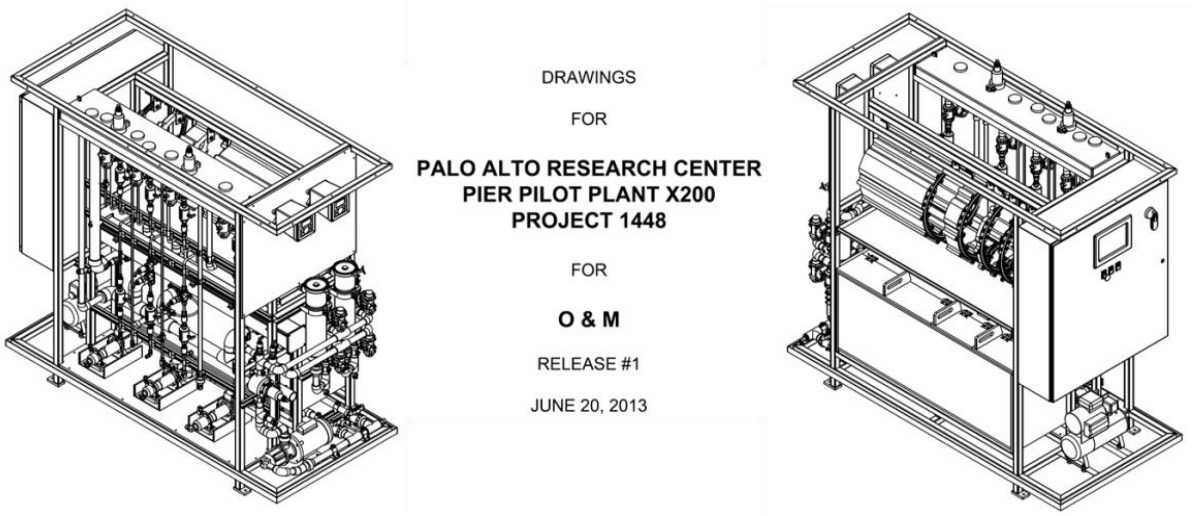

5.2 Pilot Unit Testing and Operation

The HDS pilot unit was delivered to PARC in May 2013. The pilot skid is 7′ long, 3′ wide, just over 6′ tall, and weighs 1350 lbs. It has four stages each with dedicated pumps, pressure sensors, and flow meters on the influent and effluent (diluent) lines of each stage. Primary effluent pumped into an influent tank integrated into the pilot, feeds the first stage. Components for Stage 1 are identified in figure 38. The concentrate and effluent of each stage are discharged to a small, individual weir box located at the top of the pilot. The concentrate of each stage becomes the influent to the subsequent stage, which is pulled from these weir boxes (Figure 39, left). Excess effluent and concentrate overflow the weirs and into dedicated effluent and concentrate channels. This weir box assembly approach allows each stage to be hydraulically disconnected from the others, facilitating flow and pressure control. There are also four HACH Solitax TSS meters, three of which are movable for use within the many weir box locations (Figure 38, right), while one is dedicated for inline monitoring of the influent to the pilot (Figure 4). These TSS meters are connected to two SC200 instrument controllers (Figure 39, left) that are themselves connected to the control panel (Figure 40, left). The control panel is a Human Machine Interface (HMI) that allows a user to access the PLC (programmable logic control) and record data. Finally, there are two bag-style backwash filters (Figure 39, left), pressure across the filters exceeding a threshold will shut down the pilot and the filters will require manual cleaning prior to re-start. The pilot came with engineering record drawings, an operating manual, and manuals and certifications for all of the after-market instruments and pumps installed on the pilot unit skid by Intuitech, Inc.

Figure 37: Pilot Unit Upon Delivery Without HDS Stacks and with Stage 1 Components

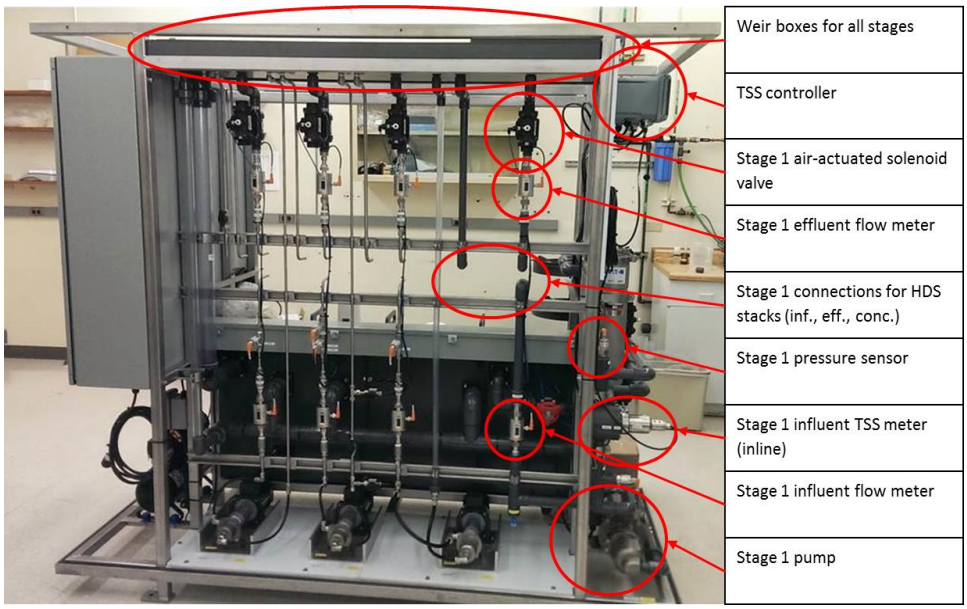

The pilot configuration was carefully checked against the process and instrumentation diagram (P&ID). Temporary pipe-plugs and valves for influent and effluent lines were used to make the pilot functional for system testing with 100 percent recirculated tap water to avoid the need to fill and drain the system within the lab. The pilot unit was operated and tested with surrogate HDS "nodes" that are simply hoses, a tee, and two manual valves to control flow rates and pressures. These were assembled and installed (Figure 39, right). With careful adjustment, throttling the valves could be adjusted to maintain a given hydraulic split (for example, 80:20 effluent:concentrate, the design split the HDS units used for the PIER pilot).

Figure 38: Weir boxes and weir configuration (left); with TSS meters and weir box lid (right)

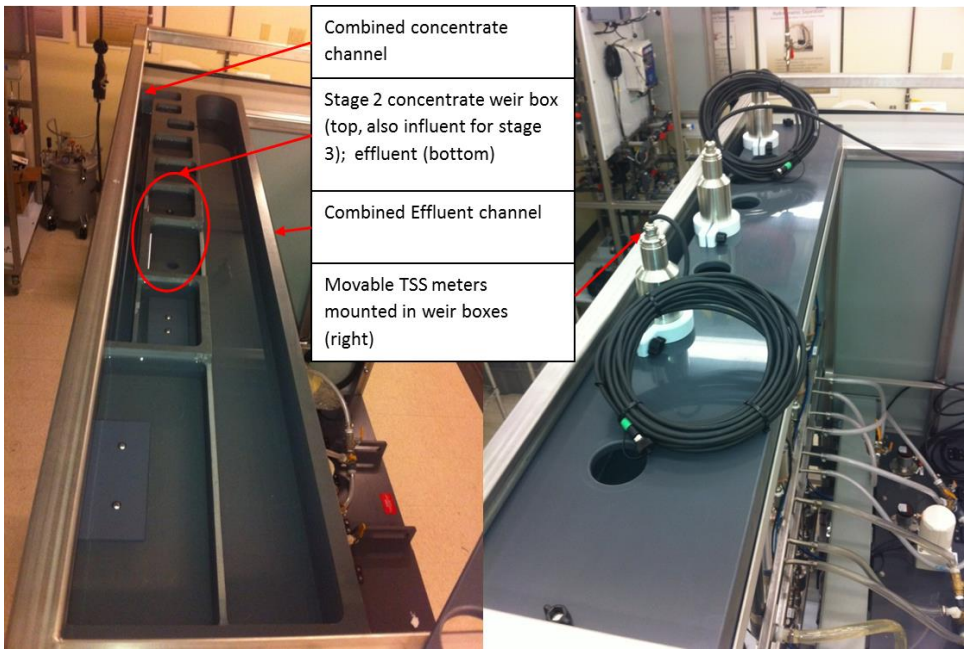

The main user display of the HMI (Figure 40, left) is access through a touchscreen on the main panel (Figure 40, middle). The operation of the different pumps are programmed via the process display (Figure 40, right). The automation control is set up according tocontrol theory, where "Proportional, Integrative, and Derivative" (PID) algorithms are used to control different process operations based on past, current, and anticipated performance through a PLC. The PID settings were "tuned" so the performance of the pumps was optimized and the flow setpoints were maintained and would change according to any unanticipated variations in flow. Pilot operation is programmable so that if flows to any of the pumps drops below a certain setpoint (alarm deadband), the pump shuts off and must be manually restarted after a given duration (alarm delay). The purpose is to protect the pumps and the equipment in the event that the system is clogged, cannot be flushed, or there is no flow to the system.

Figure 39: Bag filters and TSS Instrument Controllers (left); Surrogate Nodes for HDS (right)

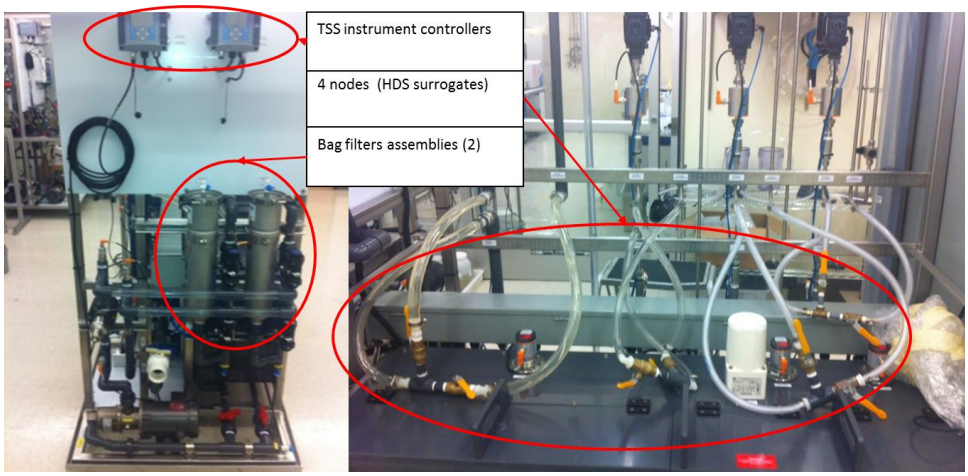

Data recorded via Excel output files automatically writes to a USB drive. Sampling frequency can be selected to give high-resolution data or to give periodic instantaneous data for monitoring long-term operation. Figure 41 shows an example of the system operating set points, gains, alarms, and dead-bands that are inputs for the PLC through the HMI for a 144:27:5:1 HDS stack configuration with an 80:20 hydraulic split. The 144:27:5:1 ratio refers to the number of channels per stack.

Figure 40: Main Control Panel with HMI (left); Overview Display (middle); Process Control Display (right)

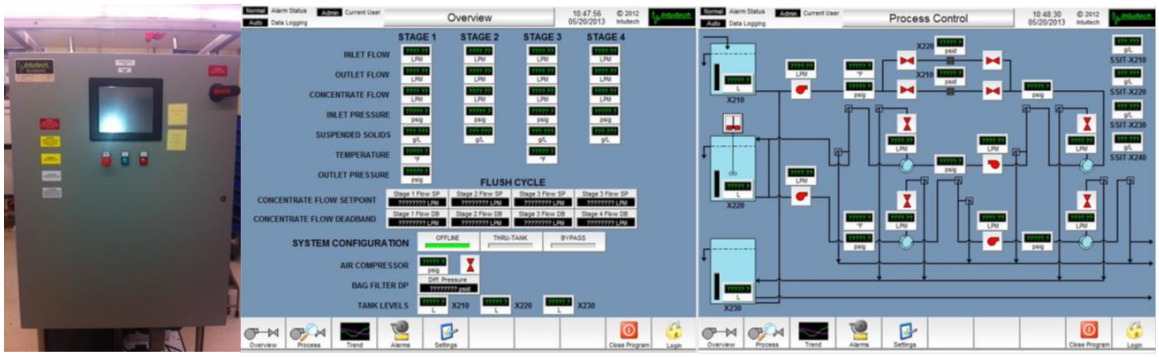

Figure 41: Process-Operating Set Points for 144:27:5:1 Channel Configuration at 80:20 Flow

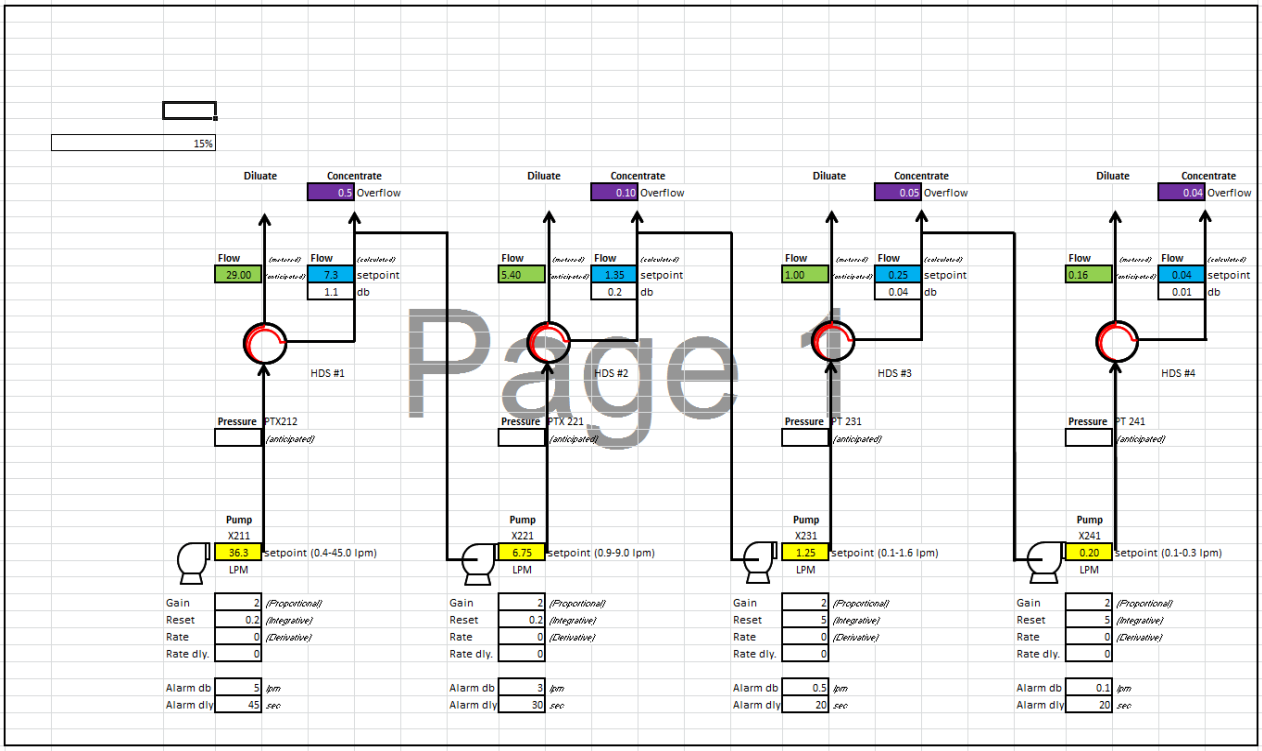

5.2.1 Pilot Unit Testing

Once the pilot system was set up and the operation procedure learned a few simple tests were performed to evaluate the hydraulic performance of the pilot without the HDS stacks in place. The tests evaluate the pilot system itself, and include a *Flow stability test*, and a *Pressure versus flow test*. These tests are described below.

5.2.1.1 Flow Stability Test

This test measured the flow rates and pressures of all four stages at two different flow conditions with clean (tap) water – a lower flow and a higher flow. The flows were somewhat arbitrary but intended to cover the possible range of flows that might be seen by the HDS stacks (~0.15 to 0.25 lpm per channel). The flow split was adjusted to about 75:25 through manipulation of valves in the nodes. The sampling frequency was every 10 seconds, and each test was run for approximately 15 minutes. The average, standard deviation (stddev), and relative percent difference (RPD) were calculated based on the data that was collected, and are presented in Table 12. Figure 42 graphically shows the amount of variability in a constant pump setting for Stage 1, while Figure 43 shows the same for Stage 4. The results presented in Table 12 (in bold, where the RPD is greater than 10 percent) suggest that Stage 4 may have difficulty in producing a sufficiently stable flow rate, especially at lower flow rates.

Table 12: Results and Statistics of Flow Stability Test

	Stage 1		Stage 2		Stage 3		Stage 4	
	high flow	low flow	high flow	low flow	high flow	low flow	high flow	low flow
average inlet flow	37.50	25.01	6.77	4.50	1.23	0.80	0.22	0.14
stddev inlet flow	0.23	0.08	0.08	0.03	0.04	0.02	0.02	0.05
RPD inlet flow	1%	0%	1%	1%	3%	3%	**10%**	**33%**
average effluent flow	29.93	19.49	5.45	3.62	0.97	0.65	0.17	0.13
stddev effluent flow	0.51	0.08	0.07	0.03	0.04	0.06	0.01	0.02
RPD effluent flow	2%	0%	1%	1%	4%	9%	6%	**13%**
average inlet pressure	7.76	4.29	2.57	1.93	1.48	1.41	1.41	1.40
stddev inlet pressure	0.11	0.01	0.02	0.03	0.01	0.01	0.00	0.01
RPD inlet pressure	1%	0%	1%	2%	1%	0%	0%	1%

Figure 42: Clean Water Through Nodes - Influent Flow, Effluent Flow, and Inlet Pressure for Stage1

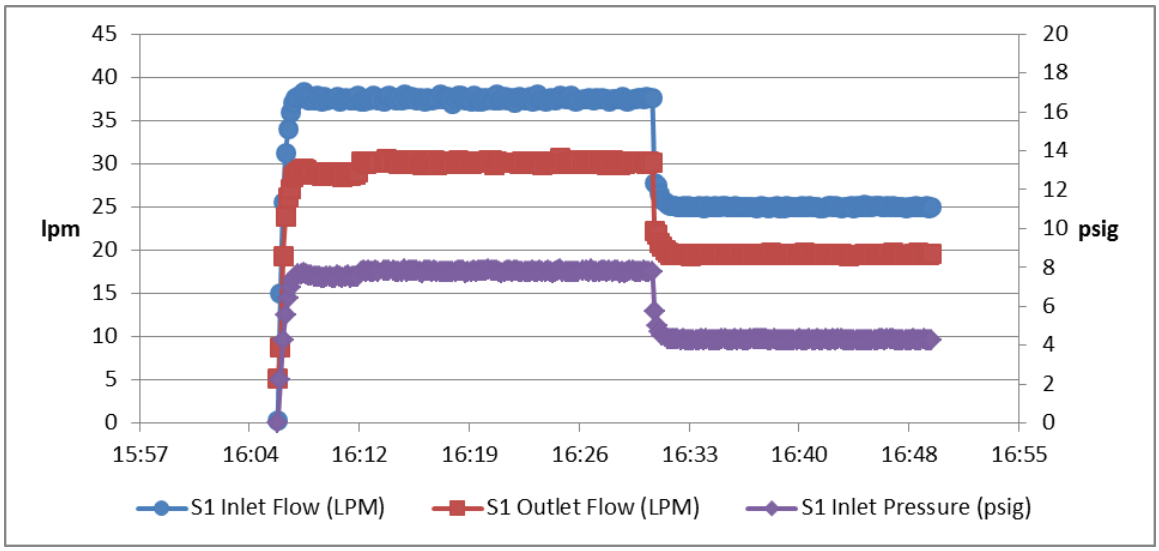

Figure 43: Clean Water Through Nodes - Influent Flow, Effluent Flow, and Inlet Pressure for Stage 4

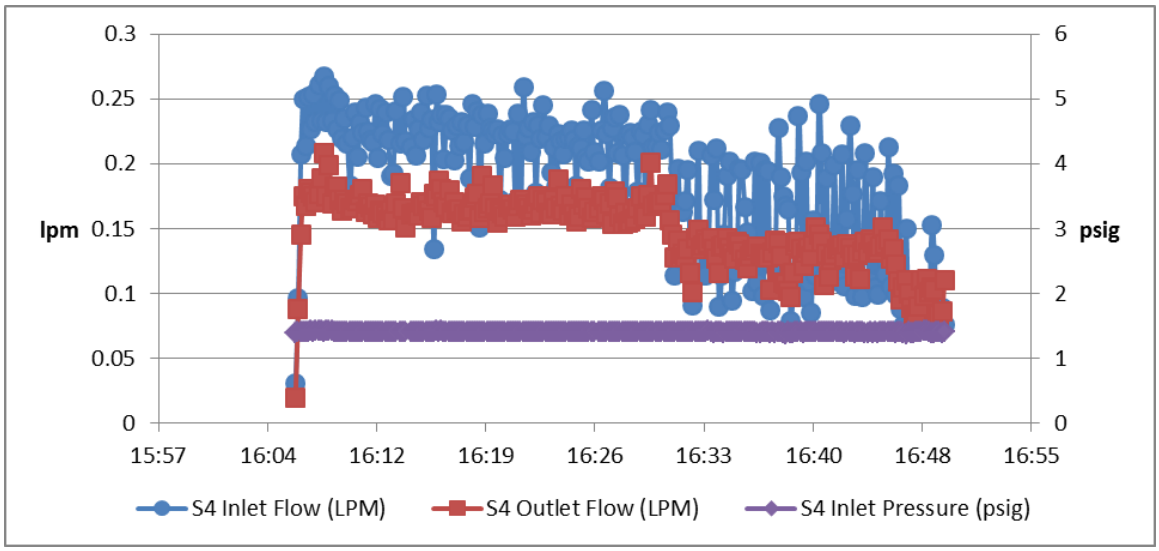

5.2.1.2 Pressure Versus Flow Test for Stage 4

This test evaluated the performance of the Stage 4 pump and system after the results from the flow stability test suggested that Stage 4 operation and performance may be subject to unstable flows (which may or may not be problematic in relation to separation efficiency). Four pressures were achieved by throttling back on the valves in the node that represented effluent and concentrate flow. As the PID control settings maintained the desired influent flow rate, all that could change was the pressure and flow stability. The results presented in Table 13 and seen in Figure 44 show that while the influent and effluent flow rates maintain the same stability (or instability), the variability of the inlet pressure increases.

Table 13: Results of the Stage 4 Pressure Versus Flow Test

S4 Inlet Flow (LPM)			S4 Outlet Flow (LPM)			S4 Inlet Pressure (psig)		
Avg	**Stdev**	**RPD**	**Avg**	**Stdev**	**RPD**	**Avg**	**Stdev**	**RPD**
0.198	0.031	16%	0.179	0.010	6%	1.459	0.047	3%
0.198	0.025	12%	0.173	0.010	6%	4.891	0.296	6%
0.202	0.029	14%	0.172	0.007	4%	9.263	0.301	3%
0.211	0.029	14%	0.172	0.008	5%	13.247	0.635	5%
0.201	0.027	13%	0.170	0.011	6%	20.512	1.465	7%

Figure 44: Pressure Versus Flow, Stage 4

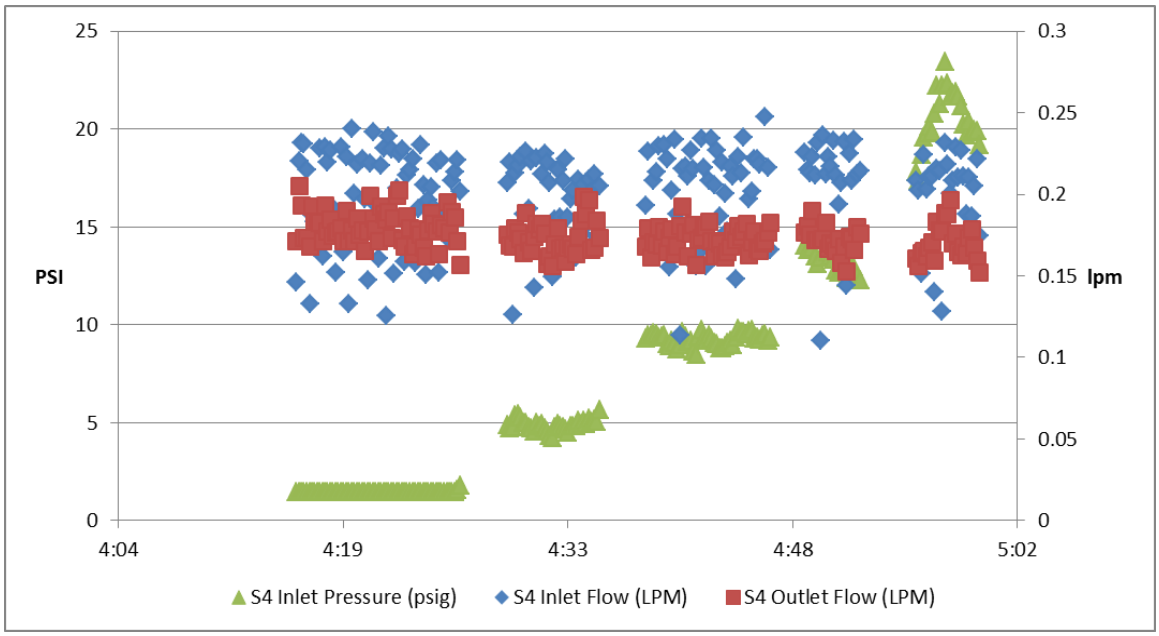

5.2.2 Pilot Installation

After testing in the lab, the pilot system was transported and installed at the Sunnyvale WPCP in November 2013. For the pilot installation site, a paved spot next to the end of the primary clarifier tanks was selected. Figure 45 shows the mechanical portion of the facility, with the 440 acres of stabilization ponds out of the image to the east. The paved spot is wide enough to fit the pilot system comfortably, has the proper strength to support the weight of the pilot system in full operation, and is close to the primary effluent source needed for testing.

Figure 45: Aerial View of the Sunnyvale WPCP Plan with the Pilot Testing Site Circled in Red (left); Pad Location at End of Primary Clarifiers for Pilot Installation

The pilot unit was set up under a carport tent to protect it and the operators from the weather (Figure 46). To allow leveling of the pilot system the researchers added adjustable feet to the 4 corners of the system.

Figure 46: Pilot system after arrival at Sunnyvale with shipping box in front (left); pilot system inside the canvas tent (right).

A simplified schematic showing the pilot system fluidic setup is shown in Figure 47. A grinder pump inside the primary clarifier effluent launder (Figure 48, left) is used to deliver primary effluent to the pilot system. A rope lowers the pump into the tank and the level of submersion can be changed during the test run to explore the performance of the pilot for primary effluent samples at different depths. After separation, the clean and concentrate streams are combined and returned to the primary effluent downstream of the pilot system intake, but before entering the secondary treatment stage. Since the discharge location is several meters away from the pilot and the water has to be lifted above the pilot exit, the authors collect the output water in an effluent storage tank (Figure 48, middle) and use a second sump pump (Figure 48, right) to deliver the effluent of the pilot back to the primary effluent channel. By running with excess flow through the influent tank, this setup prevents the pilot from running dry.

Figure 47: Schematic Diagram of the Fluidic Setup

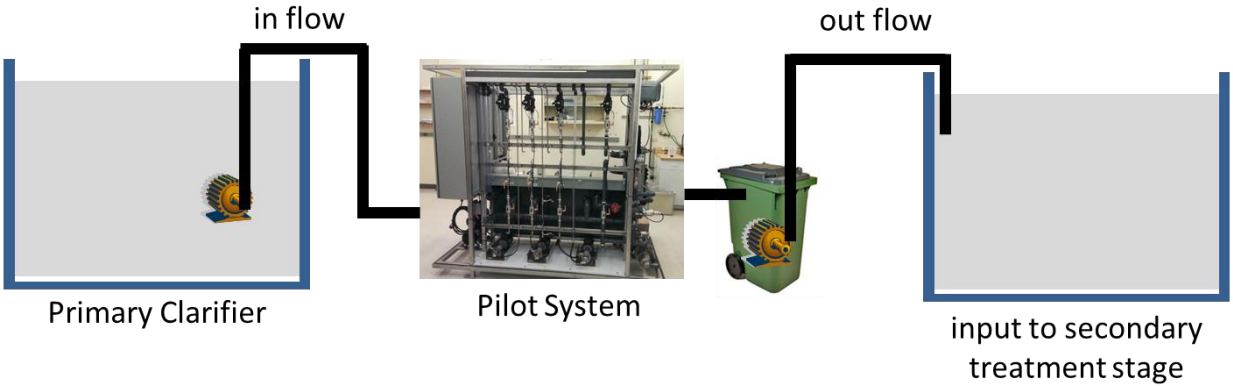

Figure 48: Components of the Fluidic Setup: Influent Grinder Pump in the Primary Effluent Launder (left); Effluent Storage Tank (a modified refuse container) (middle); Effluent Sump Pump (right)

CHAPTER 6:
Pilot Demonstration in a Wastewater Plant

This chapter summarizes PARC's efforts using HDS to separate neutrally buoyant organic solids from primary effluent at the Sunnyvale wastewater treatment plant. Two complete sets of channel stacks, each based on a different design and assembly process, were made for the pilot. The first set of stacks, herein called the first-generation stacks, was PARC's first successful attempt at mass production of injection molded parts and semi-automated assembly. The injection molding and assembly process was described thoroughly in Chapter 4. As with the production of most first articles, what was learned during the fabrication and assembly process, preliminary testing in the field, and in the lab quickly lead to the decision to make a set of second-generation stacks that improved upon the first-generation design. The pilot more rigorously tested the second-generation stacks. A brief summary of the performance of first-generation stacks will illustrate why the second-generation parts were fabricated; the results of testing of the second-generation stacks will follow.

6.1 First-Generation HDS Stacks – Summary

Figure 49: First-Generation Stacks Installed in Pilot

In an effort to expedite pilot testing, these first-generation stacks were installed in the pilot at Sunnyvale in December 2013 without undergoing laboratory performance testing with standards. The researchers were anxious to move directly to working with primary effluent.

They connected ¾ inch tubing to the influent, effluent, and concentrate manifolds of the two, first stage stacks, which totaled 144 channels; 1/2 inch tubing to the manifolds of the second stage stack that consisted of 27 channels; and 3/8 inch tubing to the manifolds of the third and fourth stage stacks, that were 5 channels and 1 channel, respectively. The five stacks that comprise Stages 1 through 4 are shown, from left to right, in Figure 49. Each stack has bleed valves on the fittings opposite the effluent tubing. Though the fluidic connections for the different stacks were chosen to reflect the different flow rates going into each stack, less consideration was done on estimating total head loss in the exit piping due to tube length and other fluidic constrictions (for example, flow meters, valves, bends, and fittings). As a result the large losses in the exit piping caused a shift of the flow split from the design value towards 50:50.

This configuration was operated and evaluated over the course of 12 days between December 2013 and March 2014 for typically no more than 1-3 hours per day. Much was learned during this time about the limitations with the pilot (the TSS meters were never successfully calibrated, the influent inline TSS meter was on the wrong side of the bag filters, the 3rd and 4th stage weir boxes accumulated solids), and about the limitations of the first-generation stacks. The poor flow split with stage 1 that improved by stage 4 was first documented (Figure 50), as was the yet-to-be-explained inlet pressure differences between the 1st and 4th stage (Figure 51). These pressure differences are now understood to have been the result of head losses caused by tube length and fluidic constrictions for the piping after the effluent and concentrate manifold exits.

Figure 50: Split Ratio Deterioration with Stack Height

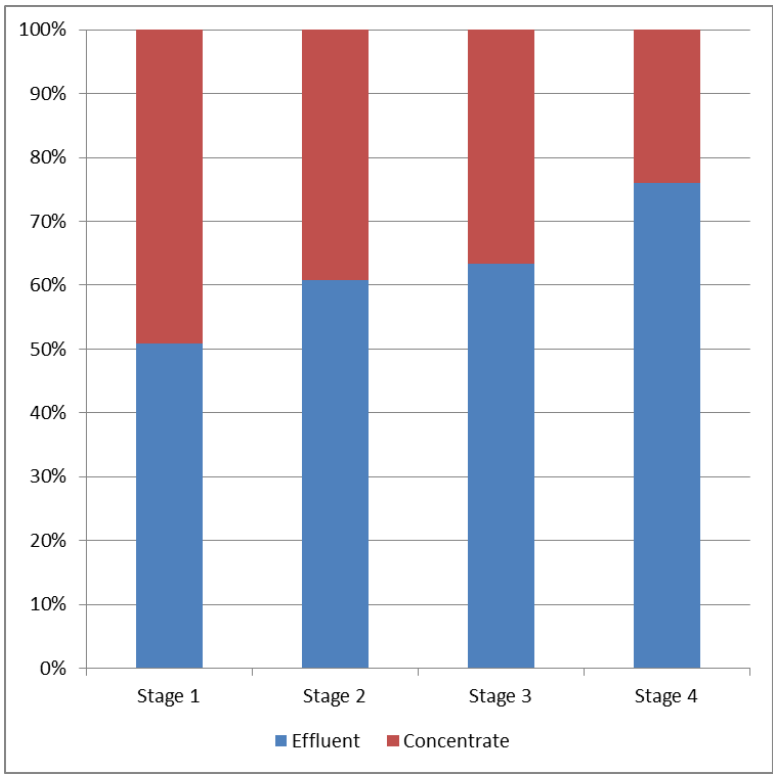

Figure 51: Pressure Anomaly Correlates with Deteriorating Split Ratio

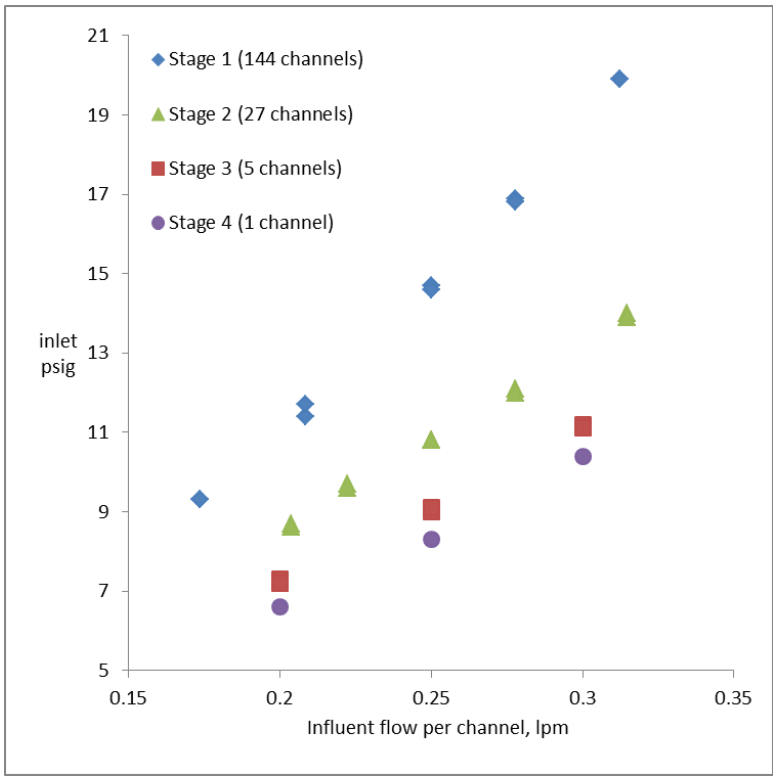

Figure 52: 10x Concentration Increase with Forced 80:20 Split

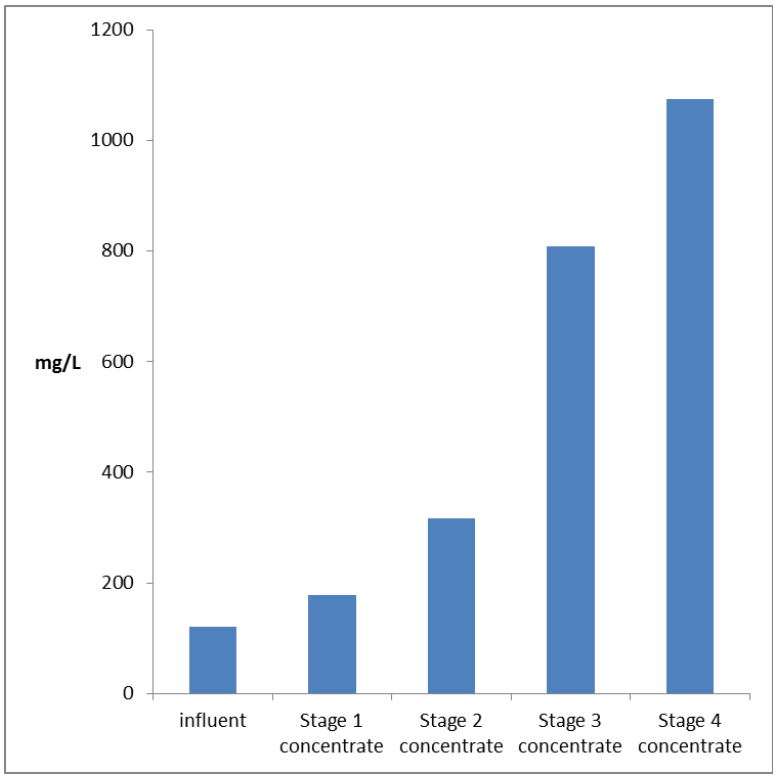

Figure 53: Influent, 4th Stage Concentrates with Forced Split

It was also learned during this preliminary pilot testing that the flow split could be forced to 80:20 by restricting the concentrate lines with clamps on the tubing, which resulted in the best possible performance with the first-generation stacks. Figure 52 shows the increase in concentration of 10x between the first stage in fluent and the 4th stage concentrate; these samples are shown in Figure 53. The 10x increase in concentration was not nearly as good as the 300x increase that was initially proposed.

As the researchers already knew there were flaws in the part manufacturing and stack assembly, the poor initial performance to the first-generation stacks prompted them in March 2014 essentially to start over. This required a new part design, a new molding tool, new parts, new programming for the gluing and assembly process, as well as a different UV curable glue. For this second effort, they collaborated with both the molding manufacturer (REVA) and the part assembler (CDI) to ensure that a part design that was easier to assemble was also easier to manufacture. CDI, who was fully responsible for stack assembly, was heavily involved in the part design process. Details of fabrication and assembly trials are presented in Chapter 4.

Figure 54: Setup for Testing First-Generation 27-Channel Stacks (left); Performance (right) with ¼" Tubing on Effluent and Concentrate Exits (which can be seen in the photo, leading from the exits to the raised tank)

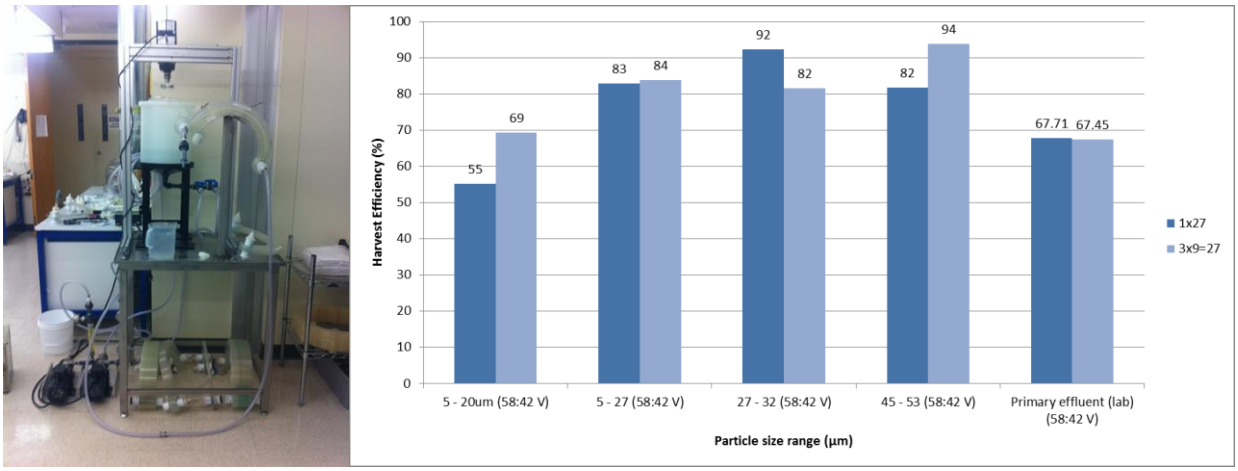

While the researchers were going through the re-design, two, 27-channel stacks (sized for the second stage) were rigorously tested in June 2014 for flow split and harvest efficiency using multiple standards (Figure 54). One stack was a single robotically glued and cured layup that resulted in 27 channels; the second was a composite of three robotically glued and cured layups of 9 channels each that were manually glued together. A progressive cavity pump (Moyno 23202) and variable speed drive (Altivar 12 20402) was used for the test setup. The harvest efficiency showed a characteristic improvement with particle size, while the flow split stayed constant at 58:42 (Figure 54). Unfortunately, it was only realized much later that the poor flow split was caused by the 1/4" tubing that was affixed downstream of the exits, adding significant downstream head losses. Without the tubing attached to the exits the 3x9=27 channel stack shows the design flow split of 73:27, which is much better than a flow split of 58:42. This was a single flow split test only, and did not correspond with harvest efficiency measurements. It is suspected that HE results without tubing attached would have been better than what is shown in Figure 54 – that is to say, similar in performance with the 2nd generation stacks.

6.2 Differences – First- and Second-Generation HDS Stacks

The second-generation stacks arrived in September and October 2014, and addressed a number of fabrication and assembly challenges associated with the first-generation stacks. Chiefly, the second-generation layers are not susceptible to warping and the stacks are easier to assemble. The new stacks are half the height of the first-generation stacks and use about 1/3 the amount of plastic (Figure 55). Also, the exit diameters are 50% larger, having been increased from 25.4 mm to 38.1 mm in diameter. The tongue and groove design was replaced with a glue cavity that allows for glue to be wicked into voids, for flush mating layers, and elimination of the glue gap that was problematic with the first-generation stacks. While the part design is vastly improved, a few design issues remain - CDI has acknowledged that the dimension of the glue cavity could be improved, there are quality control issues with automated glue delivery (the tube of glue

used sometimes emits a small air bubble, requiring manual touch-ups) and that the clamping and assembly process could be more automated. The current assembly takes approximately 6 minutes per layer.

Figure 55: 1st (top of each photo) and 2nd (bottom of each photo) Generation Stacks (bottom of each photo)

While there are improvements with the fabrication of the second-generation stacks, there is one remaining flaw and one newly introduced flaw that was not discovered until after the second-generation stacks were assembled. The remaining flaw was a design error that was propagated throughout the project. The CAD file that was used as the basis for design from the very beginning for both the 1st and the 2nd generation parts had a geometric flow split of 73:27, rather than the intended 80:20 flow split. This was not discovered until after the tool had been made for the second-generation part. While not ideal, it is not of major concern.

The new flaw is the presence of an ejector pin mark located in the middle of the exit channel (Figure 56). This raised, circular, ridged bump provides an edge that can catch debris, as will be shown in the results section. Ejector pins are used to push a freshly molded part out of a mold. This ejector pin location was not noticed during the quality assurance/quality control (QA/QC) inspection of a sample part, and the entire order was completed with the ejector pin in this undesirable location.

Figure 56: Flaws of Second-Generation Parts - Ejector Pin Mark in Middle of Effluent Channel (left); 73:27 Geometric Flow Split Design Error (right)

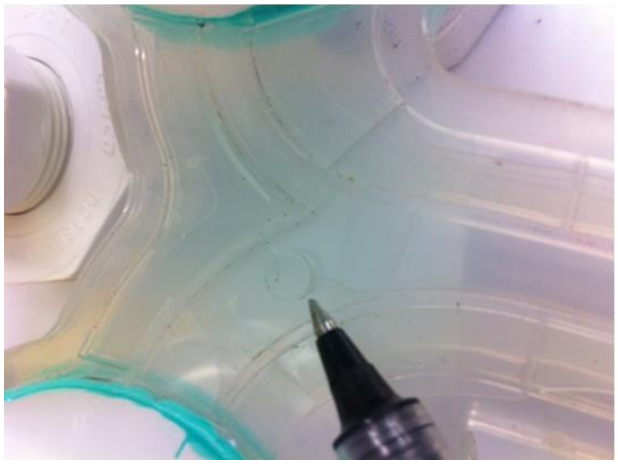

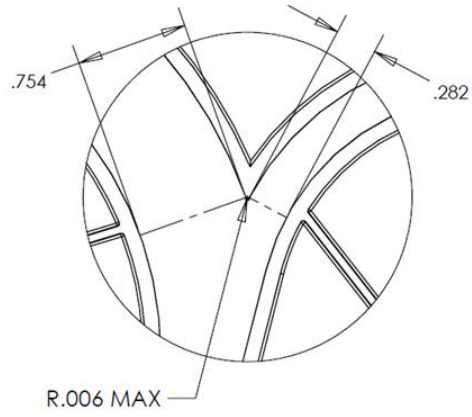

6.3 Second-generation Stacks - Performance

The second-generation stacks were tested more rigorously than the first-generation stacks. Based on what was learned during lab and pilot testing of the first-generation stacks, the second-generation stacks were tested without (or with minimal) fittings, tubing, or piping connected to the exits to prevent pressure differences from adversely influencing the flow split. Flow split and harvest efficiency metrics were first determined in the lab using particle standards using the "new" stacks once they were received from CDI. This was followed by an evaluation of the performance during 16 hours of operation at the Sunnyvale wastewater plant separating primary effluent, using the first (144 channel stack) and third (5 channel stack) stages of the pilot in series in a modified configuration. Total suspended solids, flow split, COD, and pressure changes were measured for four, 4-hour periods. The "dirty" stacks were then brought back to the lab and re-tested for flow split and harvest efficiency with neutrally buoyant standards so the performance could be compared with the "new" stacks. The first stage stack was then thoroughly cleaned and re-tested a final time (the "cleaned" stack) for flow split and harvest efficiency with neutrally buoyant standards to confirm that pre-use performance could be recovered – that is, that the effects of fouling could be reversed.

6.3.1 Baseline Testing

The four stacks of second-generation HDS channels were tested in PARC's clean water lab for both flow split and harvest efficiency using neutrally buoyant 45-53 um polyethylene spheres (Cospheric, Inc.). The setup was the same for the 1-, 5-, and 27 channel stacks, and consisted of an IWAKI model MD-70RLZT centrifugal magnet pump, with ½ inch pump inlet tubing, 3/8 inch pump outlet tubing, a flow rotometer, and pressure gauge, and a horizontal stack orientation (Figure 57, left). The 144-channel stack required a larger pump and setup (Figure 57, right) consisting of a Grundfos centrifugal pump model C4H503463 P10828, 1" pump inlet and pump outlet tubing, and a vertical stack orientation. The exits required a 1.5" fitting and hose extension to reach the discharge tank.

Figure 57: Lab Setup for Testing Second-Generation 5-Channel (left) and 144-Channel Stack (right), with a Free-Surface Discharge at the Exits

Figure 58: Lab Results of the Second-Generation 5-Channel (left) and 144-Channel Stack (right), with a Free-Surface Discharge at the Exits

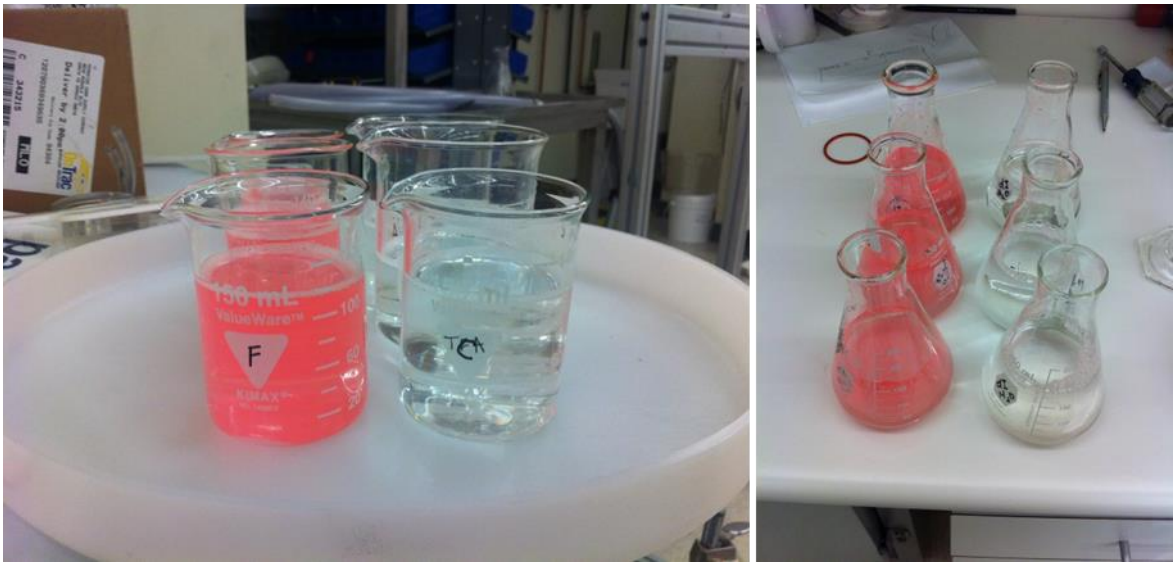

Testing the flow split involved measuring the collected volume of the effluent and concentrate flows over a set time period. The results of this baseline performance are shown in Table 14.

Table 14: Performance of "New", Second-Generation Stacks with Neutrally Buoyant, 45-53um Spheres

# of channels	Volume split, effluent:concentrate	Harvest efficiency,%	Starting conc., mg/L
1	73:27	96%	476
5	71:29	94%	379
27	69:31	92%	482
144	70:30	86%	272

It is worth noting that the harvest efficiency (HE) for the 27 channel stack is similar to the values reported for the first-generation 27 channel stacks (82 and 94 percent, Figure 54), even though the flow split is 69:31 vs 59:42. Also note that the first-generation flow split improved to 73:27 when re-tested without tubing connected to the exits. While the first-generation HE was not tested for the 27 channel stacks without flow restrictions, it is suspected that these channels would have performed at least as well as the second-generation 27 channel stack in separating neutrally buoyant 45-53 um spheres. The assumption that the poor flow split was caused by manufacturing and assembly errors was a rush to judgment. While the second-generation stacks are of far better quality, are easier to assemble cheaper to build, and address other important design flaws, the first-generation stacks likely would have performed adequately for the 1, 5, and 27 channel stacks for the pilot study. The 144 channel stacks likely would have been adversely affected by the small outlet size. A comparison between first and second-generation 27 channel stacks, with and without flow restrictions, separating 45-53 um neutrally buoyant spheres is presented in Table 15.

Table 15: Performance Between 1st and 2nd Generation 27 Channel Stacks with Neutrally Buoyant 45-53um Spheres

Generation Design	# of channels	Volume split, effluent:concentrate	Harvest efficiency,%	Starting conc., mg/L
1st	**27**	58:42 (restricted)	82%	397
1st	**3x9=27**	58:42 (restricted)	94%	407
1st	**3x9=27**	73:27 (unrestricted)	Not tested	N/A
2nd	**27**	69:31(unrestricted)	92%	482

6.3.2 Pilot Testing

6.3.2.1 Setup and Method

With the stacks of HDS channels for each stage now tested, installing and operating the channels at the Sunnyvale WPCP could begin. As it was found and presented previously that the piping configuration of the pilot adversely affects performance, the stacks were configured so as to have no (or minimal) downstream piping, tubing, or fittings that could intruduce disproportionate headlosses between the exits. Redesigning and modifying the pilot at this point in the project, with less than 2 months remaining in the schedule, was impractical. The

researchers decided to hook up only two stages to the pumps of the pilot (the first and the third stage (the 144 and 5 channel stacks, respectively)), and disconnect them from downstream piping so as to allow for each to have a free discharge. The first stage pump drew from the influent tank as was originally designed, but the first stage concentrate and effluent discharged into the intermediate and effluent tanks built into the pilot. The third stage pump drew from the intermediate tank, and effluent and concentrate from the third stage stack discharged into the final effluent sump. The intermediate tank had a build-in mixer, so the research team was able to ensure that the input to the third stage was representative of the concentrate leaving the first stage. Figure 59 shows the positions of the first and third stage stacks of second-generation HDS channels installed at the pilot at the Sunnyvale WPCP.

Figure 59: Pilot Testing of the First Stage (left) and Third Stage (right) Stacks, with a Free-Surface Discharge at the Exits

Pilot testing was then conducted over the course of four days, with each day consisting of four-hours of steady state operation. The flow split, TSS, and filtered and unfiltered COD of each stream were measured at the beginning and end of each four-hour run. Because the stacks were disconnected from all downstream piping and therefore also the flow meters, flow measurements had to be performed manually. Measuring flow for the first stage stack involved draining the intermediate tank, turning on the first stage pump, priming the first stage stack, and then monitoring the digital level indicator over a fixed period of time with a stopwatch. Only the concentrate flow could be measured. As the influent flow was still measured with the digital flow meter, the effluent flow was the difference. Measuring flow for the third stage stack involved the use of a graduated cylinder and a stopwatch.

TSS analyses were performed via conventional gravimetric methods, as were COD analyses. Figure 60 shows all TSS results taken over the course of the study. Figure 61 shows the particulate COD results taken over the course of the study. Particulate COD was calculated as the difference between the filtered and unfiltered COD analyses.

Figure 60: TSS Results for 4 Days of Pilot Testing

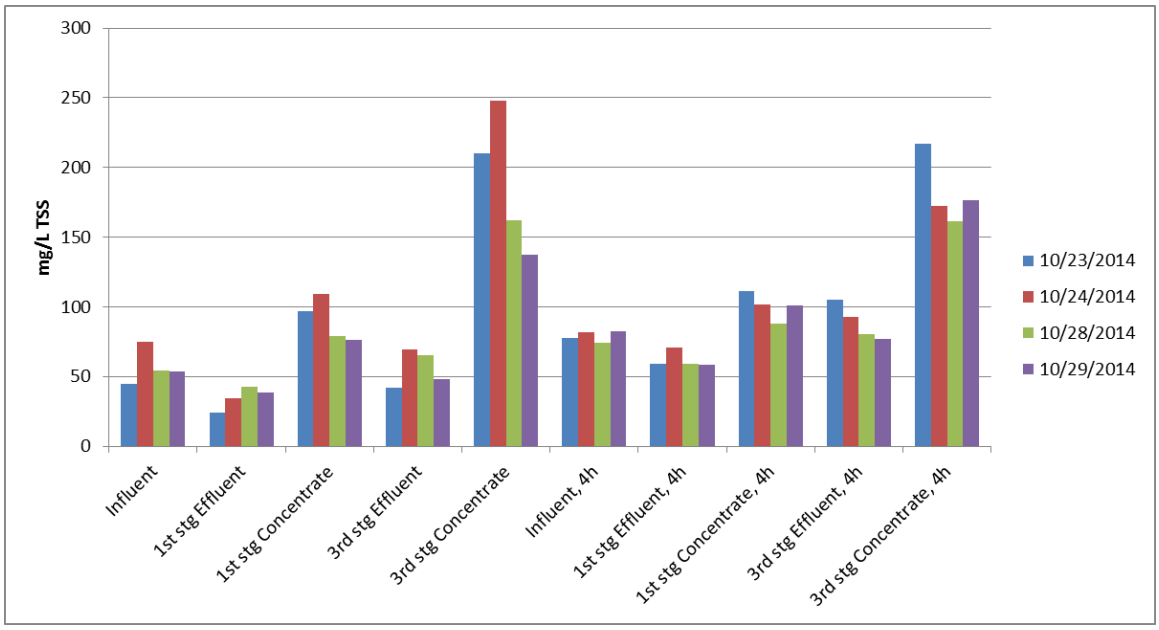

Figure 61: Particulate COD Results for 4 Days of Pilot Testing

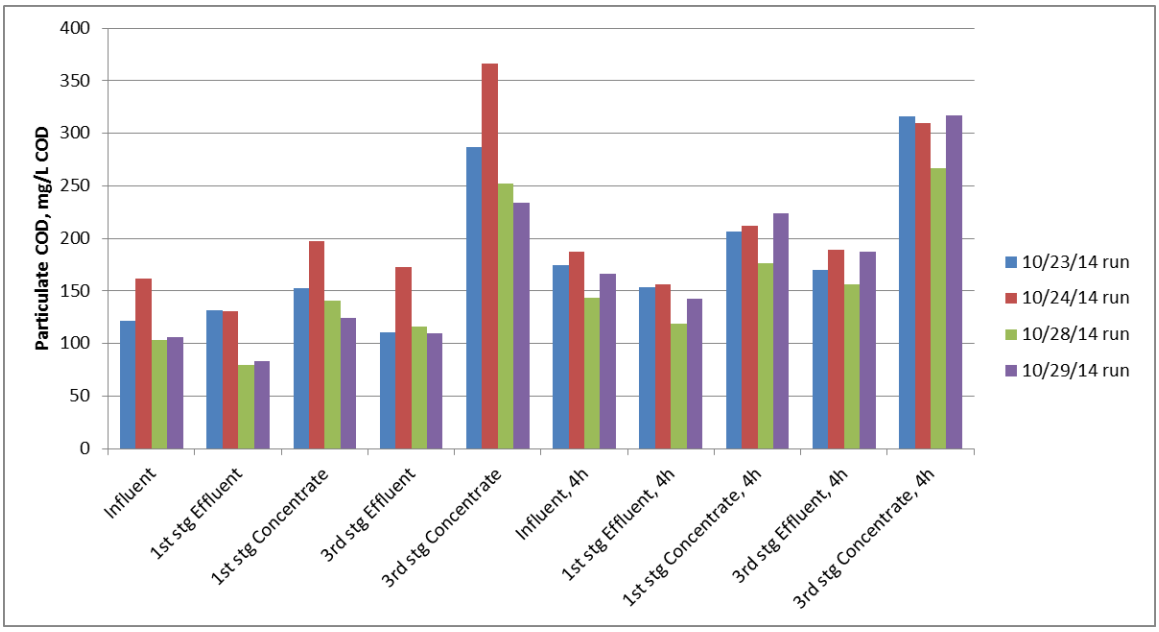

A summary of the harvest efficiencies and flow splits are shown in Tables 17 and 18, respectively. Harvest efficiency generally deteriorated from beginning to the end of a four hour period of operation, and generally deteriorated from the first to the fourth day of operation. This is attributed to channel clogging. Also, the third stage generally performed worse than the

first stage, for unknown reasons. The impact of channel clogging on flow split was inconsistent – in some cases, clogging improved flow split.

Table 16: Harvest Efficiencies with Primary Effluent During Four-Days of 4-Hour Pilot Operation

Test date	Timepoint	Stage 1 HE	Stage 3 HE
23-Oct	Startup (t=0hrs)	70%	66%
	t = 4hrs	49%	35%
24-Oct	Startup (t=0hrs)	62%	60%
	t = 4hrs	42%	32%
28-Oct	Startup (t=0hrs)	51%	35%
	t = 4hrs	39%	36%
29-Oct	Startup (t=0hrs)	53%	50%
	t = 4hrs	47%	51%

Table 17: Split Ratios During Four-Days of 4-Hour Pilot Operation

Test date	Timepoint	Stage 1 split ratio	Stage 3 split ratio
23-Oct	Startup (t=0hrs)	63:37	72:28
	t = 4hrs	66:34	79:21
24-Oct	Startup (t=0hrs)	66:34	80:20
	t = 4hrs	66:34	80:20
28-Oct	Startup (t=0hrs)	64:36	82:18
	t = 4hrs	70:30	78:22
29-Oct	Startup (t=0hrs)	64:36	74:26
	t = 4hrs	66:34	69:31

Figure 62 shows a visual comparison of samples between the first stage influent and 3rd stage concentrate at the beginning (left) and at the end (right of a 4-hour period of operation at the pilot. These photos were taken October 28th, and have corresponding HE, flow split, TSS, and particulate COD measurements in Table 16, Table 17, Figure 60, and Figure 61, respectively.

Figure 62: 1st Stage Influent (left of each photo) and 3rd Stage Concentrate (right of each photo) for Beginning (left) and End (right) of 4-Hour Run of Pilot Operation (October 28rd)

Finally, the inlet pressures to each stage were monitored manually during the course of the run, as the data logging feature of the pilot shut down inexplicably, likely due to sitting outdoors at the wastewater treatment plant site for over a year even though it was covered. Data was read from the HMI that displayed pressures every 15-30 minutes. The inlet pressures generally increased between 2-4 psi over the course of a four-hour run, likely caused by inlet manifold clogging and channel clogging. The inlet manifold cleaning between days of operation significantly lowered the starting pressure on the following day, but there was an increase in starting pressure between the first through the fourth day, only slightly for stage 1, but dramatically for stage 3 (Figure 15). Note that the final day of testing, October 29th, was conducted without a bag filter to remove particles larger than 200 um.

Figure 63: 1st Stage Inlet Pressure

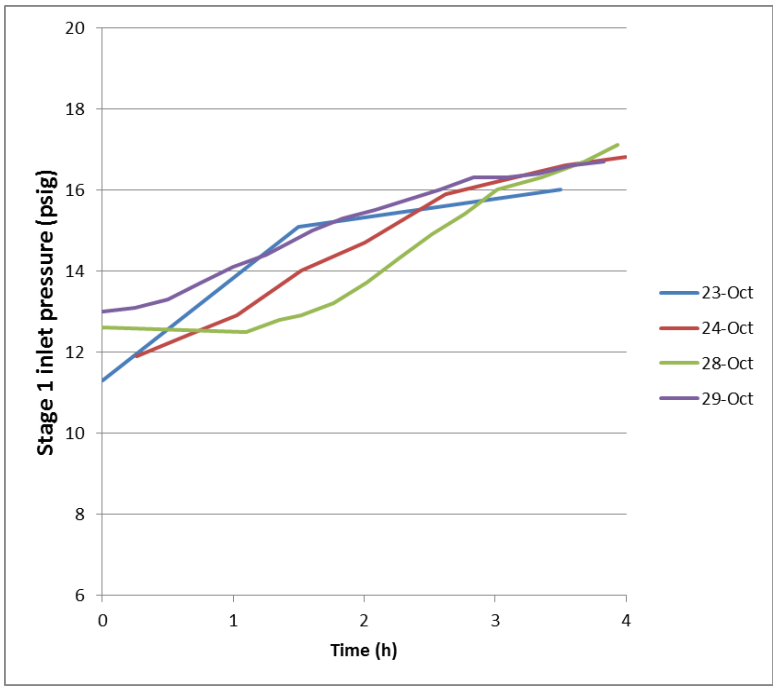

Figure 64: Stage 3 Inlet Pressure.

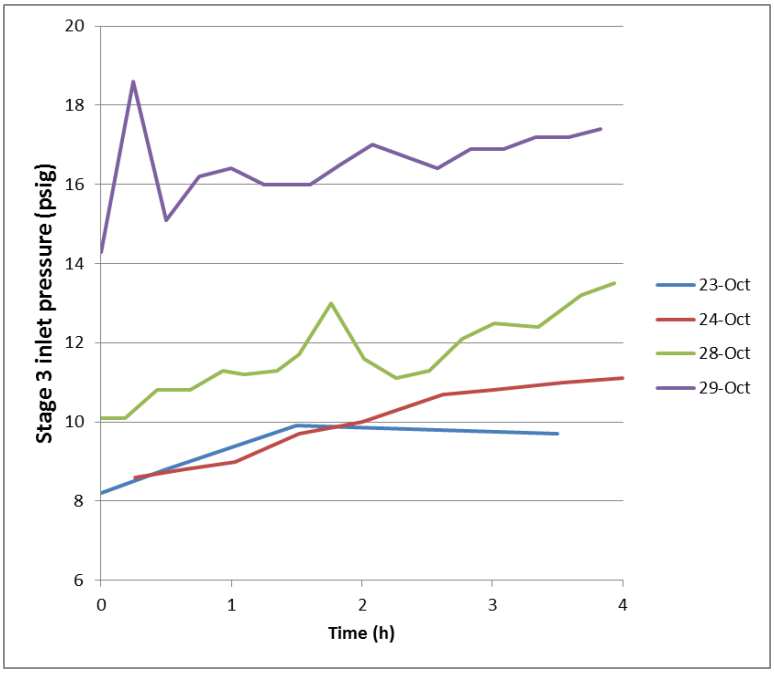

6.3.2.2 Fouling

The first three days were run with the bag pre-filter in place, with the expectation to remove particles larger than 200um; the fourth day was run without it. After four hours, the bag filter was blinded with solids – so blinded, in fact, the bag would hold water (Figure 65, left). After each four-hour period the inlet manifolds were cleaned with a brush and the stacks were rinsed with clean water and a dilute solution of bleach for approximately 15 minutes. Figure 65 also shows typical accumulation of debris in the inlet manifold of the 144-channel stack after 4-hours of operation (Figure 65, middle) with the bag filter in place, and after cleaning with a brush (Figure 65, right) (from October 23rd testing).

Figure 65: 200um bag filter holds water after 4 hours of operation (left); Inlet manifold debris accumulation (middle); after cleaning with a brush (right).

Figure 66: Solids accumulating on the splitter and ejector pin marks for the 1st Stage (left); 3rd Stage (right).

Figure 67: Algae pieces lodged in channel near inlet channel (left); lodged in effluent channel (right).

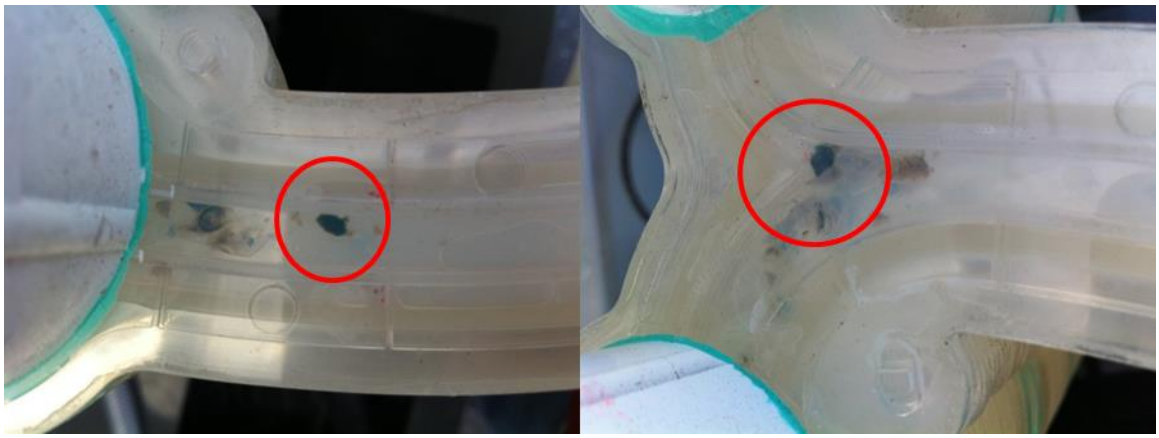

The channels themselves were also subject to fouling. Figure 66 shows fluffy organic solids accumulating on the splitters and getting caught on the ejector pin marks for the 144 channel stack (left), and 5-channel stack (right). Also, as the pilot unit had set idle for at least 6 months, algae growth accumulated on the inside of the clear piping downstream of the bag filter. Films of algae sloughed off during the 16 hours of pilot operation, perhaps the result of the dilute bleach treatment after each 4-hour run, with larger pieces of green algae contributing to the accumulated debris in the inlet manifold (Figure 65, middle), and becoming lodged inside the channels (Figure 67). There was no way to remove the algae as it was growing in parts of the pilot unit that could not be reached.

While not measured, the particles that accumulated in the inlet manifolds (Figure 65, middle) seemed to be larger than 200um, the reported equivalent mesh size for the bag filter. The installation of the bag filter was checked and confirmed, and seemed secure. Bag filters were replaced daily. The bag filter was removed for the fourth day of testing to evaluate the impact of the bag filter. Aside from the significantly higher pressures seen for the stage 3 inlet, there was little to no difference for any performance metric (Tables 16 and 17, Figure 60 and 61). Interestingly, visual observation after four hours of operation of the stage 1 inlet manifold (Figure 68) showed what appeared to be smaller particles than those that accumulated with the bag filter in place (Figure 65, middle). There is no clear explanation for this.

Figure 68: Stage 1 Inlet Manifold Debris Accumulation after 4 Hours without the Bag Filter

6.3.2.3 Confirmation Testing

After the four days of pilot testing, the first and third stage stacks of HDS channels were brought back to PARC's lab to be re-tested with standards. The inlet manifolds were brushed clean as before, but no efforts were made to clean the insides of the channels. The channels were tested as before with neutrally buoyant spheres between 45 and 53 um, using starting concentrations between 200 and 400 mg/L. The results are presented in Table 18. The conclusion is that after 16 hours of steady state operation, with regular cleaning of the manifold inlets, the mass capture deteriorated from 94 to 65 percent for the 5-channel stack, and from 86 to 75 percent for the 144 channel stack.

Table 18: Performance of "Dirty", Second-Generation Stacks with Neutrally Buoyant Spheres Between 45-53um

# of channels	Volume split, effluent:concentrate	Harvest efficiency,%	Starting conc., mg/L
5	74:26	64%	235
144	66:34	75%	402

As a final test, the researchers cleaned the 144 channel stack using a combination of hot tap water, back flushing, soapy water, and high pressure (20 psi) both forward and backwards through the inlet, concentrate, and effluent channels in combination and individually. Approximately 40L of clean water was used in the system shown in Figure 1 and pumped through the stack for about 5 minutes for each rinse, with the rinse water replaced with clean water approximately 15 times. A separation experiment was repeated with a solution of neutrally buoyant spheres between 45 and 53um, as before, to determine if the initial "new"

performance could be recovered with cleaning. The difference between "new" and "cleaned" performance was negligible, indicated that the stacks could indeed be cleaned (Table 19). Figure 69 shows the performance of the cleaned 144 channel stack separating ~ 300 mg/L of 45-53um neutrally buoyant spheres with an HE of 85 % and a volume split of 69:31.

Figure 69: Confirmation test of the 1st stage second-generation stack, flow rate of 36 lpm, showing 85 percent mass capture of neutrally buoyant 45-53um standard spheres.

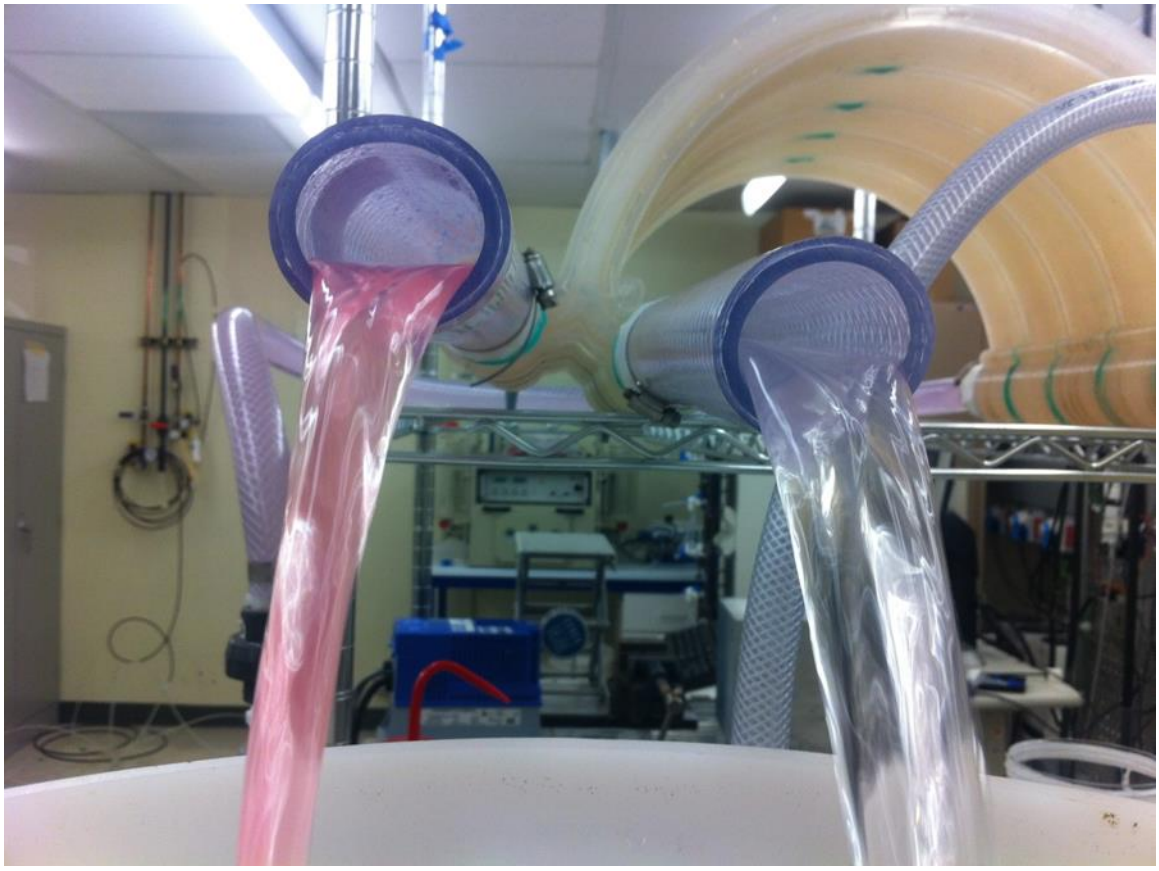

Table 19: Performance of the 144 channel second-generation stack with neutrally buoyant spheres between 45-53um – the impact of fouling and cleaning.

# of channels	Volume split, effluent:concentrate	Harvest efficiency,%	Starting conc., mg/L
"new"	70:30	86%	272
"dirty"	66:34	75%	402
"cleaned"	69:31	85%	296

CHAPTER 7:
Energy Benefits of HDS

This chapter presents an analysis of energy benefits that could result from implementing a full-scale HDS system at a wastewater treatment facility. Harvesting neutrally buoyant organic solids from primary effluent could positively impact the energy balance at a wastewater treatment facility in two ways: 1) by decreasing the organic load on the secondary treatment system, the oxygen demand and the need to supply air to bioreactors is reduced, and 2) by increasing the organic load to digesters the biogas production and potential energy generation through cogeneration is increased. The energy used for pumping to an HDS system negatively impacts the energy balance. An accounting for all three energy impacts are presented herein for a facility without HDS (the baseline condition), a facility with an ideal HDS system, representing the best-case scenario), and a facility with an HDS system that had similar performance to what was observed during the operation of the pilot (an actual HDS system, representing a worst-case scenario).

In chapter 2, a theoretical wastewater treatment facility was modeled with wastewater process simulation software (BioWin) both without an HDS system and with an ideal HDS system. The assumptions for the ideal HDS system were presented in chapter 2, and included 51 % mass capture from a four-stage system that could concentrate neutrally buoyant organics to over 3% solids in less than 0.2 % of the flow. It was also assumed that each stage delivered exactly enough flow to each subsequent stage, minimizing the number of channels to 13,104 per mgd. Tables with these assumptions are repeated in Tables 20 and 21, below.

Table 20: Table of performance assumptions for an ideal HDS system of 4 stages in series.

	Flow split		Harvest Efficiency	
Stage	**Effluent**	**Concentrate**	**Effluent**	**Concentrate**
Stage 1	80%	20%	30%	70%
Stage 2	80%	20%	10%	90%
Stage 3	80%	20%	10%	90%
Stage 4	80%	20%	10%	90%

Table 21: Implications for 1 mgd HDS system of 4 stages in series starting with 100 mg/L TSS with the ideal performance presented in Table 20.

		flow rates [gpm]			mass flow rates [%]			solids concentration [mg/L]		
stage	#channels	Inf.	Eff.	Conc.	Inf.	Eff.	Conc.	Inf.	Eff.	Conc.
1	10500	694	556	139	100%	30%	70%	100	38	350
2	2100	139	111	27.8	70%	7%	63%	350	44	1575
3	420	27.8	22.2	5.56	63%	6%	57%	1575	197	7088
4	84	5.56	4.44	1.11	57%	6%	**51%**	7088	886	**31,894**

Using the average flow splits, harvest efficiencies, inlet pressures, and relative flow rates (to accommodate the necessary overflow needed to prevent downstream pumps from "starving") documented during pilot testing, the performance and impact of a full-scale HDS system based on "actual" performance was similarly estimated. It was assumed that the first and second stage of this theoretical system had performance similar to the first stage tested in the pilot, while it was assumed that third and fourth stage had performance similar to the third stage tested in the pilot. Also, the primary effluent TSS concentration was assumed to be 100 mg/L for comparison (rather than the average primary effluent concentration measured during pilot testing, which was about 70 mg/L). To accommodate extra channels to prevent "starving" and to allow for up to 80:20 flow split (even though actual flow splits were less), 12,906 channels are needed for a 1 mgd system. This is less than for an ideal HDS system, but that is only because an actual system operates at lower volume splits and needs to have an overflow for each stage to prevent pump starving, so each stage and corresponding pump is smaller). Also, while the actual HDS system captured 1.35 % of the mass of solids, and assuming an influent concentration of 100 mg/L, the final concentrate will only be about 800 mg/L. In practice, this is far too dilute to send to an anaerobic digester. While additional thickening would be needed to make this stream suitable for anaerobic digestion, requiring additional energy, and the amount is small – in this 1 mgd example, this amounts to about 1,600 gpd of dilute sludge to process per mgd, which, assuming centrifuges (at 1.0 kWh/m^3), amounts to only 6 kWh/mgd – additional processes are required. Table 22 and Table 23 present the assumptions for an actual HDS system for 1 mgd.

Table 22: Table of performance based on average, actual results measured during pilot testing.

	Flow split		Harvest Efficiency	
Stage	**Effluent**	**Concentrate**	**Effluent**	**Concentrate**
Stage 1	65%	35%	48%	52%
Stage 2	65%	35%	48%	52%
Stage 3	76%	24%	54%	46%
Stage 4	76%	24%	54%	46%

Table 23: Implications for 1 mgd HDS system of four stages in series starting with 100 mg/L TSS with the actual performance presented in Table 22.

		flow rates [gpm]			mass flow rates [%]			solids concentration [mg/L]		
stage	# channels	Inf.	Eff.	Conc.	Inf.	Eff. (& overflow)	Conc.	Inf.	Eff.	Conc.
1	10500	694	456	239	100%	48%	52%	100	74	149
2	1969	130	85.4	44.8	28%	38%	14%	149	110	221
3	365	24.1	18.5	5.61	8%	11%	4%	221	157	423
4	73	4.82	3.70	1.12	2.9%	2%	**1.35%**	423	301	**811**

Using the modeling results presented in Chapter 2, the assumptions in tables 20 through 23, and the assumptions presented in table 24, the impact to the energy balance for a wastewater

treatment facility without HDS, with an ideal HDS system, and with an actual system was calculated. Only the impacts to energy generation through anaerobic digestion, aeration, and pumping are considered, as all other plant energy demands will be equal. Table 25 presents the results of this analysis in kWh/mgd and $/mgd for each of these three components, and then summed (positive for anaerobic digestion, negative for total aeration requirements, and negative for HDS pumping requirements). To summarize, an ideal HDS system saves about 40 kWh/mgd and about $1,650/mgd/year in energy costs when compared to a conventional activated sludge plant. Were an HDS system installed that had performance similar to what was achieved during the pilot study, it costs about 220 kWh/mgd more and about $9,335/mgd/year more in energy costs than a conventional activated sludge plant. Clearly this iteration does not provide a benefit over conventional treatment, but there is much that can be improved. However, the best-case savings of $1,650/mgd/year is an unlikely incentive for commercialization of HDS for harvesting of organics from primary effluent.

Table 24: Assumptions Used for the Three Components Used to Calculate Energy Benefits of HDS

Cogeneration assumptions	
Anaerobic digestion VSS destruction, % =	60%
Biogas yield, Primary Sludge, ft3 biogas/lb VSS digested =	15
Biogas yield, Secondary Sludge, ft3 biogas/lb VSS digested =	13
Biogas yield, HDS Sludge, ft3 biogas/lb VSS digested =	15
methane content of biogas, % =	66%
methane, BTU/ft3 =	1000
BTU/kWh =	3412
methane, kW/cfm =	17.6
biogas, kW/cfm =	11.6
Microturbine efficiency, % =	26%
Microturbine power yield, kW/cfm =	3.02
Biogas energy utilization, % =	90%
electricity cost, $/kWh =	$0.114
Aeration assumptions	
oxy transfer efficiency, lbs O_2/kWh =	2.99
HDS pumping assumptions	
Hydraulic efficiency, %	65%
Motor efficiency, %	90%

Table 25: Energy comparison of a theoretical plant without HDS (baseline), with an ideal HDS system, and an HDS system based on average performance documented during the pilot study.

Energy generation through anaerobic digestion, cogeneration	**Baseline**	**Ideal HDS**	**Actual HDS**
VSS of primary sludge to digester, lbs/mgd =	852	852	852
VSS from HDS sludge to digester, lbs/mgd =	N/A	363	10
VSS from secondary sludge to digester, lbs/mgd =	669	491	665
Total Biogas Production, ft3/d/mgd =	12890	14763	12940
Biogas production rate, cfm/mgd =	8.95	10.25	9.0
Potential Power Generation (kW/mgd) =	27	31	27
Actual Power Generation (kW/mgd) =	0	28	24
Energy generation (kWh/mgd) =	583	668	586
Electricity revenue from digestion, cogeneration ($/mgd/yr) =	*$ 24,277*	*$ 27,805*	*$24,371*
Energy consumption through aeration for secondary treatment			
BOD removed, lbs/day/mgd =	1453	1195	1446
BOD5 aeration energy requirement, kWh/mgd =	486	400	484
Electricity expenditures for aeration, $/mgd/yr =	*$20,231*	*$16,643*	*$20,137*
Energy consumption for HDS pumping			
1st stage operating pressure, psi =	N/A	8.5	14.7
2nd stage operating pressure, psi =		8.5	14.7
3rd stage operating pressure, psi =		8.5	12.7
4th stage operating pressure, psi =		8.5	12.7
1st stage flow rate, gpm =		694	694
2nd stage flow rate, gpm =		139	130
3rd stage flow rate, gpm =		27.8	24.1
4th stage flow rate, gpm =		5.56	4.82
Power needed, kW =		5.5	9.3
Energy needed, kWh/mgd =		132	223
Annual pumping requirements, $/mgd/yr =		*$5,472*	*$9,278*
Energy consumption for centrifuge thickening to accommodate poor HDS performance			
Energy needed kWh/mgd =	N/A	N/A	6
Annual pumping requirements, $/mgd/yr =			*$245*
Total Energy balance, kWh/mgd	**97**	**137**	**-127**
Total cost benefit, $/year	**$ 4,046**	**$ 5,689**	**$ (5,289)**

CHAPTER 8:
Technology Transfer Activities

PARC submitted monthly and interim reports for this project to the California Energy Commission, and also presented posters and presentations related to PARC's HDS technology at conferences around the country. This are listed below.

Reports to the California Energy Commission:

- 27 monthly progress reports
- Pilot Test Plan
- Pilot System Report
- Pilot Installation Report
- Pilot Demonstration Report
- Measurement and Verification Report

Conferences and Workshops:

- WEFTEC 2012 – Water Environment Federation Technical Exhibit and Conference. New Orleans, LA, September 29th – October 3rd, 2012. Exhibitor.
- Biogas Technology Summit – Diamond Bar, California, February 2013. Presenter.
- Filtech 2013 – International filtration and separation conference, Wiesbaden, Germany, October 22-24, 2013. Presenter. "Reducing energy footprint of a wastewater treatment plant by increasing harvest efficiency during primary clarification".
- Cleantech 2014 – Water and Energy Symbiosis Conference, Washington DC, June 15-19th, 2014. Presenter. "Reducing energy footprint of a wastewater treatment plant by increasing harvest efficiency during primary clarification"
- WEFTEC 2014 – Water Environment Federation Technical Exhibit and Conference. New Orleans, LA, September 29th through October 2nd, 2014. Presenter. Piloting a 40 lpm, organics-harvesting hydrodynamic separation process for reducing energy needs and increasing energy recovery during wastewater treatment.
- Algal Biofuels Spring Strategy Workshop, US DoE's Bioenergy Technologies Office, Charleston, South Carolina, March 26-27, 2014. Oral presentation. "Innovative Algae Dewatering Technology".
- Biomass 2014 – Growing the future economy conference, US DoE. Washington, DC, July 29-30th, 2014. Poster presentation.

Publications:

- Lancaster, C. and A.R. Völkel. "Piloting a 40 lpm, Organics-Harvesting Hydrodynamic Separation Process for Reducing Energy Needs and Increasing Energy Recovery During Wastewater Treatment". (New Orleans: *Proceedings of the WEFTEC 2014*, 2014), September 29 through October 2.

CHAPTER 9:
Conclusions and Recommendations

9.1 General Conclusions

The following general conclusions can be drawn from the results of this study using a custom-built test-station for piloting semi-automatically assembled stacks of mass produced, injection molded parts to create working HDS channels.

- Pre-screening of particles greater than 25 % of the channel height is of critical importance. In this study, the configuration that included a 200um bag filter was not effective in removing larger particles, which contributed to fouling of the inlet manifolds, increased head losses, and likely contributed to decreased performance (harvest efficiency). Also, algae that grew within the pilot system contributed to fouling of both the inlet manifolds and the channels themselves during the study. Future pilot units could be improved by providing better or more effective pre-screening devices and reducing or eliminating the use of clear tubings.
- The splitter and ejector pin mark accumulated fluffy organic solids. While there is little that can be done to prevent accumulation of solids on the splitters, regular backwashing could easily dislodge and minimize buildup. The ejector pin mark was a manufacturing flaw. Future molded parts will not have ejector pin marks in the middle of the exit channels.
- Inlet pressure increased as a result of fouling of the inlet manifolds and the channels. Most pressure increases could be reduced by regularly removing the debris from the inlet manifolds.
- The manifold and channel fouling resulted in a slow decline in harvest efficiency over the course of the study, but did not seem to have an impact on split ratio.
- Having equal head losses downstream of the exits is critical for maintaining a desired flow split. This was achieved in this study by discharging to a free surface. The pilot unit was not designed to allow this. Future pilot units could be improved by designing the exit piping such that the downstream head losses are considered.
- The fouled channels were easily cleaned after 16 hours of operation at the Sunnyvale Wastewater treatment facility such that pre-use performance was attained after cleaning. The cleaning method involved pressure at 20 psi through the channels in both directions.
- The particle size distribution of the primary effluent has a strong impact on the separation performance of the HDS stacks. Figure 70 shows the PSD of primary effluent collected from the Sunnyvale wastewater treatment plant before and after separation. The initial size distribution results, which are presented as a percentage of volume for each size bin for the total volume of solids and is independent of total mass in a sample,

make comparisons between samples difficult. Figure 70 integrates the particle size distribution with the mass rate for each sample so as to provide distributions for influent (primary effluent), HDS effluent, and HDS concentrate streams that are relative to each other, making visual comparison easier. The mode input particle size (blue lines, primary effluent) is approximately 20 um, and the mean particle size is approximately 30 um. The theoretical cutoff size for this HDS design is 20 um, meaning a significant portion of solids are theoretically unable to be separated by HDS. This separation experiment, presented earlier, resulted in a HE of 53% by mass (in 27% of the volume). Separation efficiency is variable, and has been as high as 70% during the pilot (the first day of operation for the first stage, Table 16). Significantly higher performance for a single pass, such as 90%, is unlikely. Perhaps primary clarifiers could be designed to be smaller, or different primary treatment systems could be used (for example, Salsnes filters) to allow a slightly larger particle size (but not too large) through to an HDS system. While the net benefit in terms of organics harvesting would be the same, a smaller primary treatment systems would reduce footprint and save capital costs. To capture smaller particles, an HDS design with smaller channel dimensions could be used. However, a re-designed HDS channel would likely increase the rate of fouling, and/or would necessitate pre-screening of smaller particles. A cascade of different sized channels might be employed to capture a wider range of particle sizes – an initial, four-stage process through PARC's floc separator design (channel dimensions of 15mm by 1.1 mm high, removes particles between 70 and 250 um) could capture and thicken the larger particles while acting as a pre-screening device for a second, four-stage process consisting of stacks of HDS of the current (6 mm wide by 0.4mm high, removes particles between 20 and 100um) or slightly smaller size channels. This second process would take the cleaner effluent of the first process. While this is theoretically possible, such a two-process system of four stages each would likely be too complex to be practical and at best would provide the benefit that was initially proposed for this study. Because the larger dimension channels operate at approximately 1/10th the pressure, the pumping costs would only be slightly more than the current estimate of about 0.06 kWh/m^3 of processed primary effluent.

Figure 70: Mass rate particle size distribution of primary effluent input, single channel HDS effluent, and single channel HDS concentrate. From lab separation of primary effluent from Sunnyvale Wastewater plant performed November 21, 2013

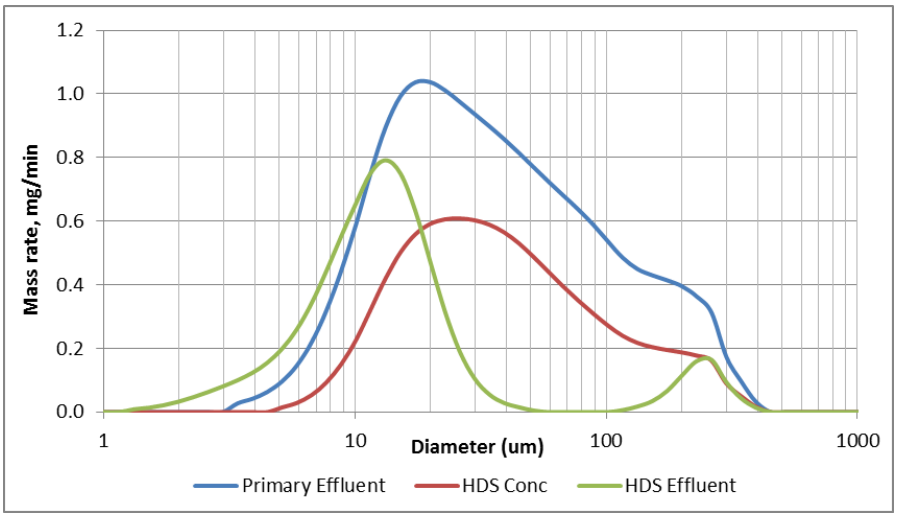

9.2 Recommendations for Future Work

PARC has made significant strides in developing this promising technology, but there is much still to be learned. Future work should focus on sources of separation other than primary clarifier effluent. This may be a different type of primary wastewater treatment, such as a Salsnes Filter, that provides a particle size distribution more amenable to HDS. It is more likely that HDS will offer a cost-effective solution for activated sludge concentration to reduce loads on secondary clarifiers rather than as a means to harvest organics from raw, filtered, or settled wastewater. The most promising application may be for algae dewatering, which is currently the bottleneck in economical algal biofuels production.

Future work should build on what was learned during the course of this study, namely in the fabrication of stacks of channels. With the proper design and QA/QC procedures in place, injection molded parts can be made within acceptable tolerances. While gluing stacks robotically was effective for assembly, other methods such as hot plate assembly, may be faster, cheaper, and provide more robust stacks. Such methods require more initial investment, however.

HDS system design is as important as the HDS channel design. Future work should be sure to incorporate system headlosses in the design to ensure that stacks of HDS channels can perform as intended.

Lastly, future work should evaluate the upper concentrations limits that are capable of being separated by HDS. This will be different for different particle types, and will be essential for understanding separability potential when placing HDS stacks in series.

GLOSSARY

ABS	Acrylonitrile Butadiene Styrene (a plastic)
BOD	Biochemical Oxygen Demand
CAD	Compter-Aided Design
CDI	Cascade Designs, Inc.
CFD	Computational Fluid Dynamics
COD	Chemical Oxygen Demand
EBMUD	East Bay Municipal Utility District
Energy Commission	California Energy Commission
gpm	Gallons per minute
HDS	Hydrodynamic Separation
IOU	Investor-owned utility
kWh/mgd	Kilowatt-hours per million gallons per day
L	Liter
lpm	Liters per minute
MGD	Million gallons per day
μm	Micrometer
mg/L	Milligrams per liter
mgd/year	Million gallons per day per year
mm	Millimeter
P&ID	Piping and Instrumentation Diagram
PARC	Palo Alto Research Center
PE	Primary Effluent
PID	Proportional, integral, derivative
PIER	Public Interest Energy Research
PMMA	Poly (Methyl Methacrylate) (a plastic)
PLC	Programmable Logic Controller

ppm	Parts per million
PSD	Particle Size Distribution
psi	Pounds per square inch
PVC	Poly vinyl Chloride (a plastic)
QA/QC	Quality Assurance/Quality Control
SFPUC	San Francisco Public Utility Commission
Sunnyvale	Sunnyvale Water Pollution Control Facility
TSS	Total Suspended Solids
TWh	Terawatt-hours
UV	Ultraviolet
VSS	Volatile Suspended Solids
WPCP	Water Pollution Control Plant

REFERENCES

Hsieh, H. B., Völkel, a. R., Chang, N., Kole, a., Melde, K., & Torres, F. 2013. "An Innovative Hydrodynamic Separation Technology (HDS) for Water Pretreatment: Harvesting Neutrally Buoyant Particles Effectively". *Water Science & Technology: Water Supply* 13(2): 524. doi:10.2166/ws.2013.053

Seo, J., Lean, M. H., & Kole, A. 2007. "Membraneless Microseparation by Asymmetry in Curvilinear Laminar Flows". *Journal of Chromatography* A, 1162(2): 126–31. doi:10.1016/j.chroma.2007.05.110